Investigating Material Behavior in Atmospheric Entry Conditions: Arc-Jet Testing Insights from Meteorite Ablation to High-Temperature Coatings.

Dr. Brody K. Bessire

National Aeronautics and Space Administration

Ames Research Center

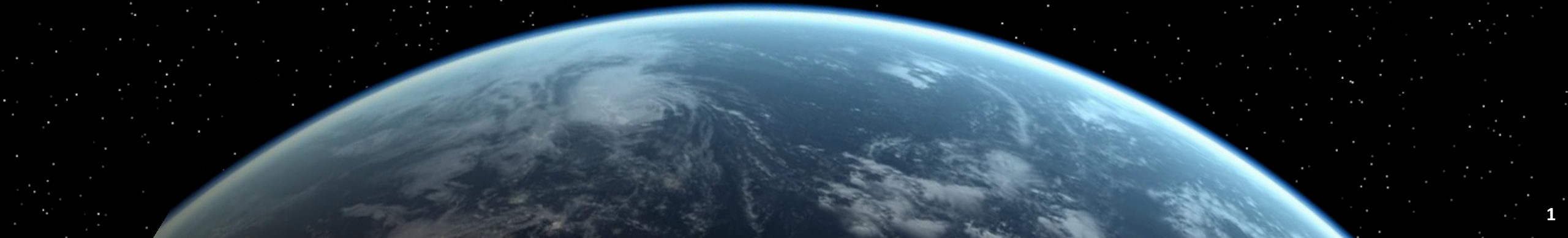

NASA Ames Research Center

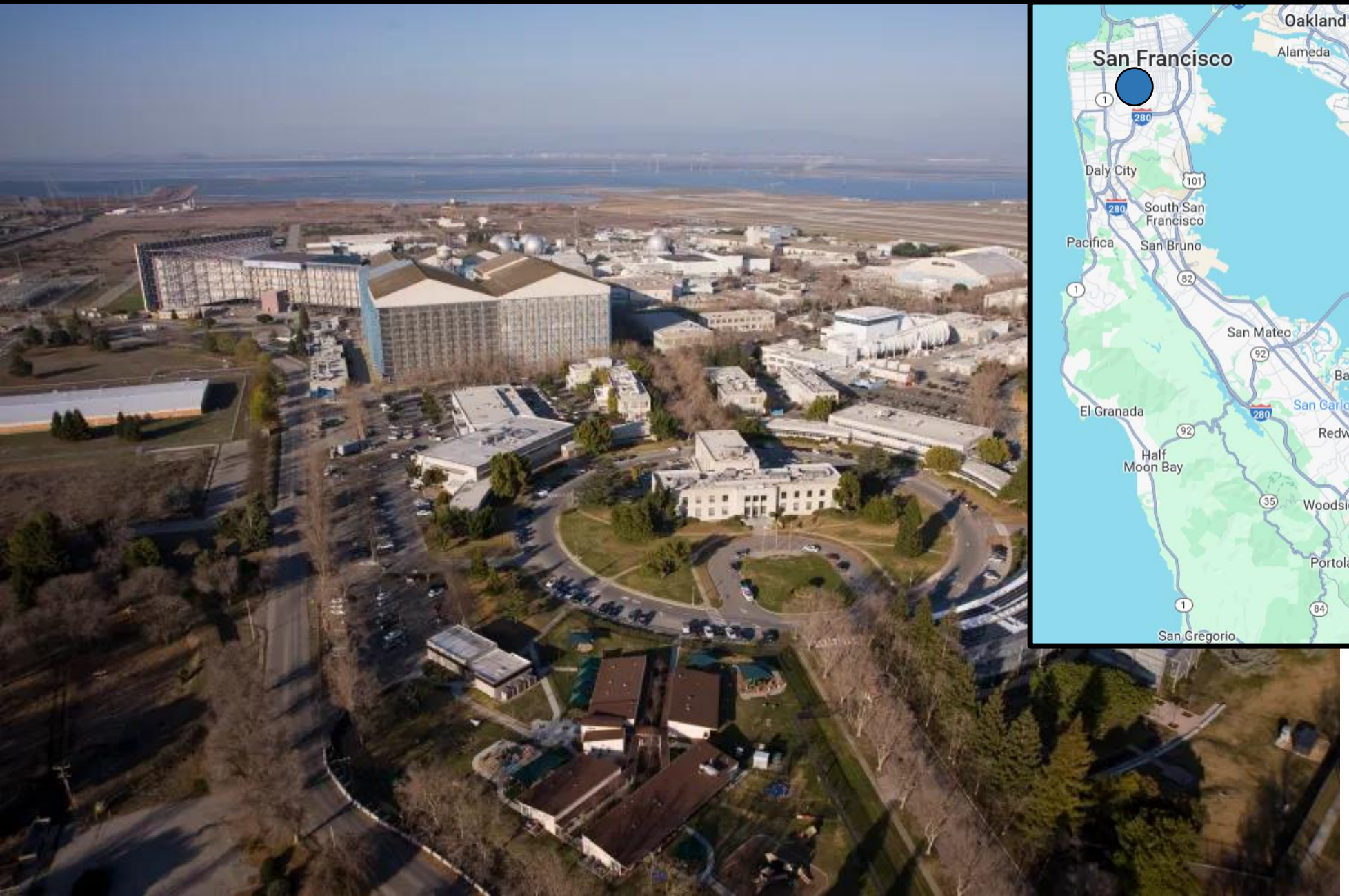

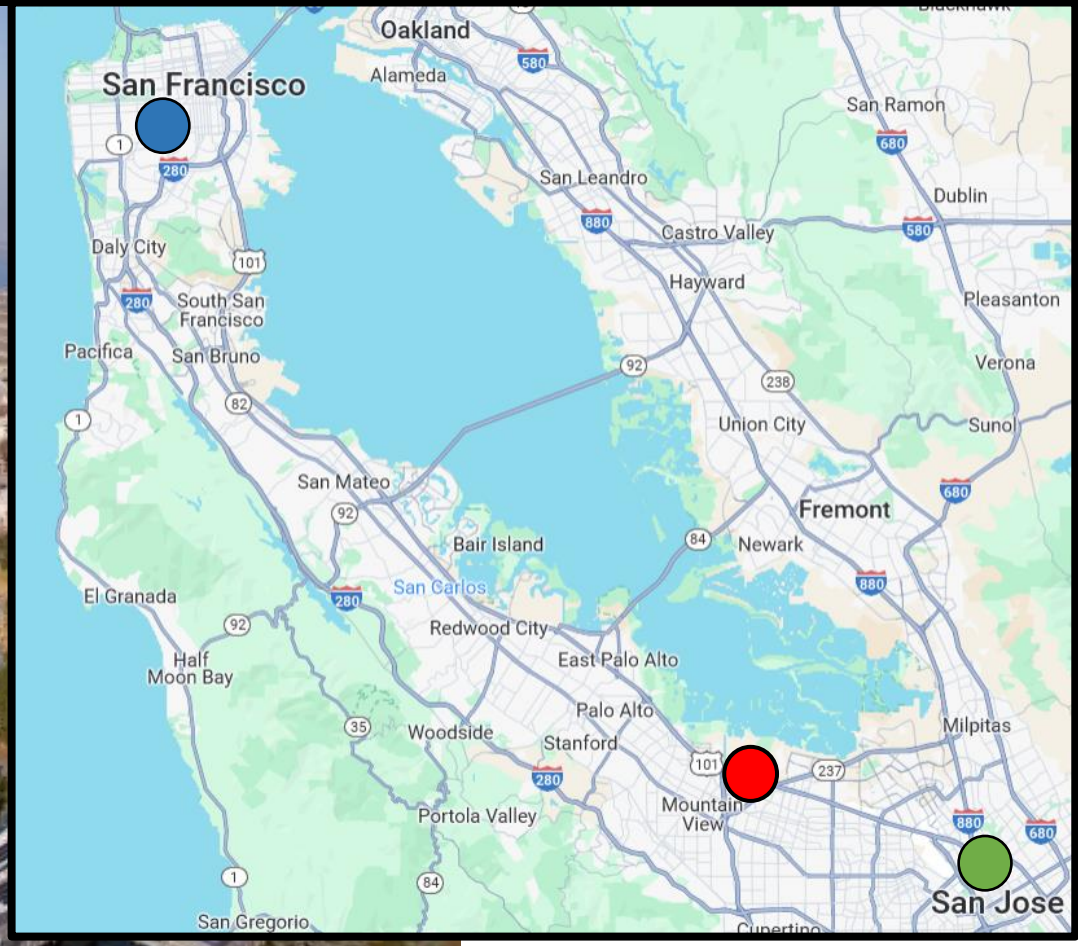

NASA Ames Research Center

NASA Team Members

Adam S. Caldwell (ARC)

Aaron M. Brandis (ARC)

Arnaud Borner (ARC)

Bohdan O. Wesley (ARC)

Brody K. Bessire (ARC)

Bruno Diaz (ARC)

Eric C. Stern (ARC)

Georgios B. Chatzigeorgis (ARC)

Gregory L. Gonzales (ARC)

Jeremie Meurisse (ARC)

John M. Thornton (ARC)

Jose F. Chavez-Garcia (ARC)

Joseph G. Mach (ARC)

Justin Haskins (ARC)

Mairead Stackpoole (ARC)

Magnus Haw (ARC)

Michael D. Barnhardt (ARC)

Michael J. Wright (ARC)

Nagi N. Mansour (ARC)

Peter E. Marshall (ARC)

Sebastian V. Colom (ARC)

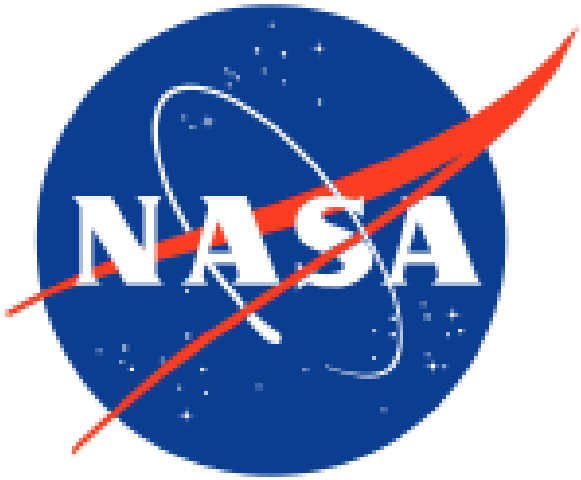

David Alan Mclain (LaRC)

Douglas M. Johnson (LaRC)

Harlen D. Capan (LaRC)

Jason M. Chenenko (LaRC)

Kate Clements (LaRC)

Michael T. Goodwin (LaRC)

Monica Hughes (LaRC)

Ryan H. Hill (LaRC)

Scott C. Splinter (LaRC)

Scott R. Zavada (LaRC)

Thomas K. West (LaRC)

Collaborators

Alathea Davies (UI)

Alexandre Martin (U. Kentucky)

Alex Zibitsker (U. Kentucky)

Doug Fletcher (U. Vermont)

Francesco Panerai (UIUC)

Ian Ballou (U. Vermont)

Jack Widmer (U. Colorado)

Joseph Bibin (U. Kentucky)

Kate R. Rhoads (U. Kentucky)

Kristen J. Price (U. Kentucky)

Kuren Patel (ISU)

Mason Anderson (UI)

Mollie Clyde (Vermont)

William T. Burke (Vermont)

Nathan Wells (SJSU)

Nicholas Anderson (UIUC)

Sander Bouchard (CSM)

Sreevishnu Oruganti (UIUC)

Steven M. George (U. Colorado)

Victoria Duplessis (U. Kentucky)

Virginia Knight (U. Texas - Austin)

Asteroid Threat Assessment for Planetary Defense

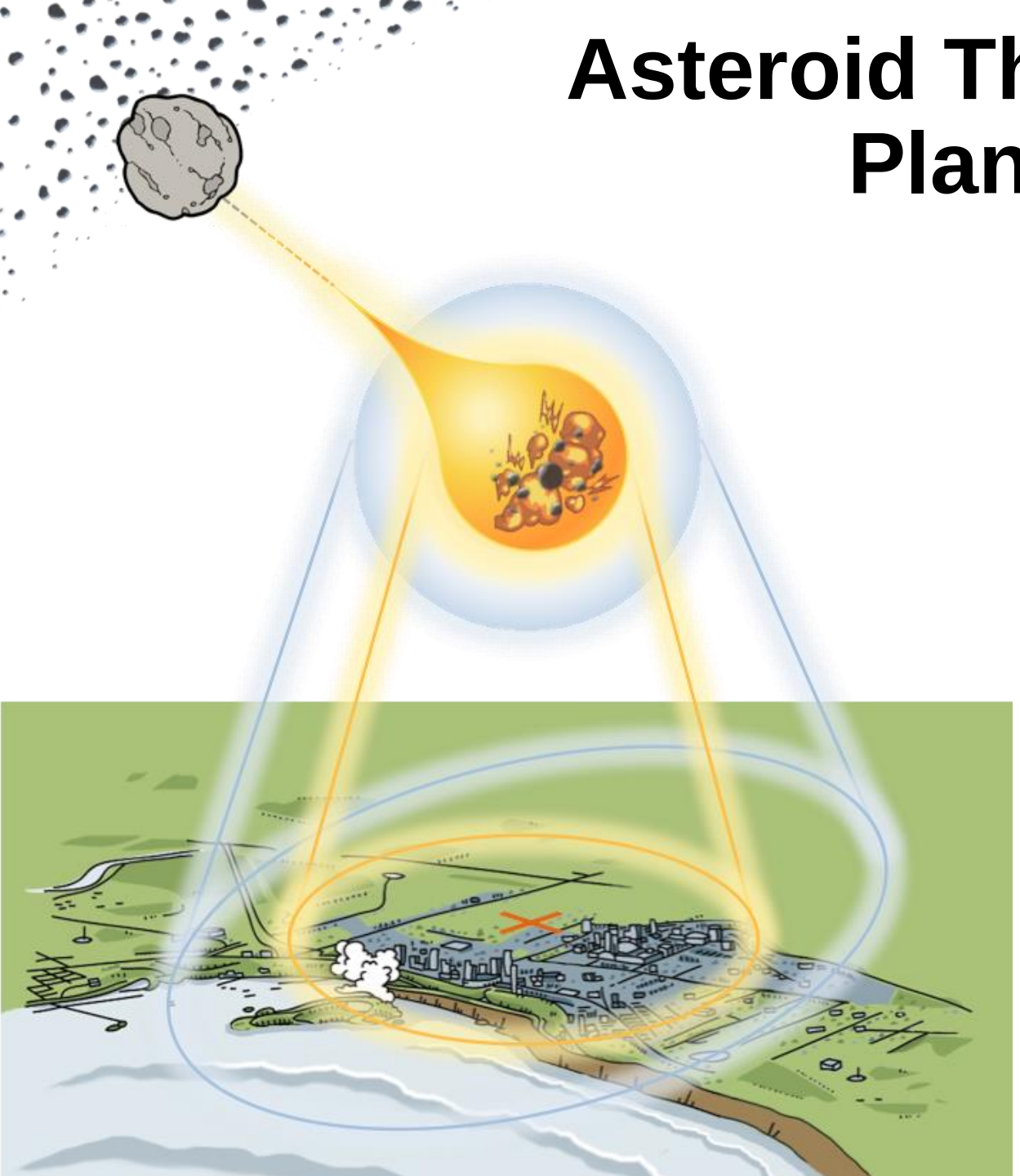

Objectives:

- Develop models and data to characterize the potential damage and risks due to asteroid strikes on Earth
- **Provide results that can help guide decisions and planning:**
  - Asteroid surveys
  - Mitigation systems
  - Disaster response

Meteorite Classification & Composition

Stony

- Primarily composed of rock forming silicates with decreased concentrations of iron alloy.

Stony-Iron

- 50% iron alloy imbedded in a silicate matrix.

Siderites

- Composed of 90-95% iron-nickel alloy (e.g., kamacite and taenite) with trace elements.
- Rare! 5.7% of all witnessed falls.

Chondrites

Carbonaceous

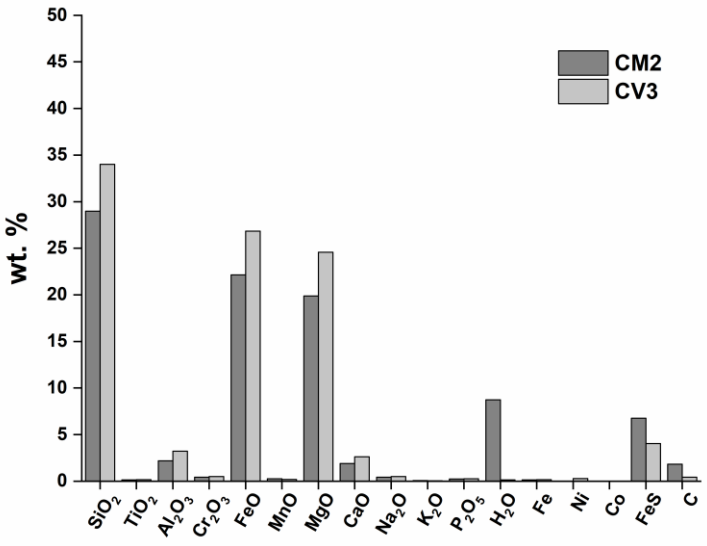

Ordinary

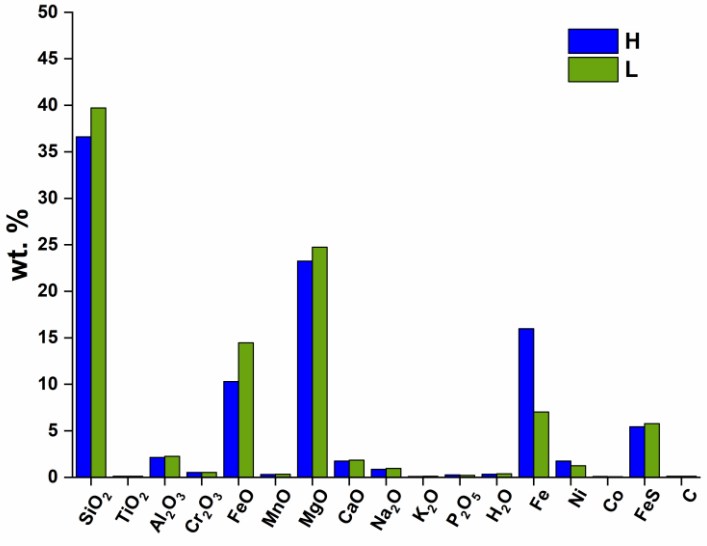

Enstatite

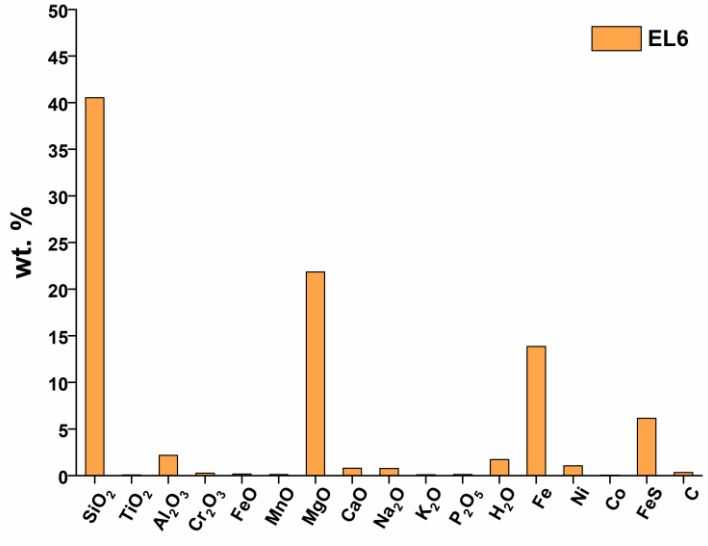

85% of observed falls!

Jarosewich, E., Meteoritics 1990, 25, 323-337

Sample Architecture and HyMETS Facility

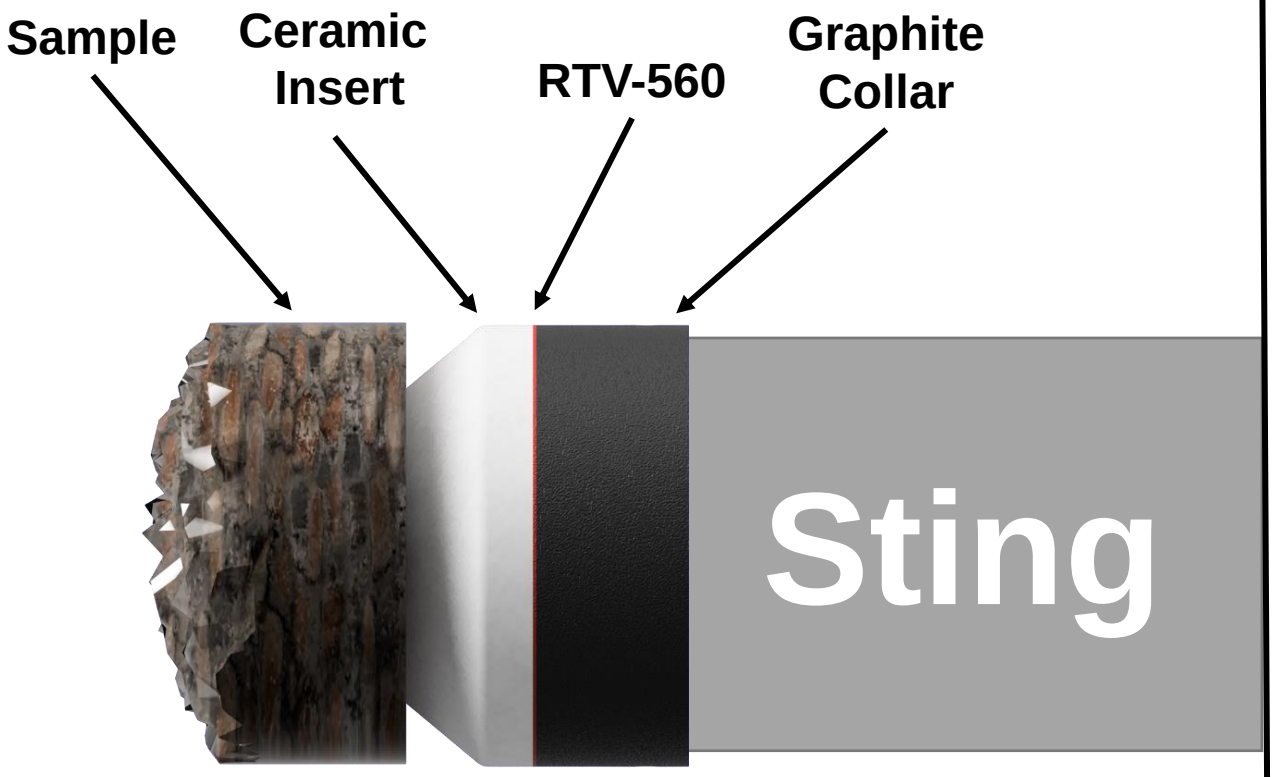

- Compare the material response of basalt vs. ordinary chondrite (Tamdakht).
- Models subjected to testing in air flow.
- Heat flux range: 150 – 350 W cm^{-2}.
- Stagnation pressure range: 3-7 kPa.

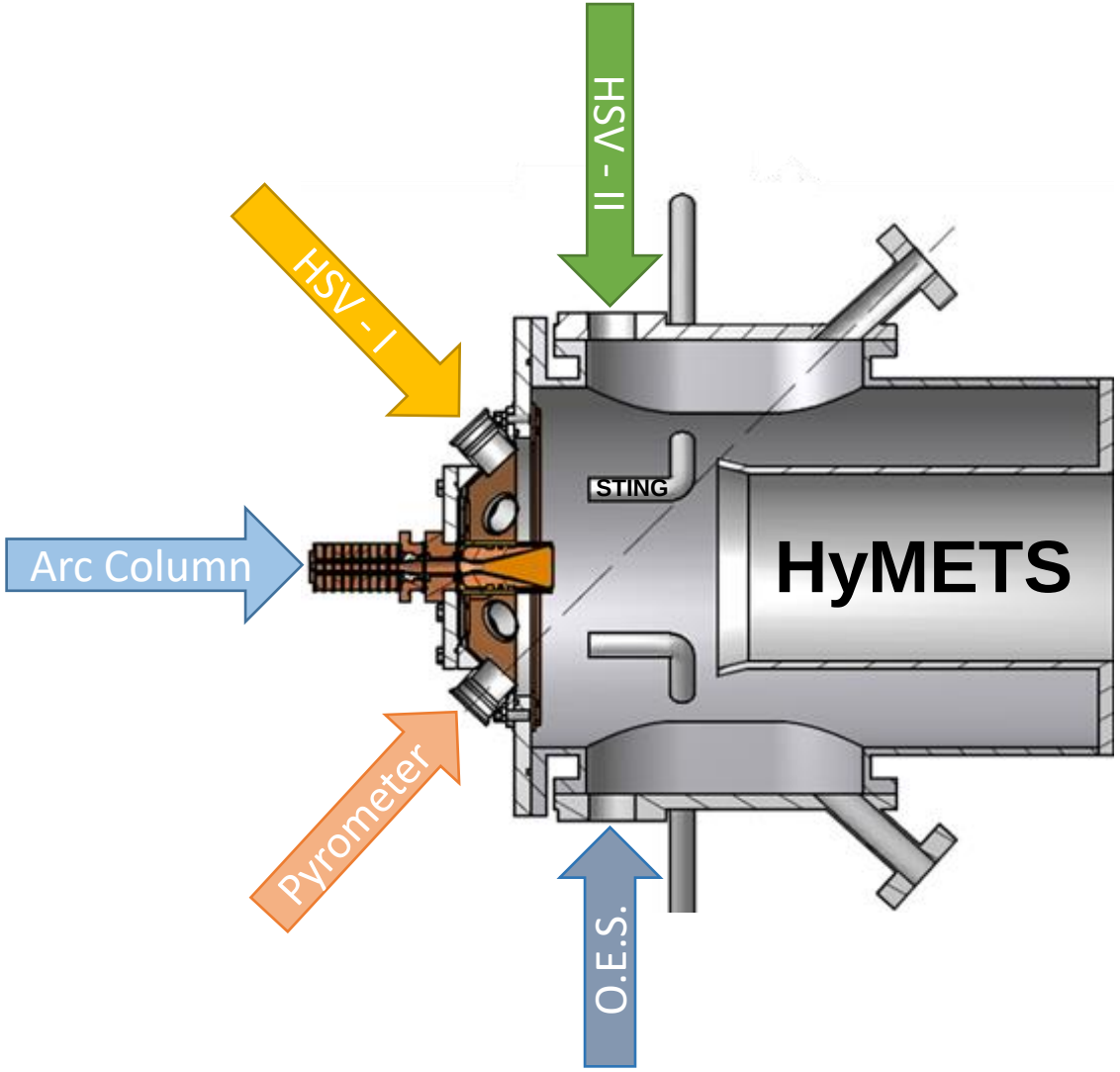

Surface Temperature (T_s) Measurements

- The plot shows surface temperatures (T_s) collected on Tamdakht and Basalt as a function of heating rate.
- Surface temperatures of Tamdakht (green traces) slowly rise to a steady state.
- Surface temperatures of basalt (orange traces) increase rapidly when compared to Tamdakht.
- However, the surface temperature is not stable as evidenced by periodic oscillations.

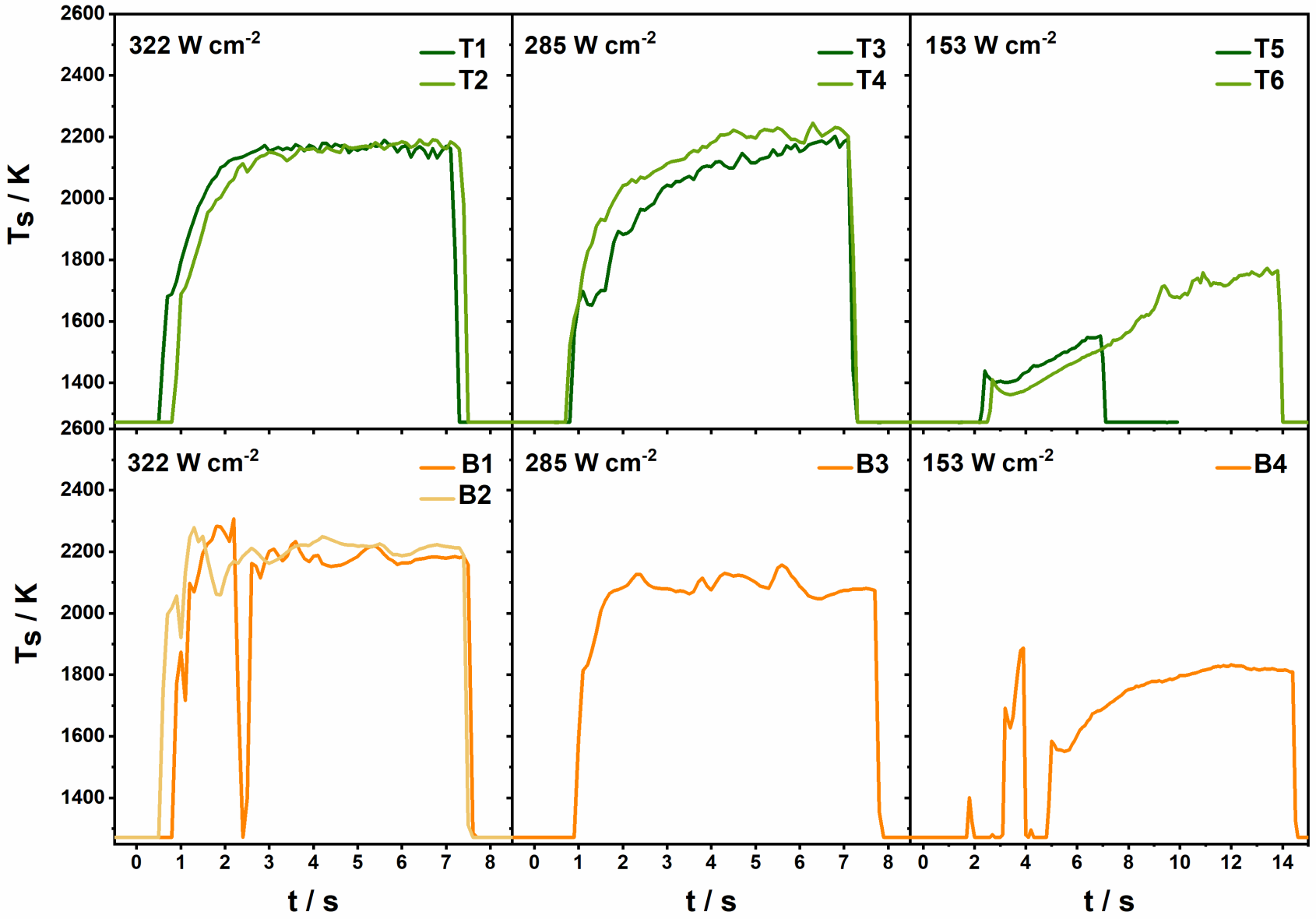

Ablation Mechanisms / High-Speed Video

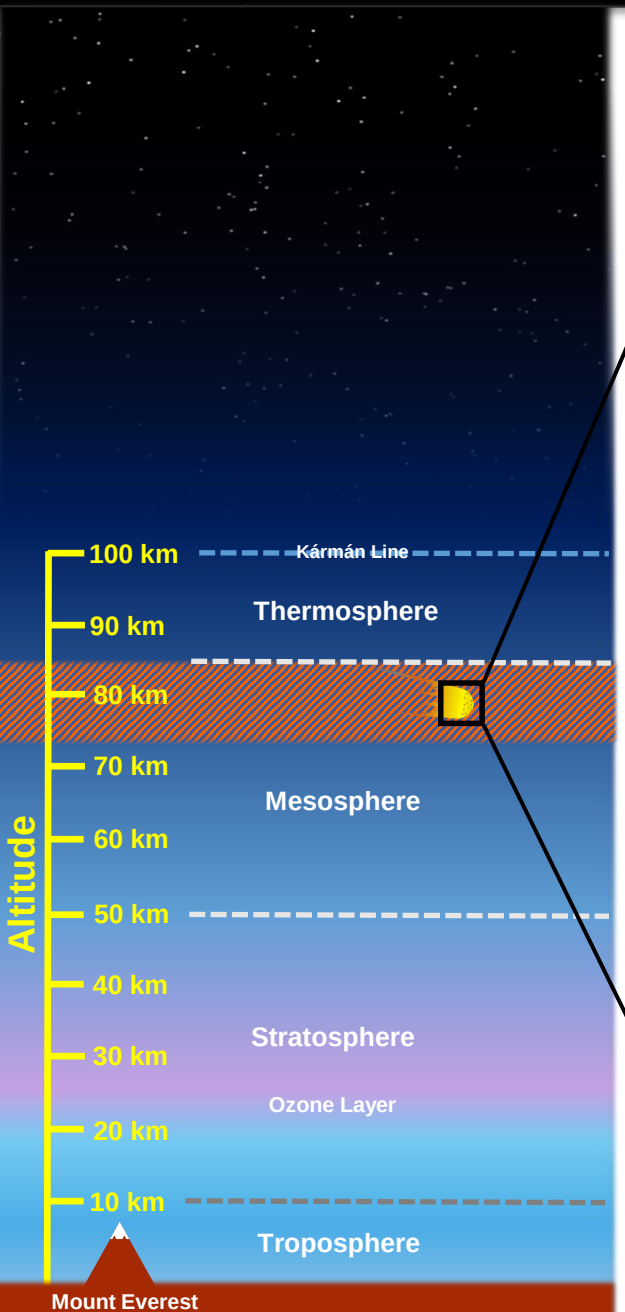

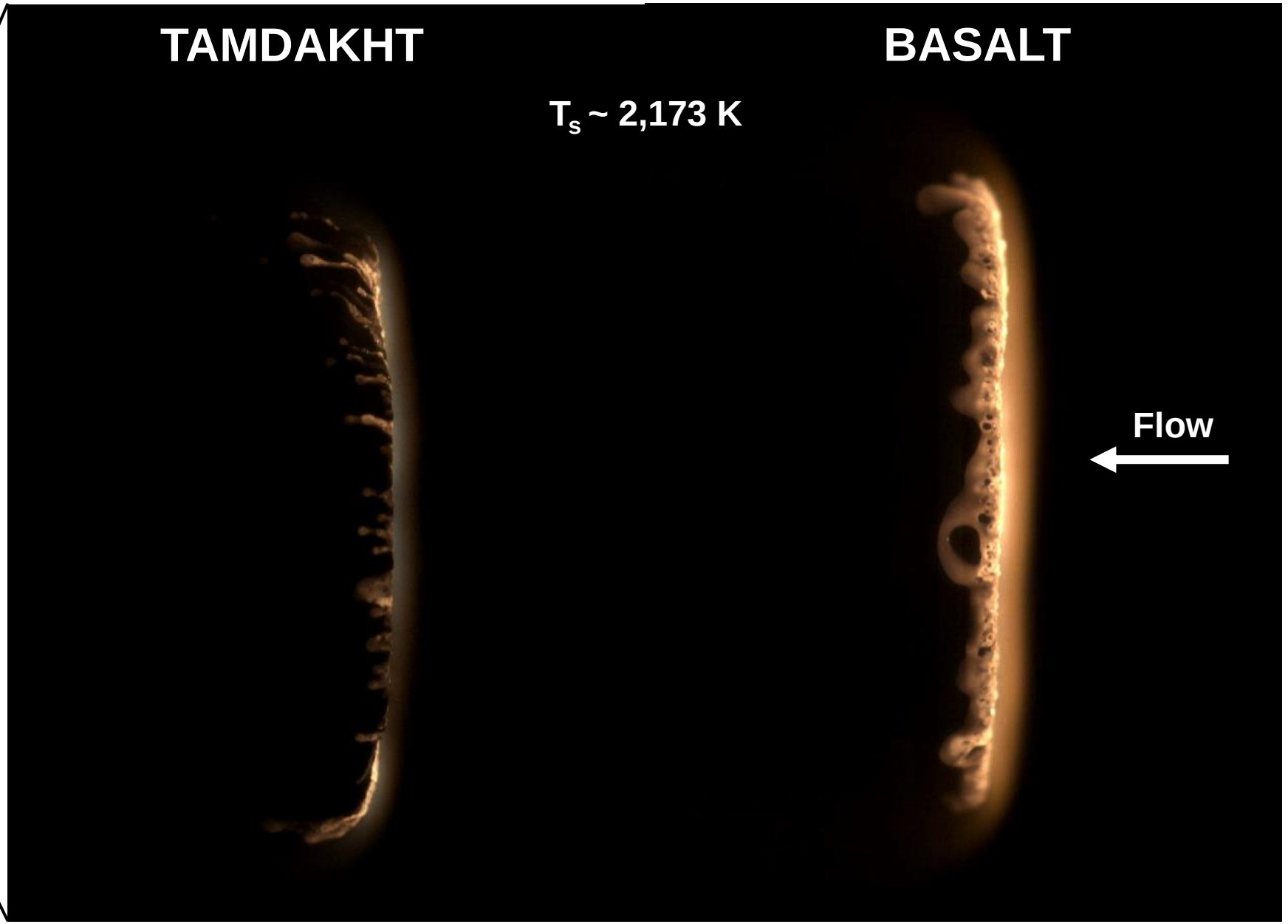

Recession Rates and Mass Loss

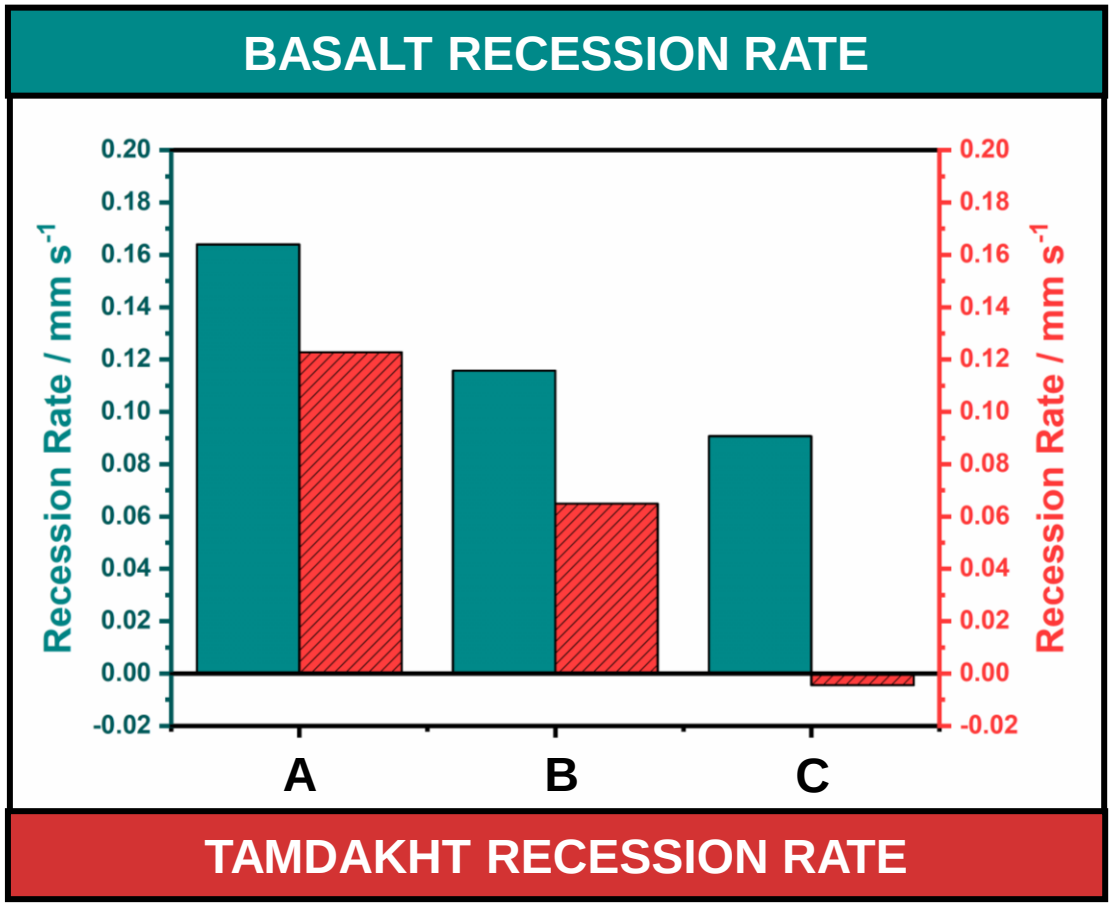

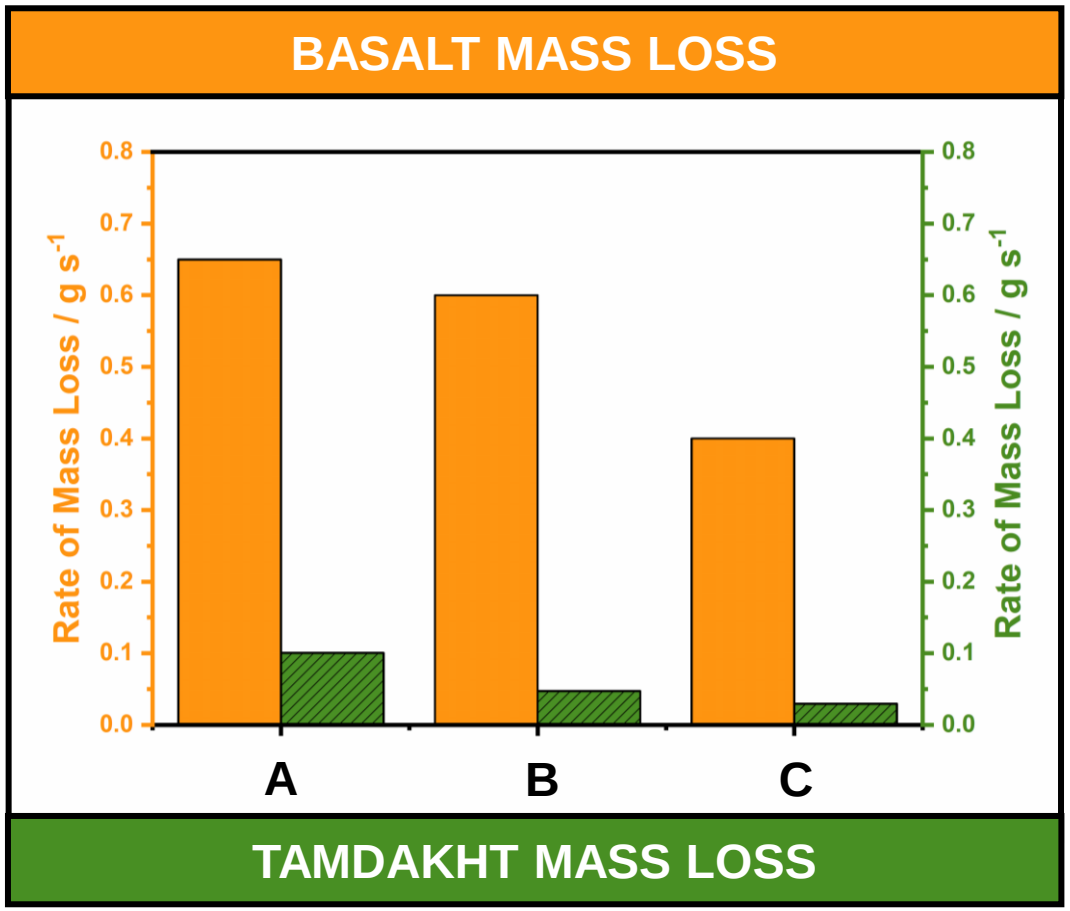

Mass loss and recession rates are higher for basalt.

Meteor Ablation Mechanisms

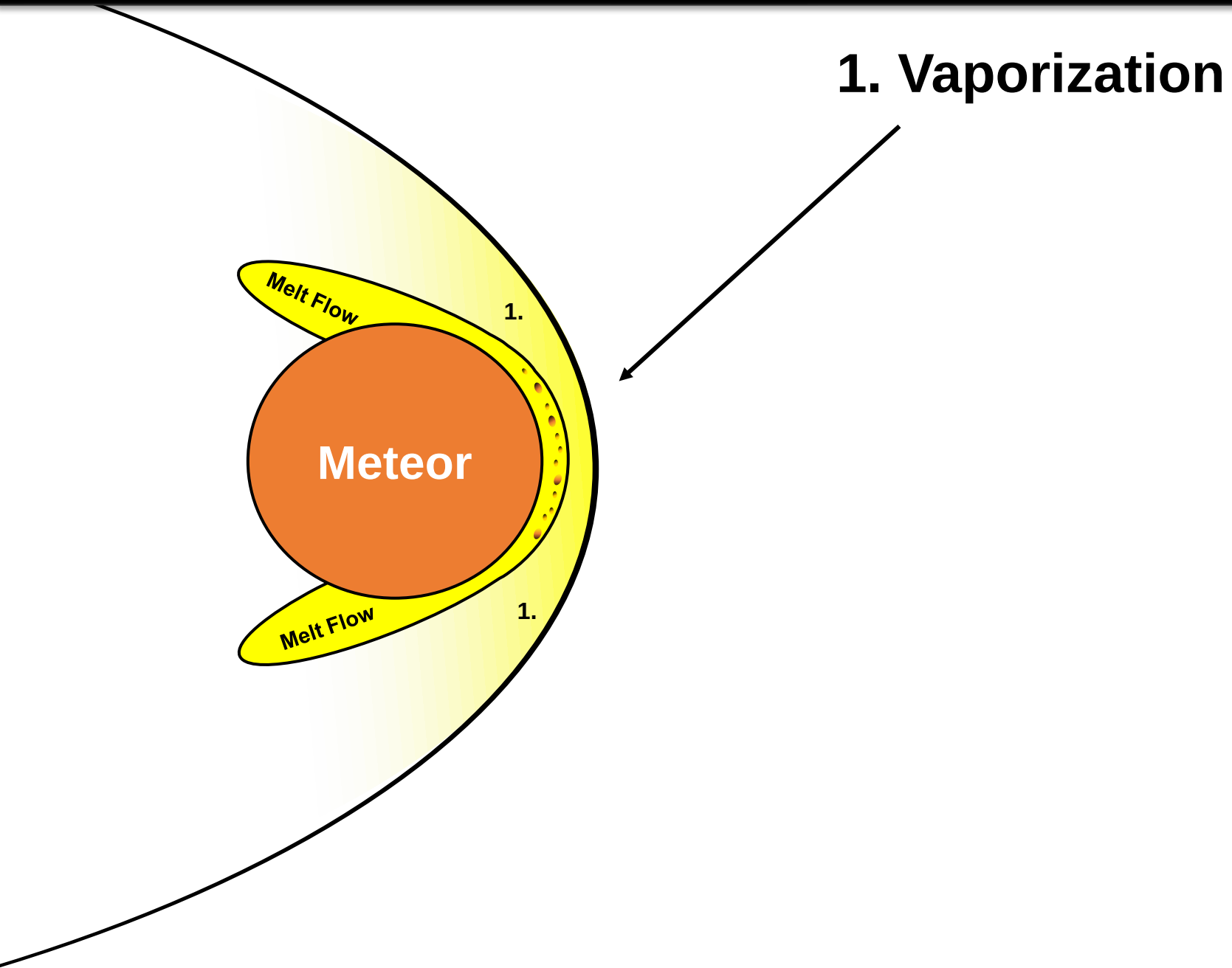

Optical Emission Spectroscopy

Emission Data

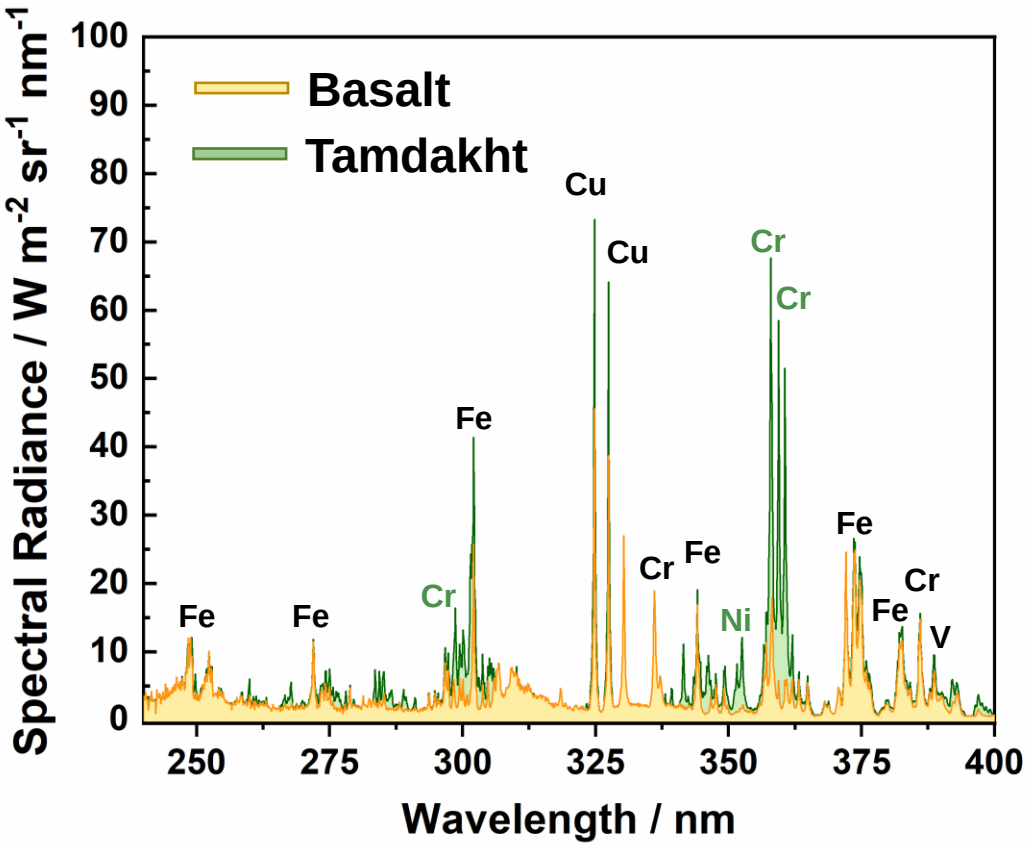

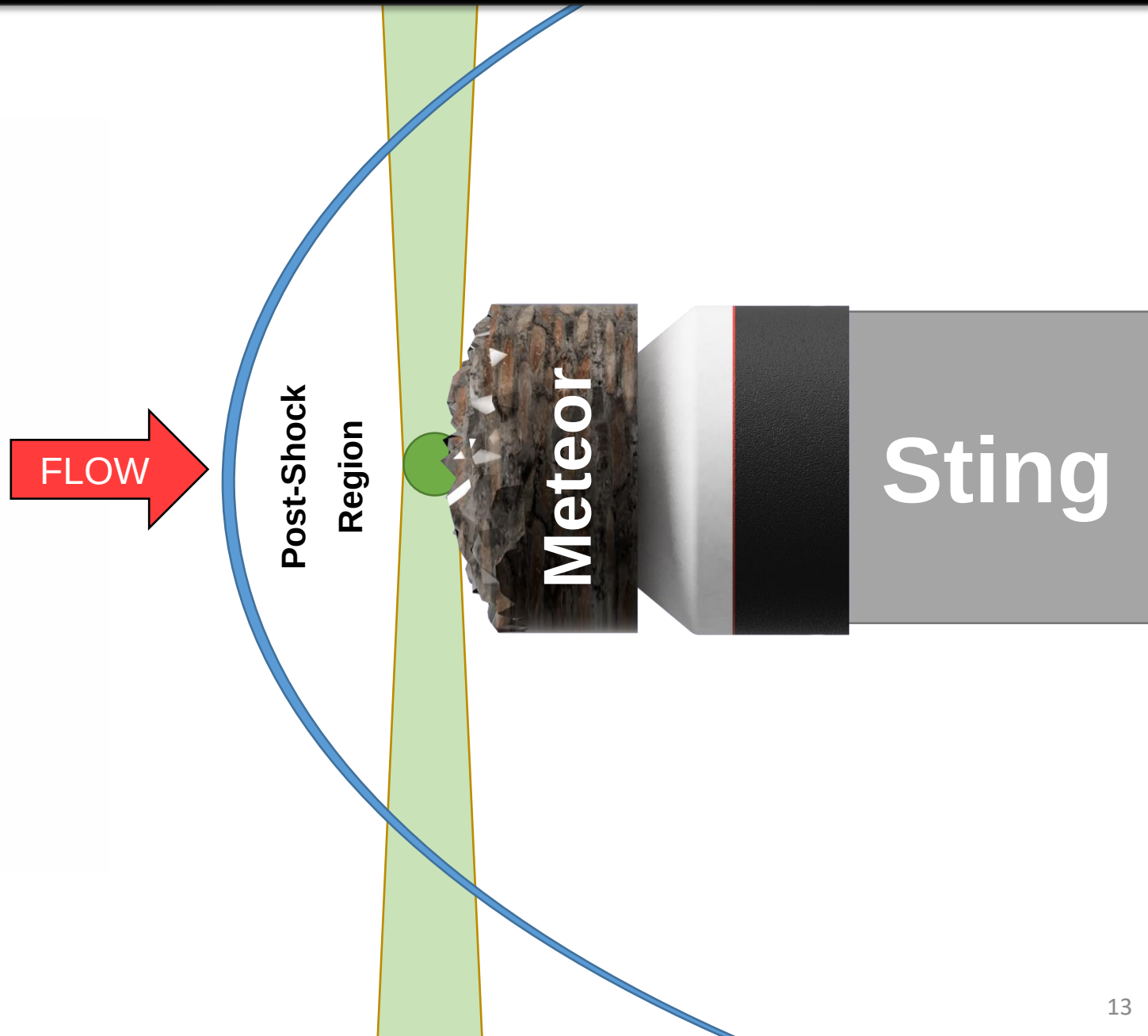

X-ray Fluorescence (XRF) / Post-Test Melt

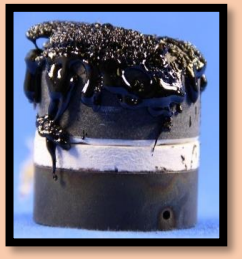

- Primary compounds of the post-test melt are invariant with respect to the virgin material.
- Volatile compounds decrease under more severe test conditions.

Basalt / Primary Compounds

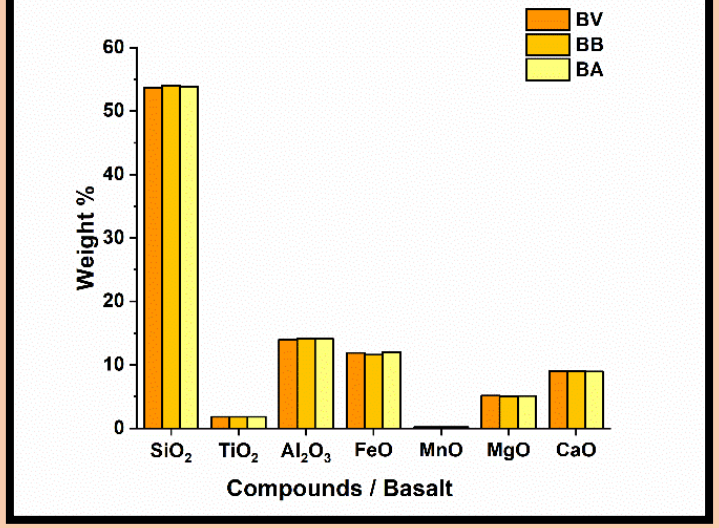

Basalt / Volatile Compounds

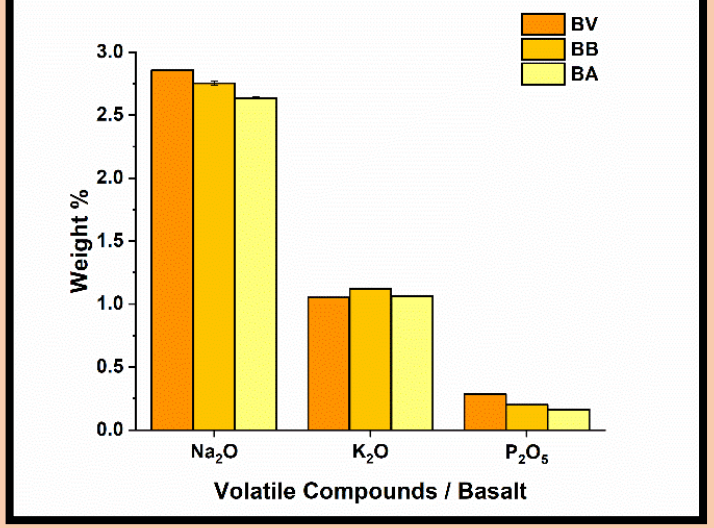

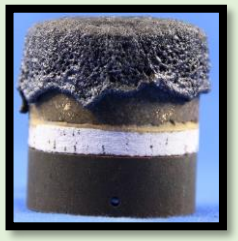

- Concentrations of primary compounds change significantly as a function of test condition.
- Volatile species decrease relative to the bulk material.
- Analysis does not account for FeS.

Tamdakht / Primary Compounds

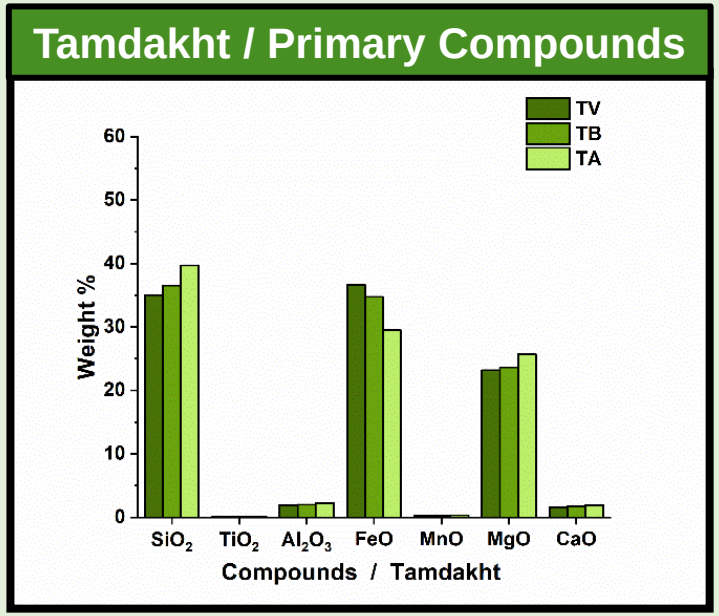

Tamdakht / Volatile Compounds

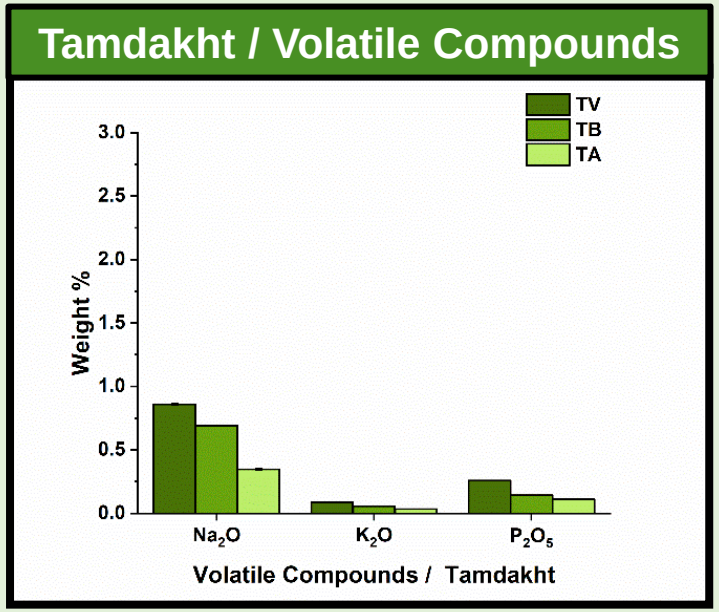

Meteor Ablation Mechanisms

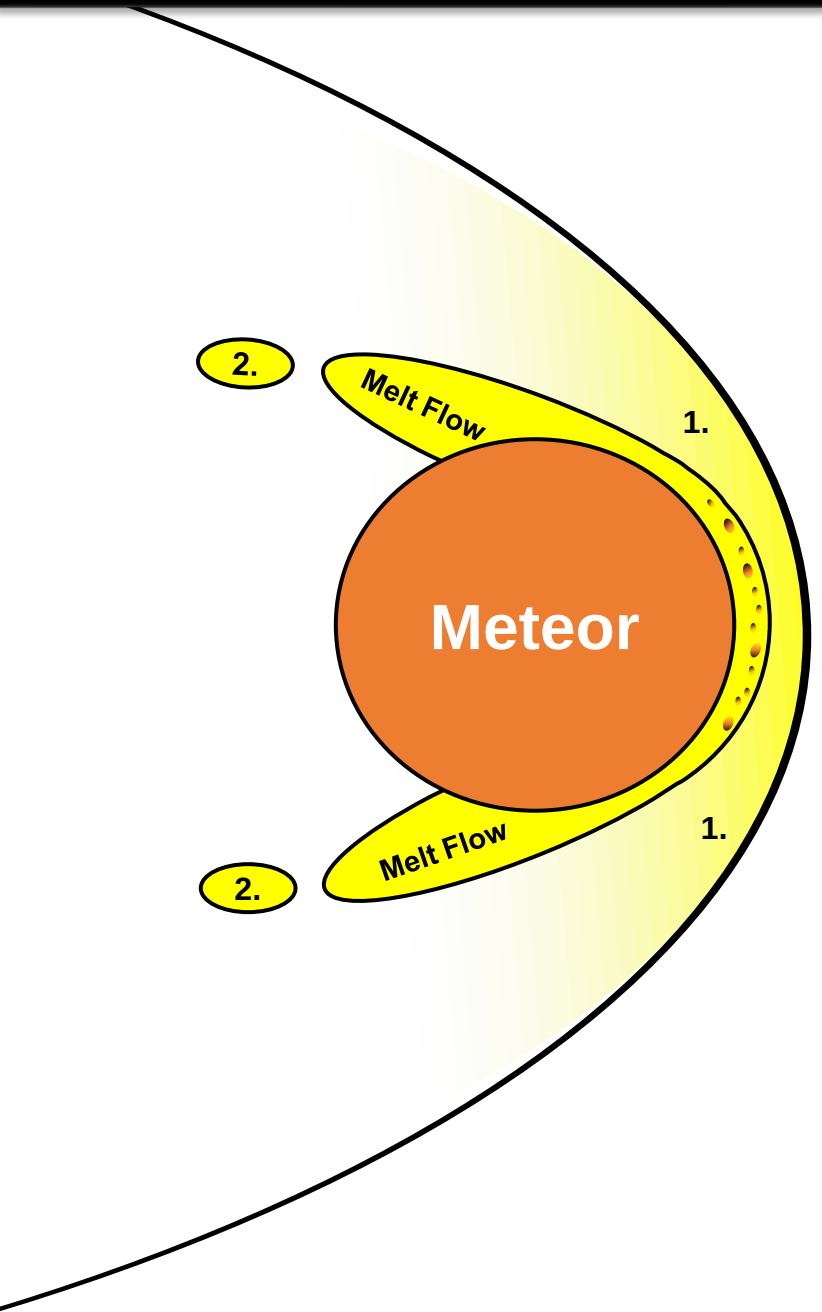

1. Vaporization

2. Melt Flow Spray

Melt Viscosity

1. Giordano model used to predict silicate melt viscosities as function of temperature and composition.

2. Vogel-Fulcher-Tammann.

$$Log\ \eta = \frac{A + B}{(T(K) - C)}$$

3. XRF data used as input.

4. Viscosity of basalt is higher than Tamdakht.

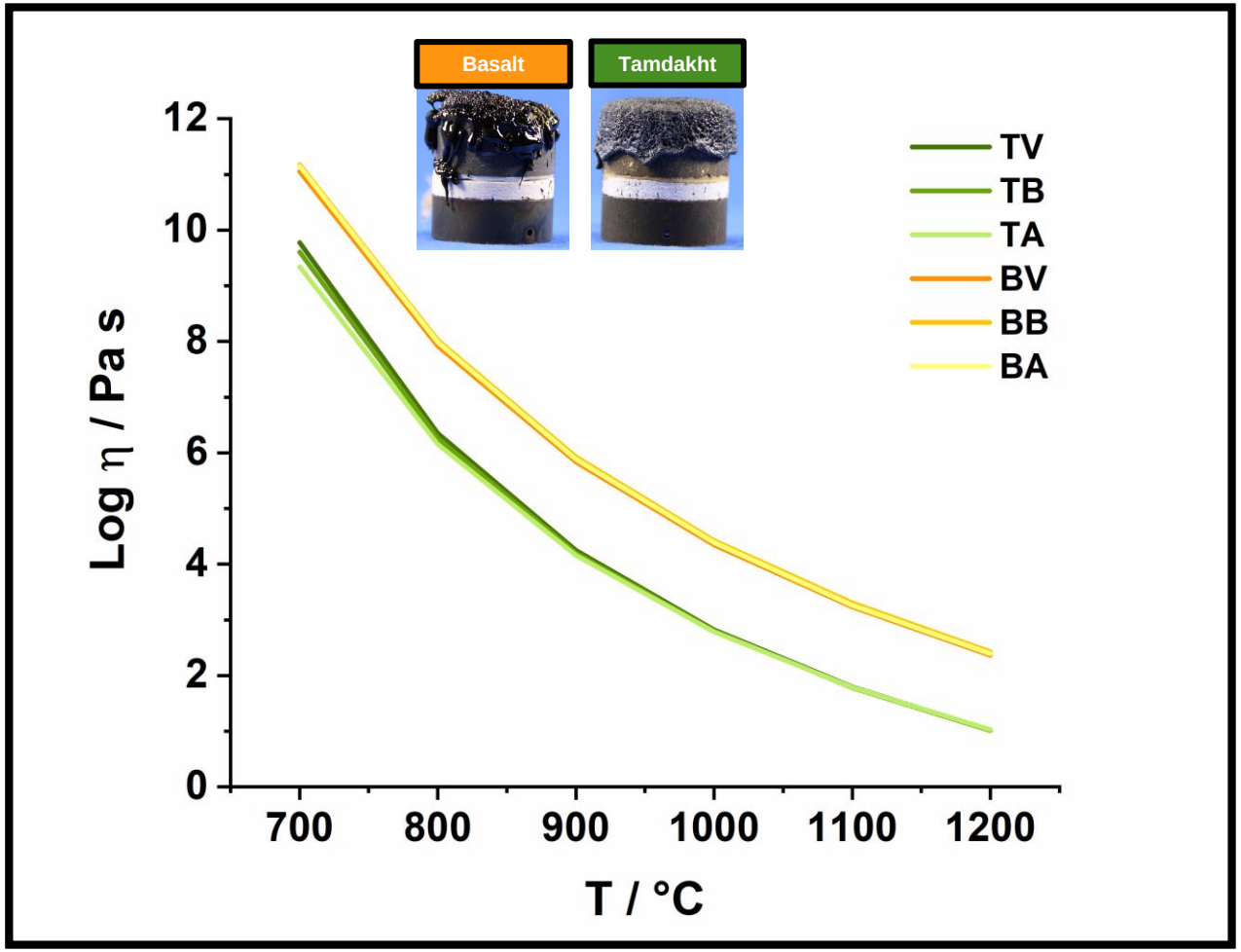

Melt Viscosity Calculated Using Giordano Melt Model

Giordano, D., Earth Planet. Sci. Lett. (2008)

OH Emission

Emission Data

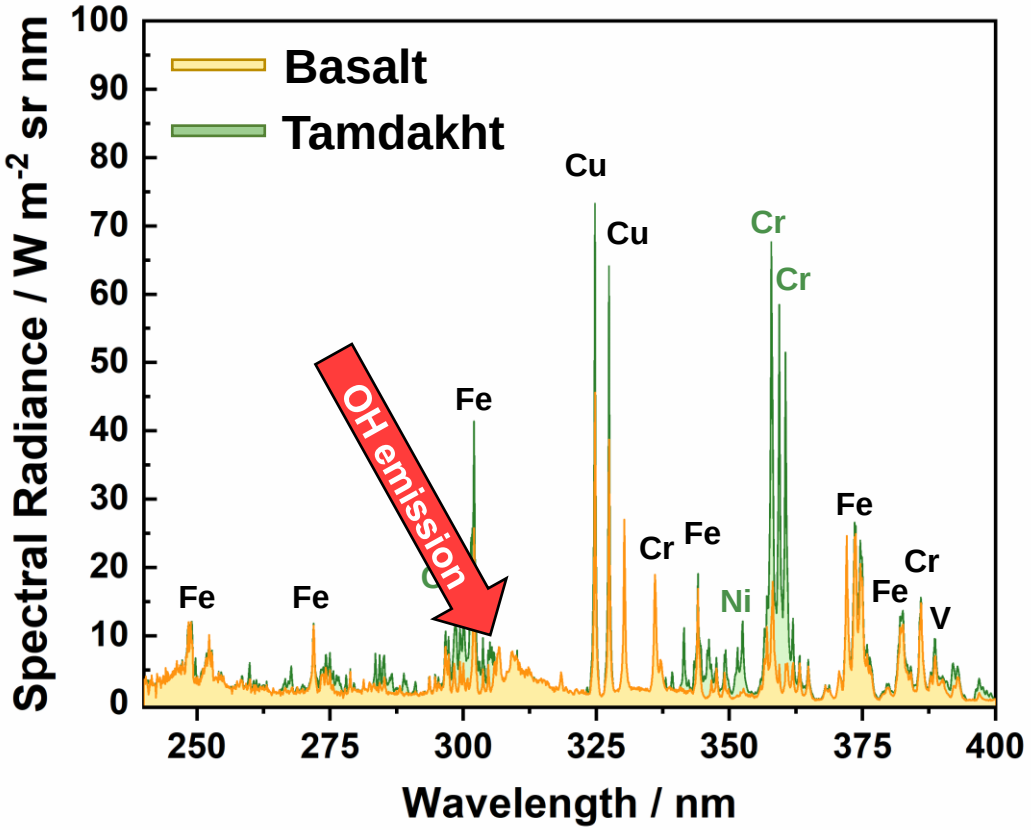

- **Emission band heads near 306.7 nm and 308.9 nm indicate the presence of OH in the post-shock region of basalt.**
- **Emission bands for OH are not present in Tamdakht.**

Melt Viscosity

1. Total water content in the Columbia River Basalt Group can be as high as 1-2 wt.%.

2. Water is a network modifier and has a significant influence on the melt viscosity.

3. Melt viscosities converge to the same value at high temperature.

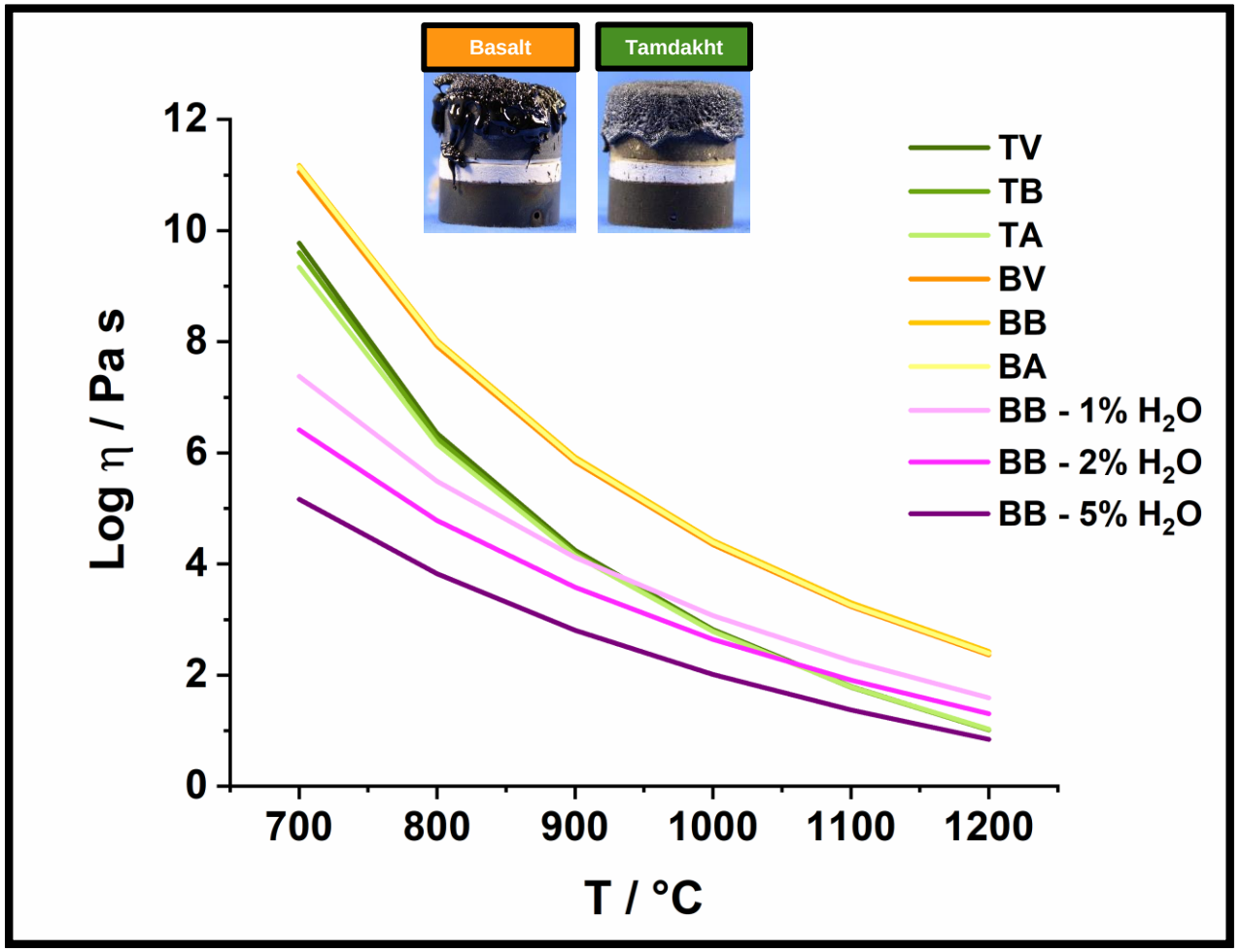

Melt Viscosity Calculated Using Giordano Melt Model

Giordano, D., Earth Planet. Sci. Lett. (2008)

Meteor Ablation Mechanisms

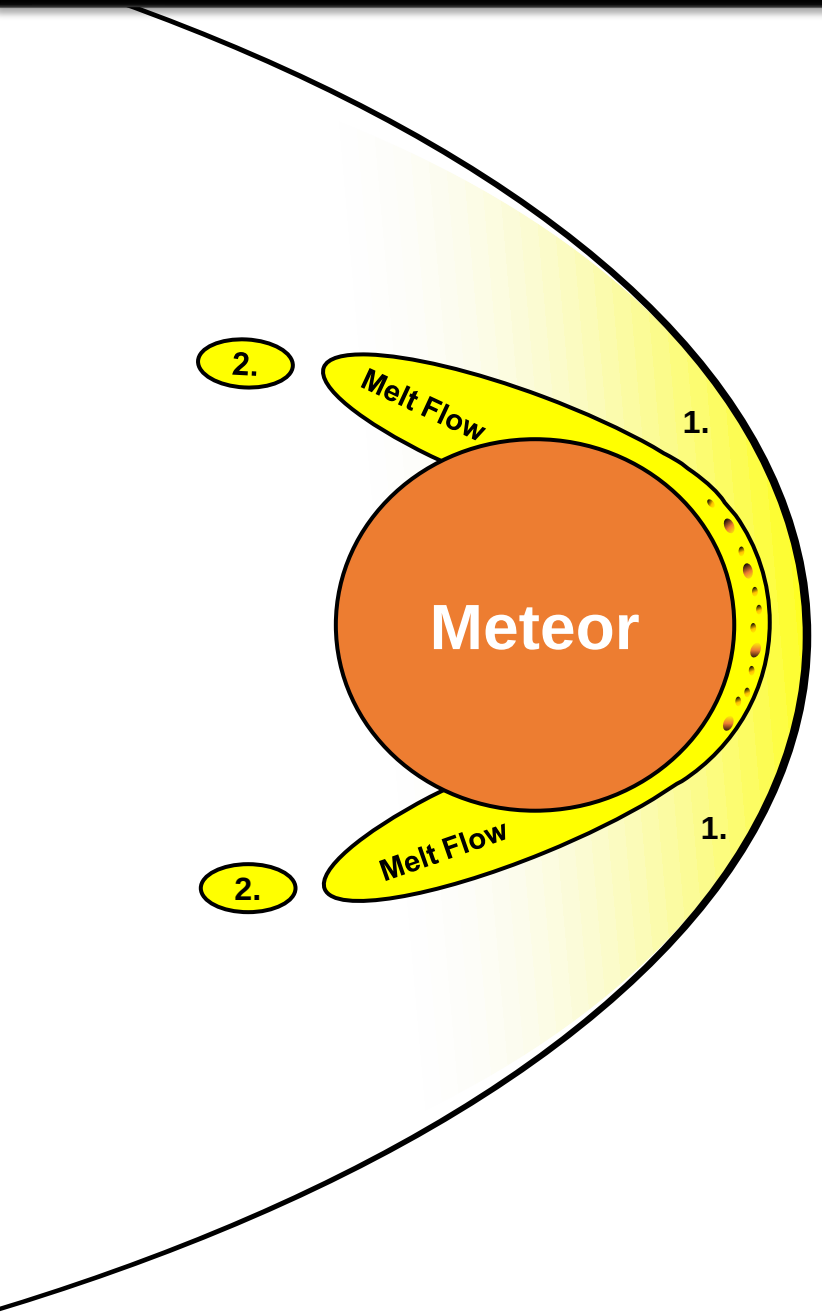

1. Vaporization

2. Melt Flow Spray

- **Melt models predict higher melt viscosities for basalt unless water is present.**
- **The viscosities of both materials converge to the same value as the temperature increases.**

3. Fracture and Spallation

Thermal Spallation Mechanisms of Brittle Materials

Surface of Brittle Material

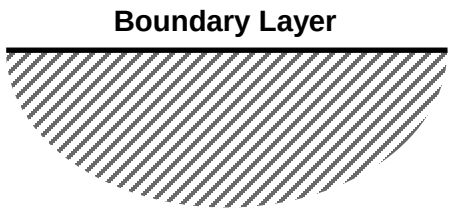

1.

Thermal Spallation Mechanisms of Brittle Materials

Surface of Brittle Material

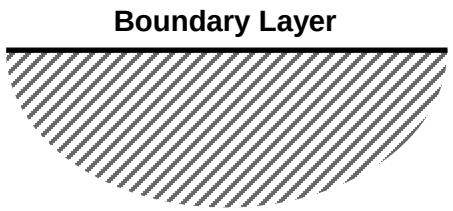

1.

Thermal Load Applied to Surface

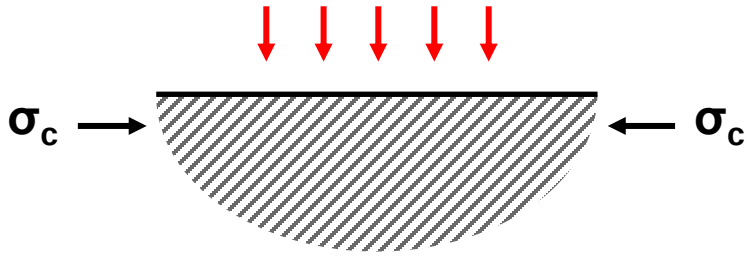

2.

Thermal Spallation Mechanisms of Brittle Materials

Surface of Brittle Material

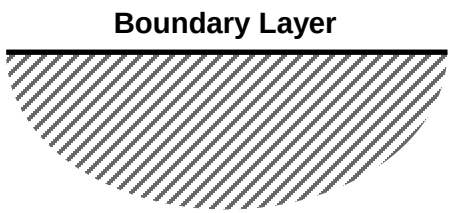

1.

Thermal Load Applied to Surface

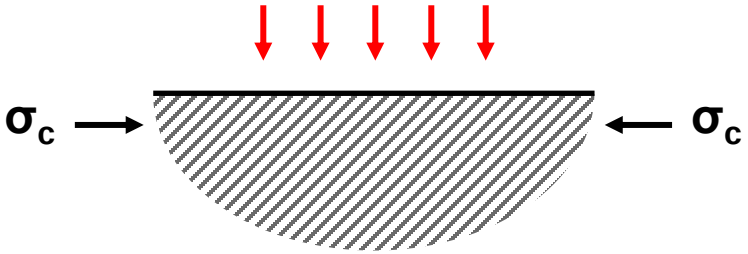

2.

In-Plane Crack Formation

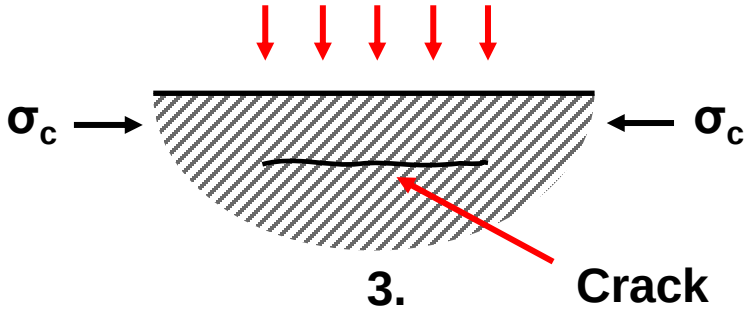

3.

Thermal Spallation Mechanisms of Brittle Materials

Surface of Brittle Material

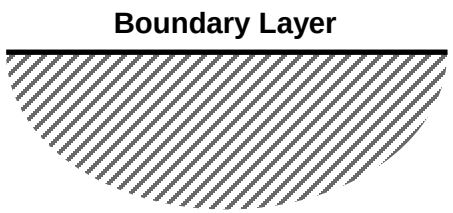

1.

Thermal Load Applied to Surface

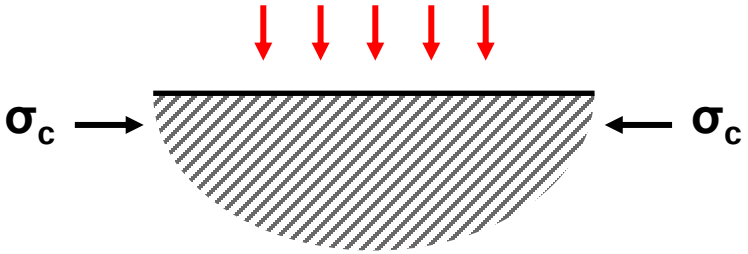

2.

In-Plane Crack Formation

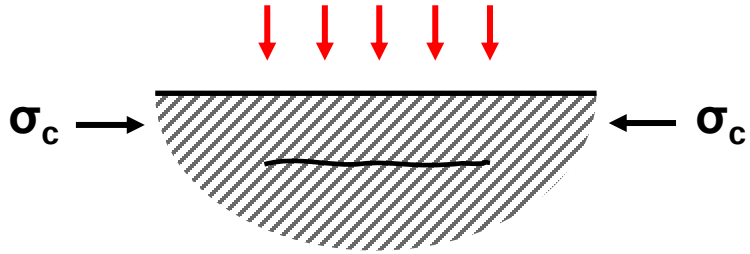

3.

Buckling & Void Formation

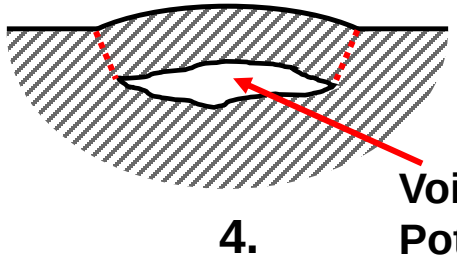

4.

Void Formation & Potential Pore Pressure Increase From Volatile Species

Thermal Spallation Mechanisms of Brittle Materials

Surface of Brittle Material

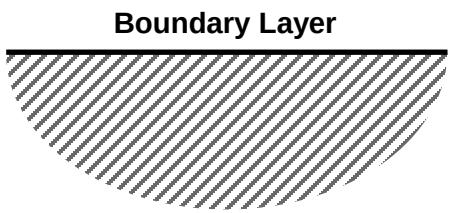

1.

Thermal Load Applied to Surface

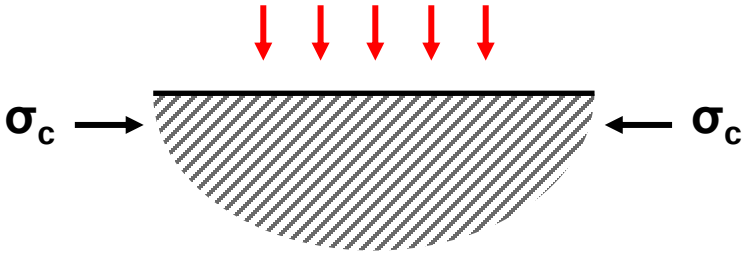

2.

In-Plane Crack Formation

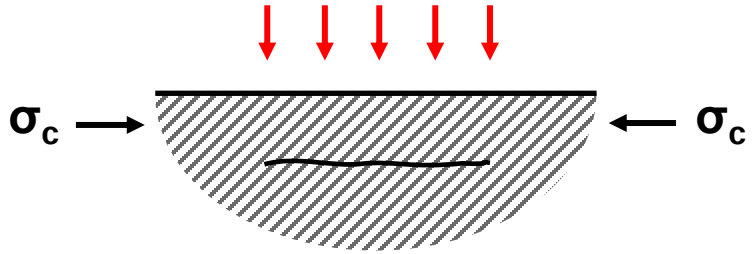

3.

Buckling & Void Formation

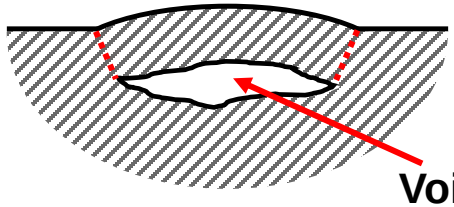

4.

Void Formation & Potential Pore Pressure Increase From Volatile Species.

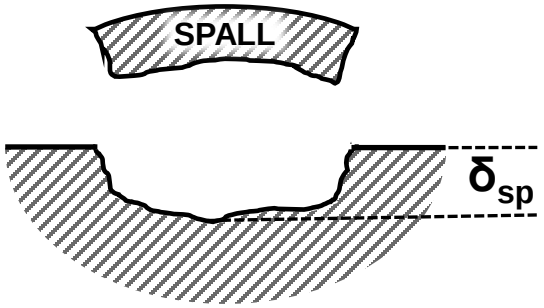

5.

The spall thickness (δ_{sp}) is inversely proportional to the heating rate (Q_w).

Thermal Spallation Mechanisms of Brittle Materials

Surface of Brittle Material

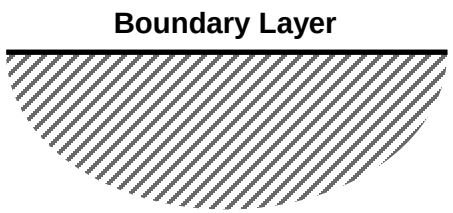

1.

Thermal Load Applied to Surface

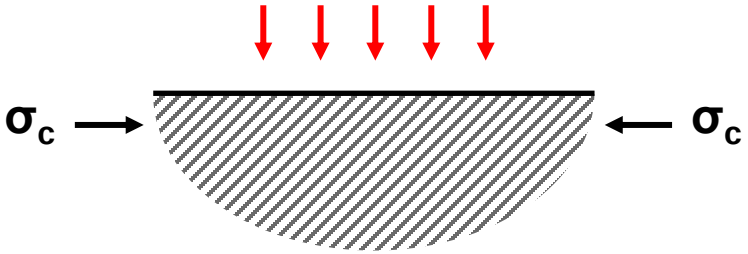

2.

In-Plane Crack Formation

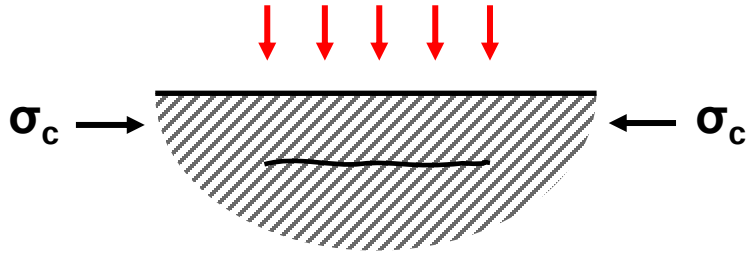

3.

Buckling & Void Formation

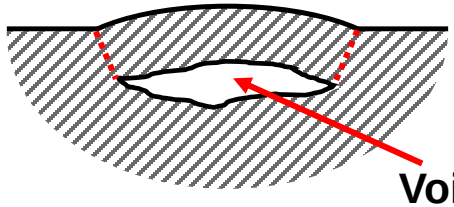

4.

Void Formation & Potential Pore Pressure Increase From Volatile Species.

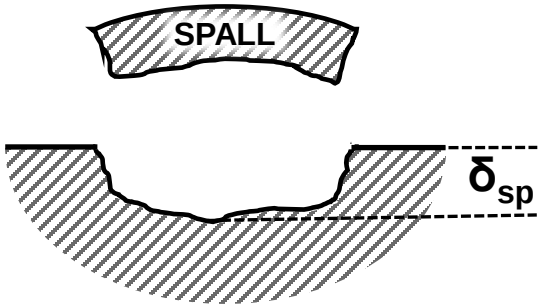

5.

$$\Delta T_s = \frac{(1-\nu)\,\sigma_c}{\beta_r\, E}$$

Thermal Spallation of Basalt and Tamdakht

- Dashed line of T_s is the average surface temperature of basalt and Tamdakht observed during B1 and T1.
- T_m = temperature at which the surface is covered in melt as evidenced by facility video.
- Basalt curves represent a range of surface temperatures required to observed spallation as a function of compressive strength and the upper and lower bounds of moduli.
- Tamdakht curves represent a range of surface temperatures required to observed spallation as a function of compressive strength and the upper and lower bounds of linear thermal expansion coefficients of olivine (Ol) and orthopyroxene (Opx).

$$\Delta T_s = \frac{(1-\nu)\,\sigma_c}{\beta_r\, E}$$

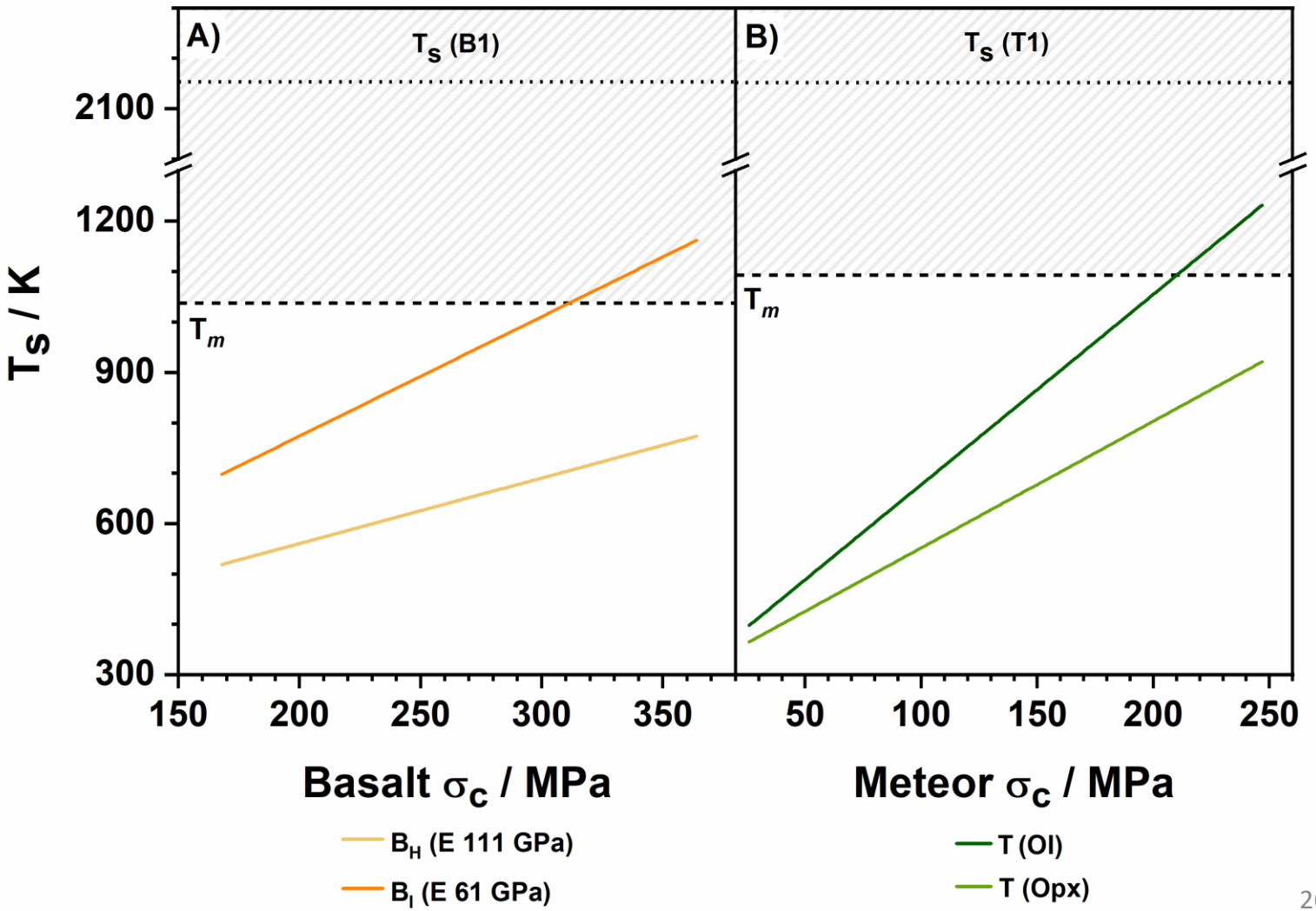

Basalt – Spallation

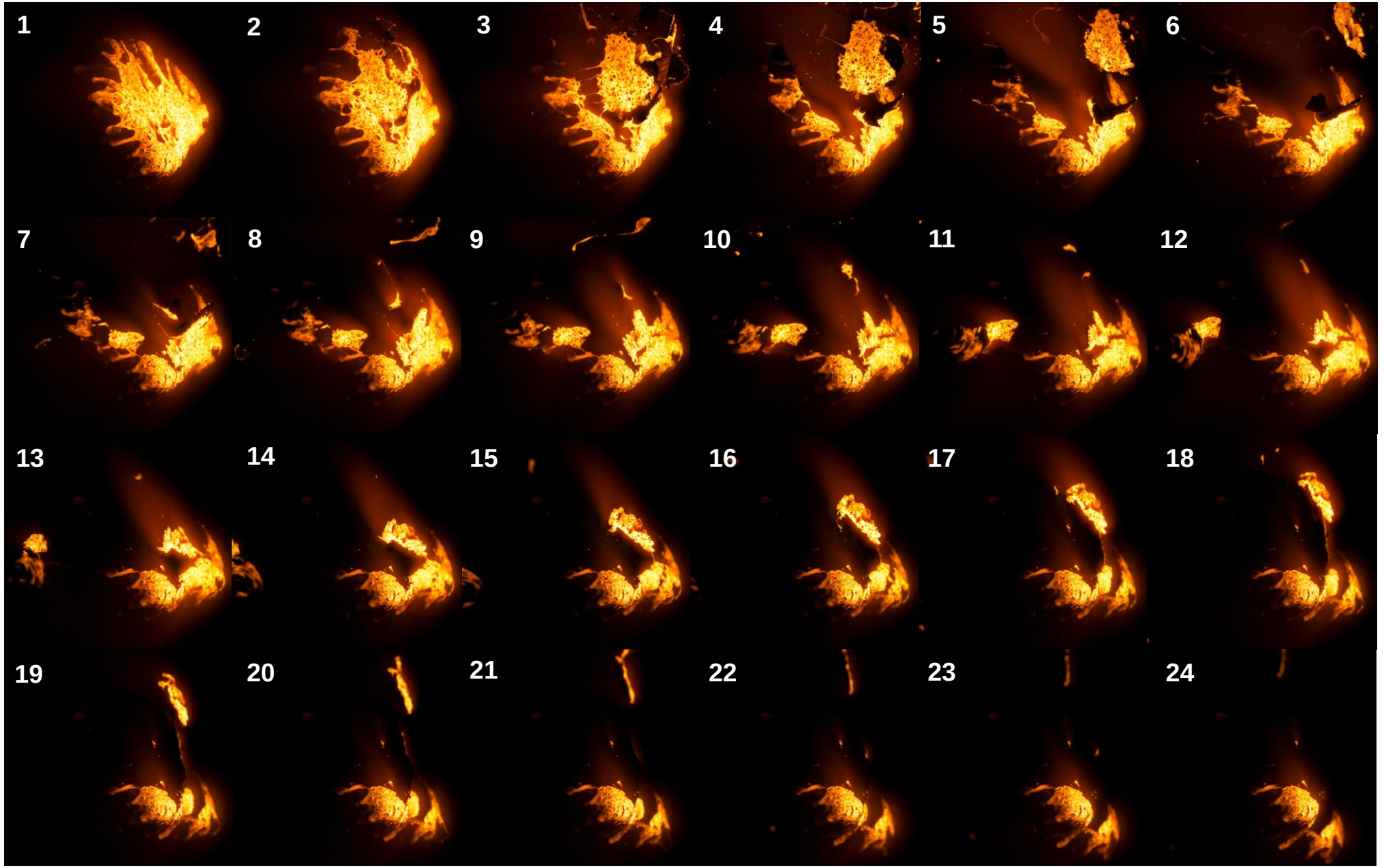

Flow

Basalt - Secondary Minerals

- Analysis of basalt samples indicates the presence of secondary minerals.
- A) Reflected light microscopy image of secondary mineral.
- B) Plane polarized light image of secondary mineral indicating thin needles radiating from a central mass which is indicative of clay minerals.
- C) SEM image highlighting cracks at the interface between the secondary mineral and bulk.
- D) EDS line scan indicating primary elements present over the dashed line in image C.

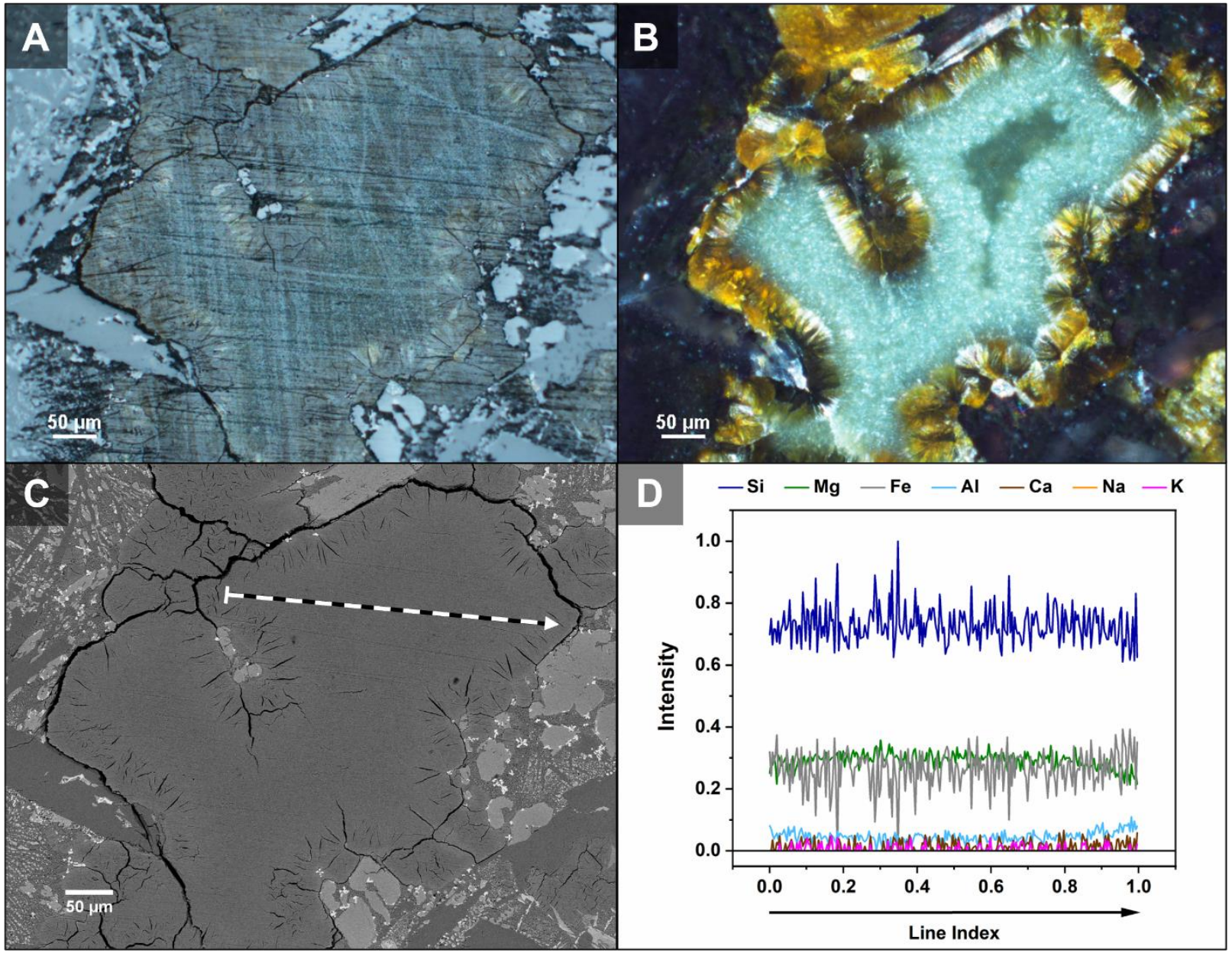

Basalt – Mineral Identity

- Raman spectrum shows features that help identify and distinguish mineral morphologies.
- Water and hydroxyl groups are present.
- Primary band located at 664 cm^{-1} indicates that the mineral is trioctahedral.

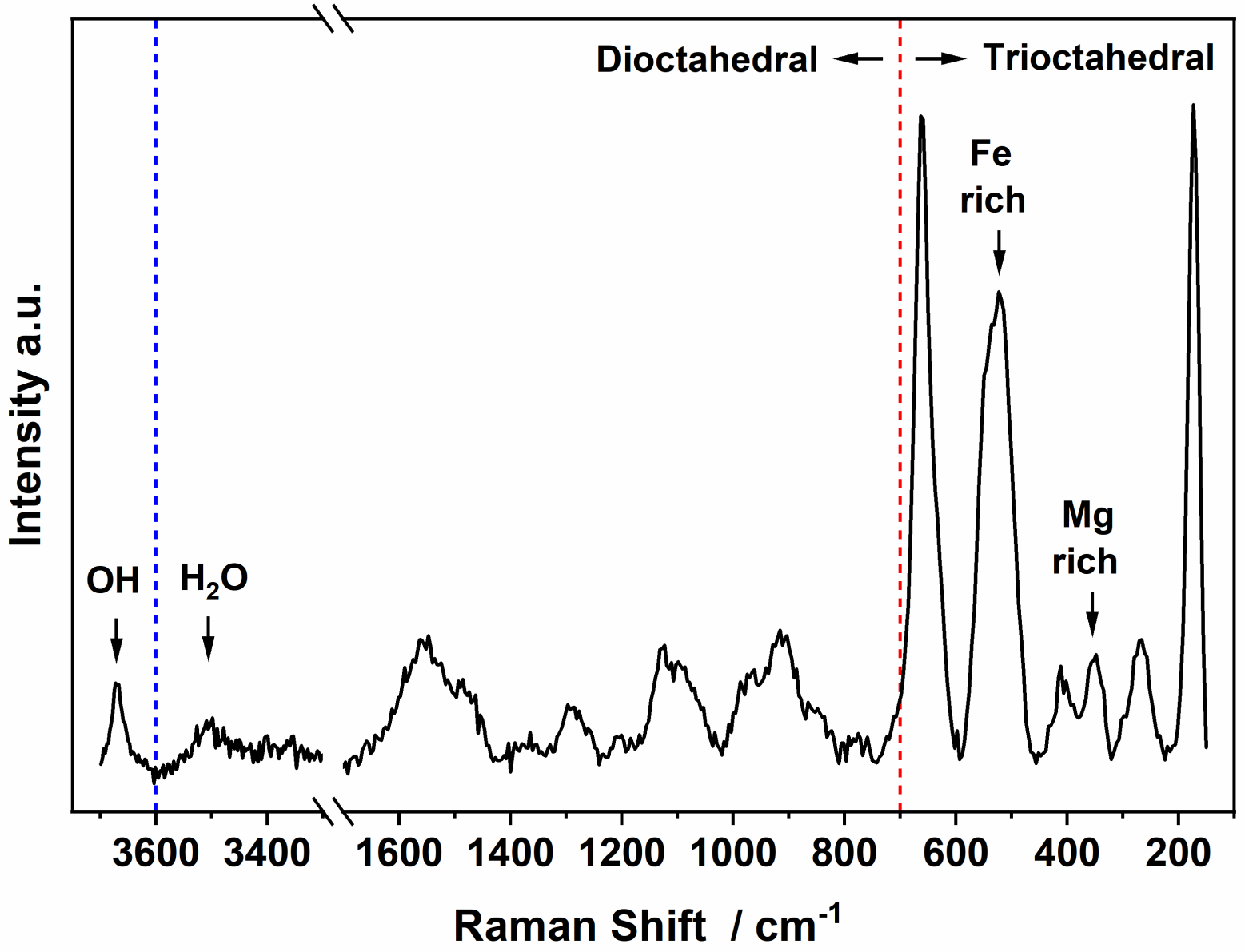

Basalt – Thermal Decomposition

- TGA of basalt and Tamdakht show a lower temperature peak which is associated with the loss of adsorbed water.

- TGA of basalt shows additional peaks at higher temperatures associated with the loss of coordinated water that exists in the interlayer spaces of the clay structure and water that forms during dehydroxylation of the clay.

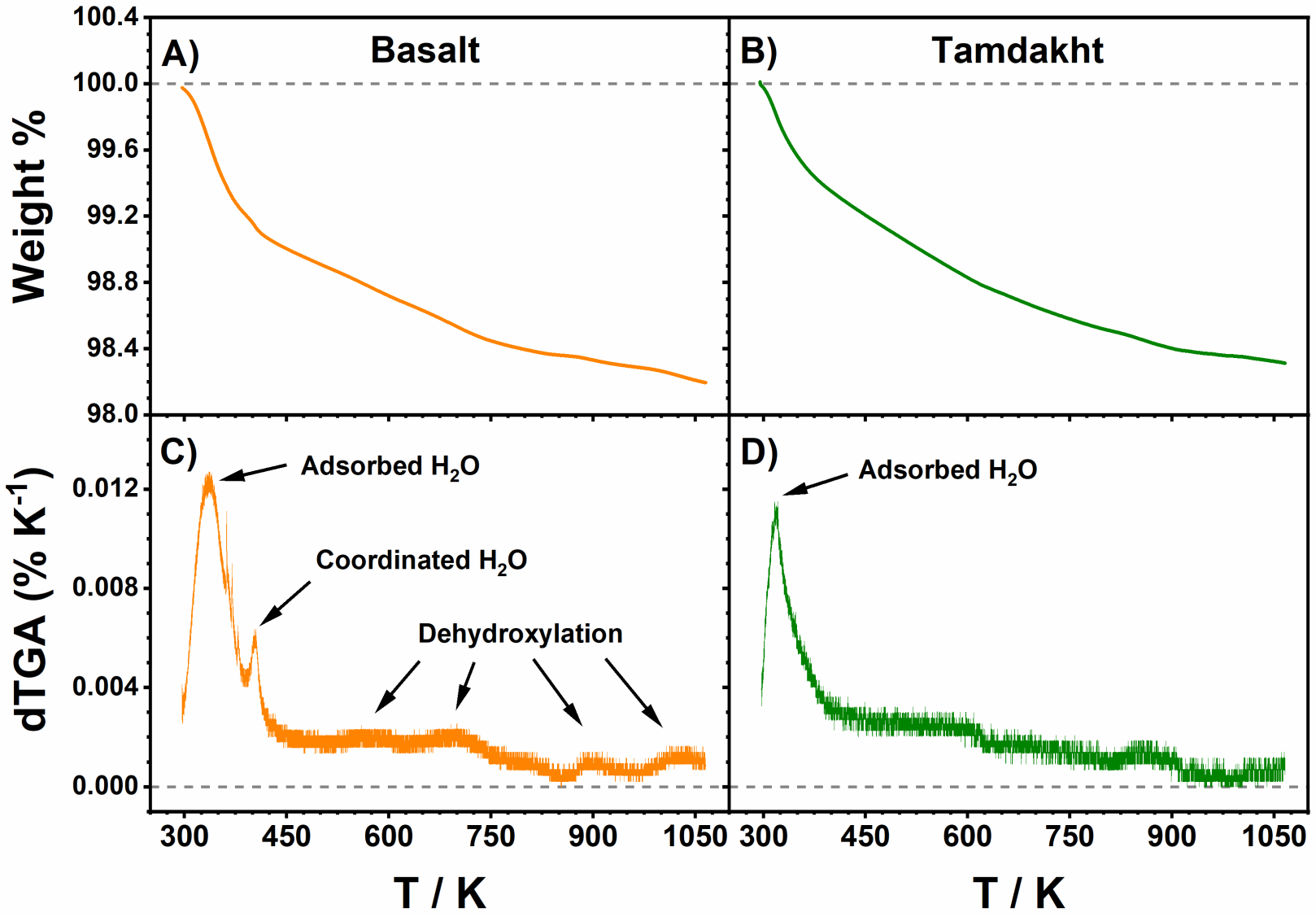

Fracture Mechanism / Basalt

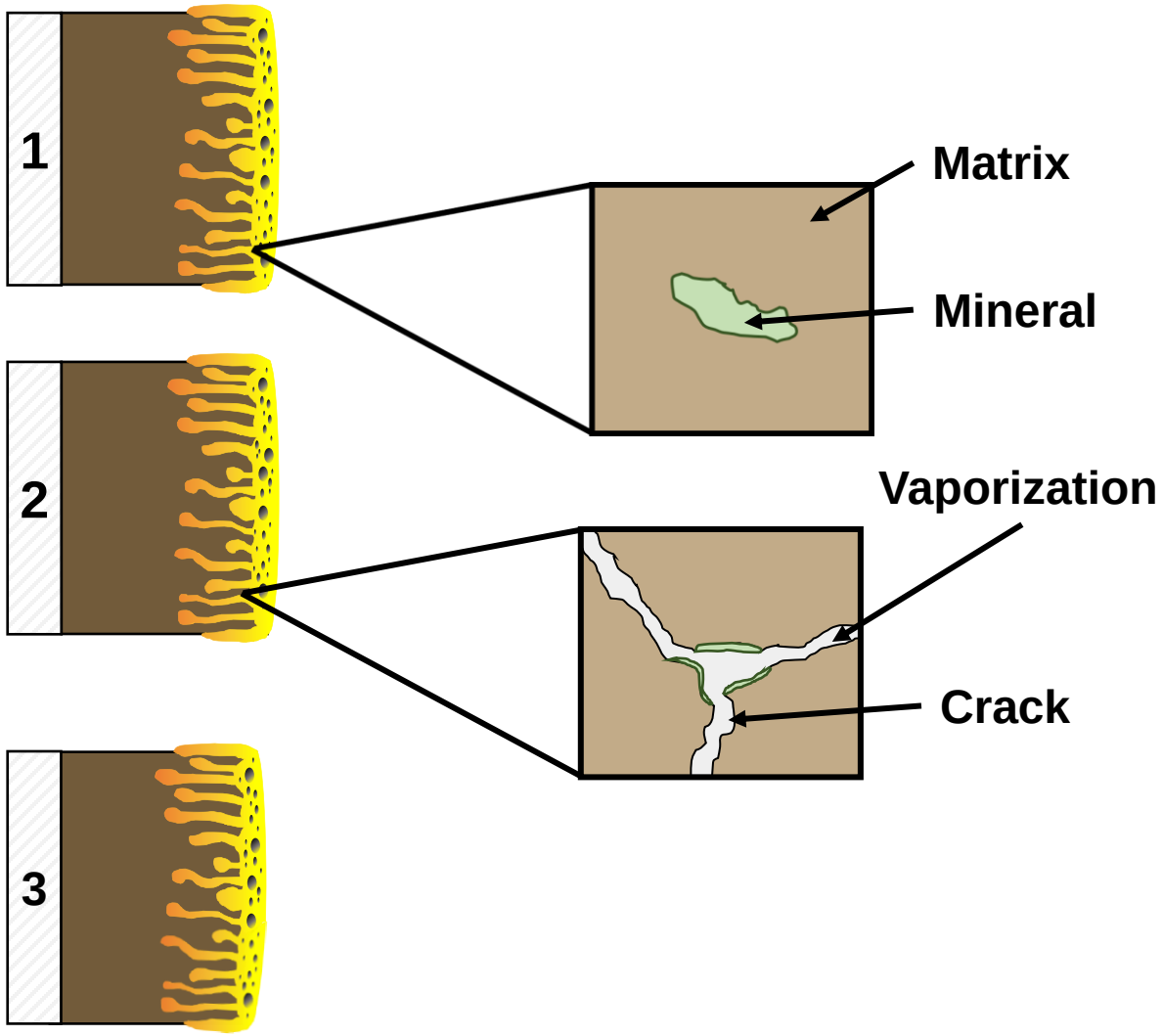

1) Basalt from the Columbia River Group likely contains hydrated minerals and inclusions.

2) Hydrated minerals decompose to yield water vapor which fills adjacent voids cracks.

3) Large sections of the sample are lost to the flow due to mechanical action from subsurface water vapor and shear at the edge of the sample.

Conclusions

Tamdakht

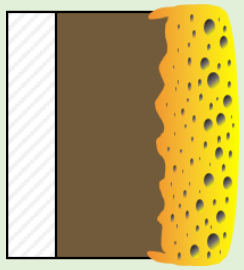

- Ablation is dominated by vaporization.
- Recession rates are lower than basalt.
- Mass loss 6.5x lower than basalt.
- Viscous melt forms a flange at the edge of the sample and loss of mass via melt spray is low.

Basalt

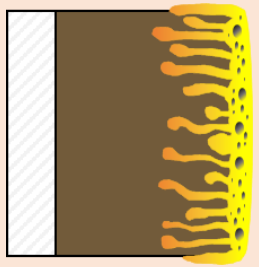

- Ablation mechanisms are driven by the presence of water.
- Mass is lost through separation of a tenuous melt.
- Mass loss is dominated by the separation of large sections of the surface through fracture and shear.

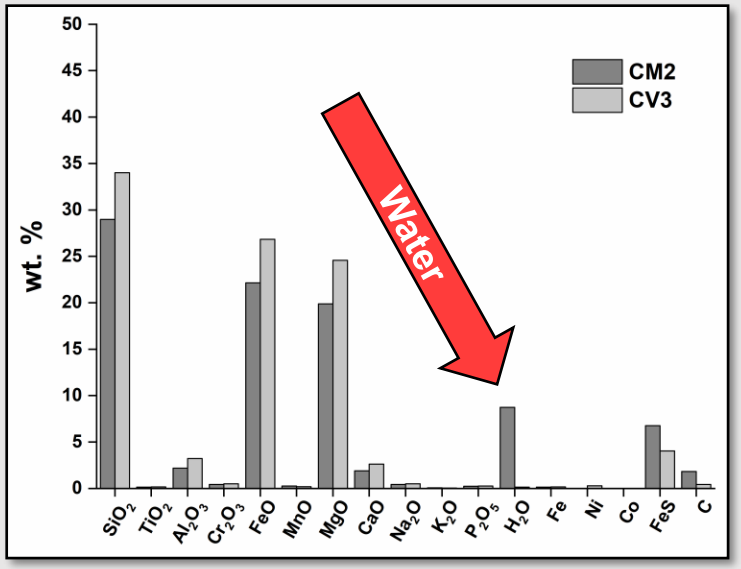

Future Testing

- Basalt is inexpensive but is it a relevant analog?
- The composition of carbonaceous meteorite material is similar to ordinary chondrites (e.g., Tamdakht).
- However, the concentration of water is much higher in carbonaceous chondrites.
- Are the ablation mechanisms of carbonaceous chondrites comparable to basalt?

Carbonaceous Chondrite Simulants

The Meteoritical Society

Meteoritics & Planetary Science 54, Nr 9, 2067–2082 (2019)
doi: 10.1111/maps.13345

Simulated asteroid materials based on carbonaceous chondrite mineralogies

Daniel T. BRITT[1], Kevin M. CANNON[1*], Kerri DONALDSON HANNA[1,2], Joanna HOGANCAMP[3], Olivier POCH[4], Pierre BECK[4], Dayl MARTIN[5], Jolantha ESCRIG[4], Lydie BONAL[4], and Philip T. METZGER[1,6]

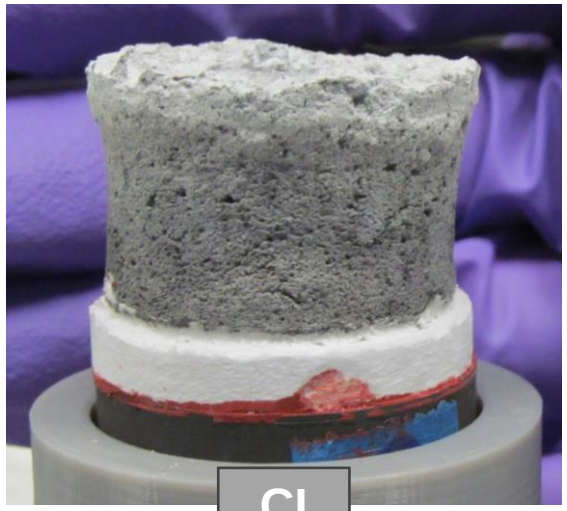

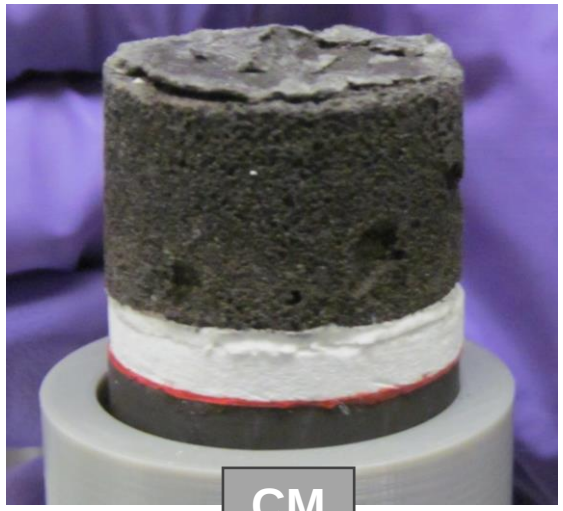

Table 2. Initial simulant recipes used to create prototypes, and suggested updates to the recipes based on analyses of these prototypes. All values in wt%.

Mineral	CI prototype	CI future update	CM prototype	CM future update	CR prototype	CR future update
Mg-serpentine	48.0	51.3	72.5	73.8	9.2	6.8
Epsomite	6.0	–	–	–	–	–
Magnetite	13.5	10.0	10.4	5.0	14.3	2.5
Palygorskite	5.0	5.3	–	–	–	–
Olivine	7.0	7.0	7.8	11.2	33.7	33.1
Pyrite	6.5	7.0	2.6	3.3	4.1	5.8
Vermiculite	9.0	9.6	–	–	–	–
Coal	5.0	5.0	3.6	3.6	2.0	2.0
Pyroxene	–	–	2.1	2.1	31.6	29.6
Siderite	–	–	1.0	1.0	–	–
Iron metal	–	–	–	–	4.6	10.6
Nickel metal	–	–	–	–	0.5	–
Ferrihydrite	–	4.8	–	–	–	–
Amorphous silicate	–	–	–	–	–	9.6

CI

198.1 W cm^{-2} 176.8 W cm^{-2} 145.6 W cm^{-2} 108.4 W cm^{-2} 72.6 W cm^{-2}

CM

209.5 W cm^{-2} 179.4 W cm^{-2} 146.1 W cm^{-2} 111.5 W cm^{-2} 72.0 W cm^{-2}

What is PICA – NuSil?

PICA

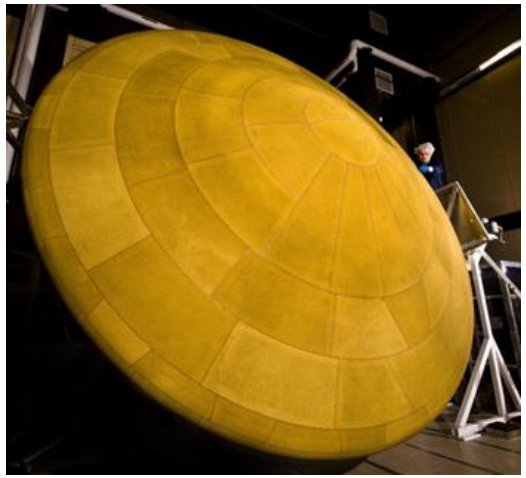

Siloxane Copolymer Backbone

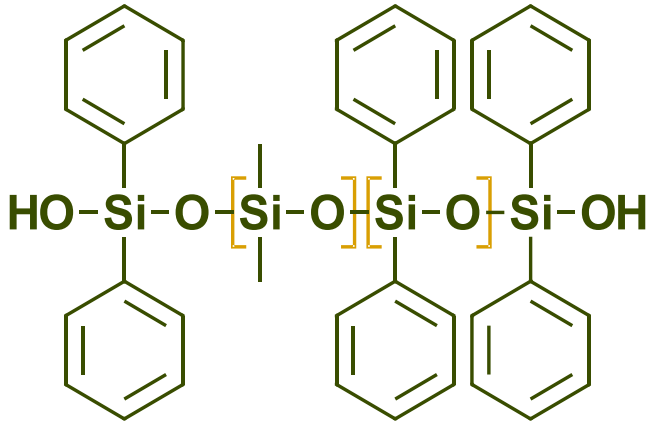

m = 0.95 ; n = 0.05

Oxime Crosslinking Agent

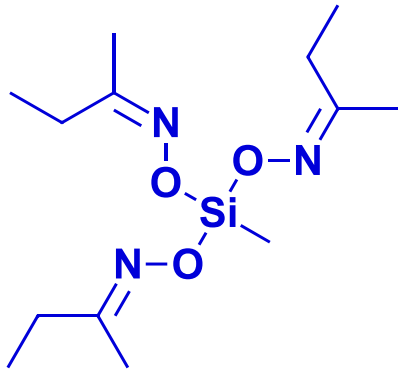

MEKO

- **The phenolic phase of PICA is friable.**
- **A thin coating of NuSil (CV-1144-0) is applied to the surface of flight hardware to mitigate particulate shedding during pre-flight activities.**
- **Does NuSil have an impact on the performance of PICA during arc-jet testing?**

Coating Process Terminology

General Application Process

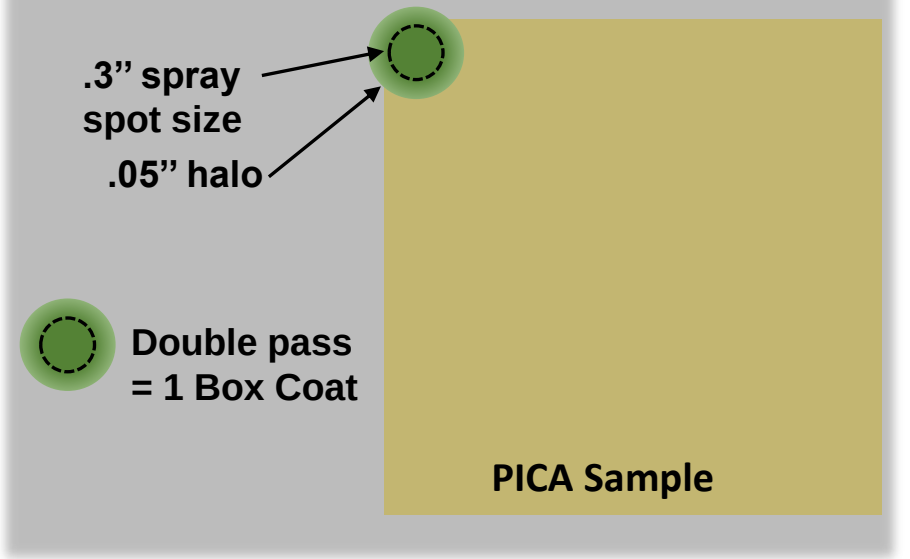

Application of NuSil to PICA Mini-Sprite

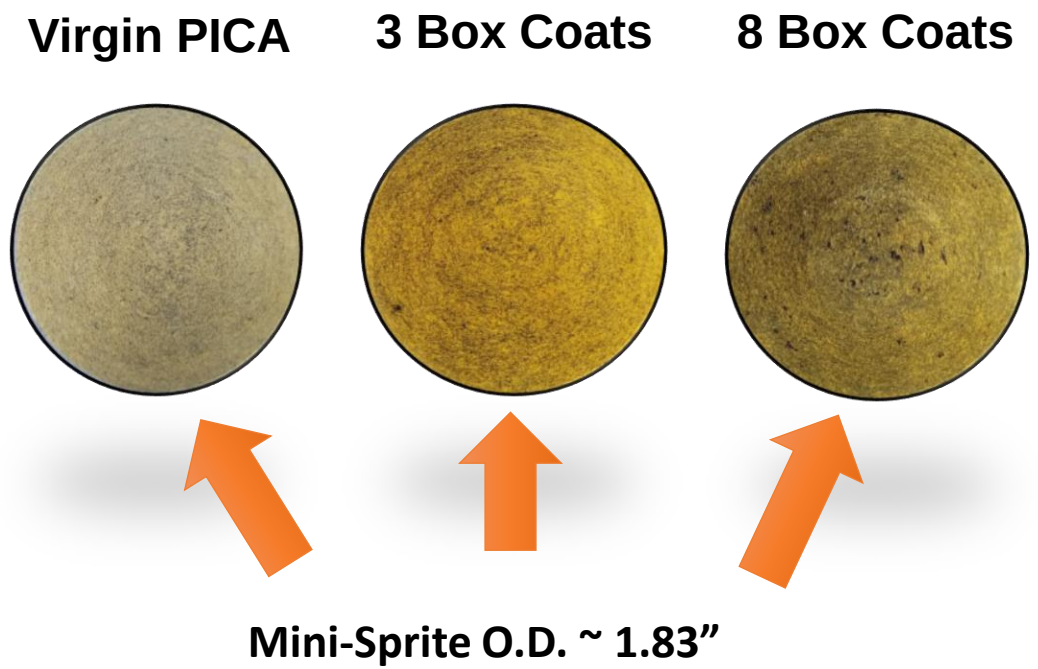

Flight Hardware ≤ 1.5 Box Coats

Polysiloxane Resin Structure

Siloxane Copolymer Backbone

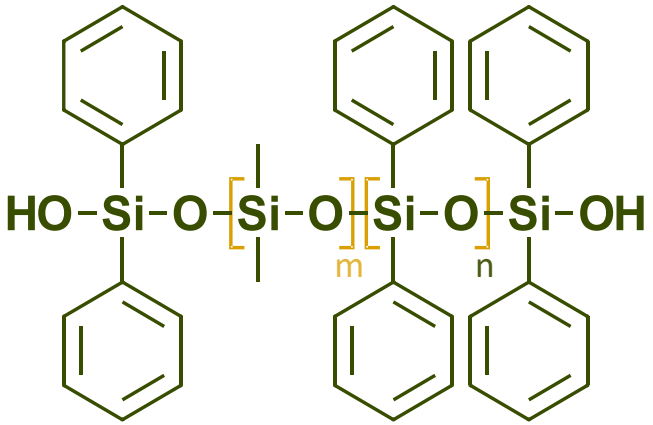

m = 0.95 ; n = 0.05

Oxime Crosslinking Agent

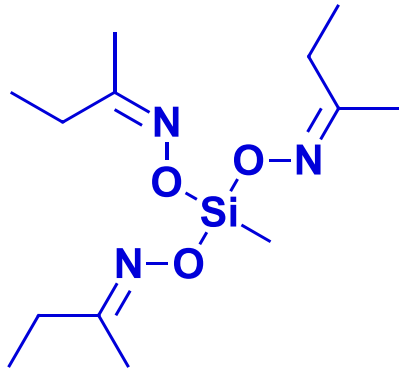

Molecular Structure / NuSil

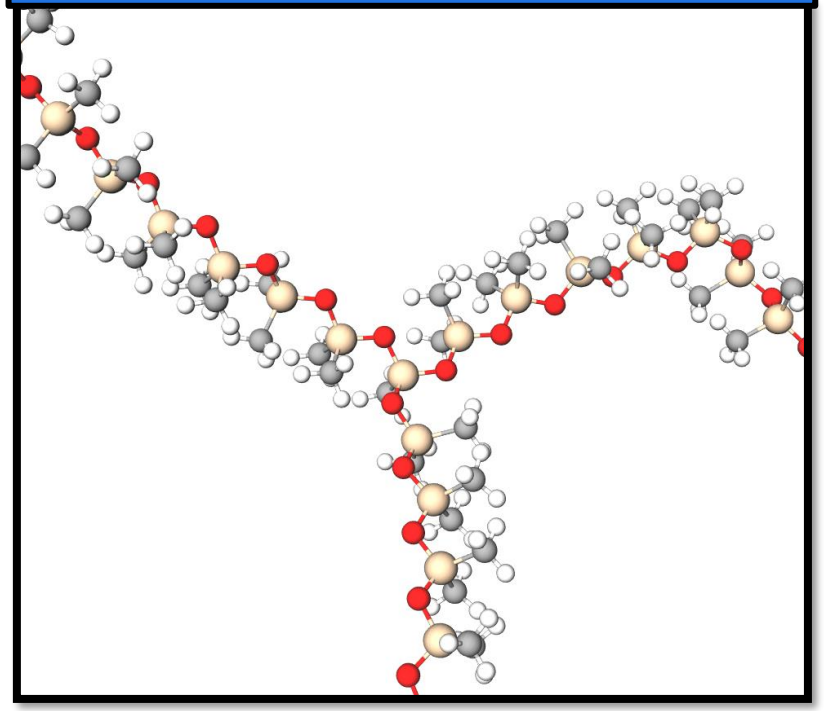

- **The main constituent of NuSil is a siloxane copolymer with monomer units that are functionalized with phenyl and methyl groups. (~ 974 monomer units / polymer chain)**
- **The end of the polymer chain is functionalized with hydroxyl groups.**
- **NuSil contains an oxime crosslinking agent (5 – 10 wt. %) that reacts with pendant hydroxyl groups when exposed to atmospheric moisture.**
- **The crosslinking agent influences the material properties of NuSil (e.g., thermal stability, mechanical, etc).**

Polysiloxane Resin Curing Process

1B) Crosslinking compounds react with hydroxyl functional units of phenolic resin.

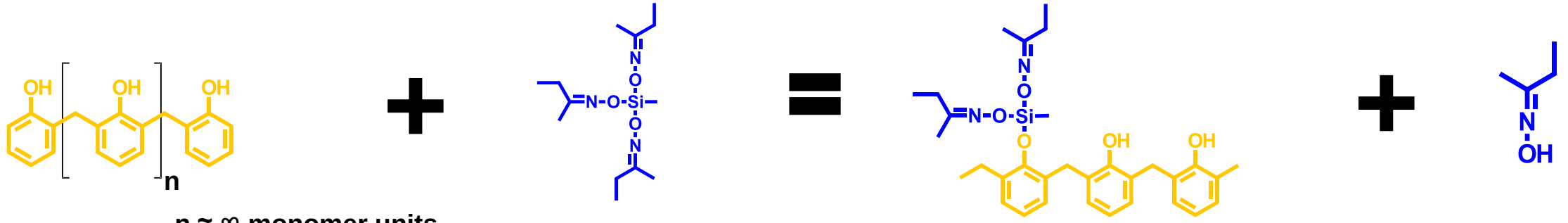

n ≈ ∞ monomer units

2B) Crosslinking compounds react with water.

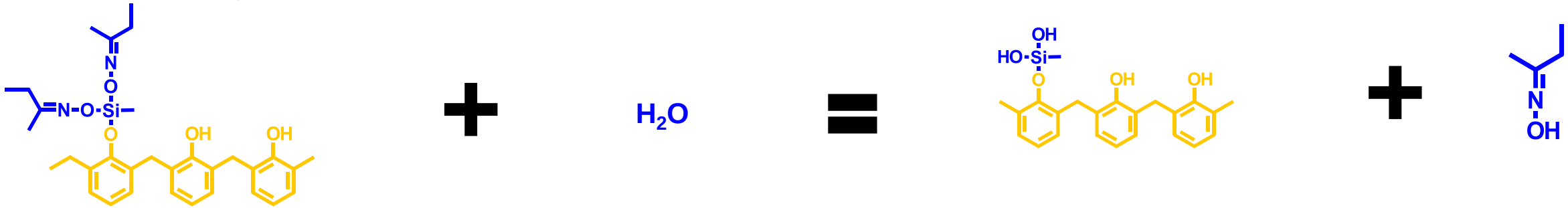

3B) Crosslinking compounds react with hydroxyl functional units of phenolic resin.

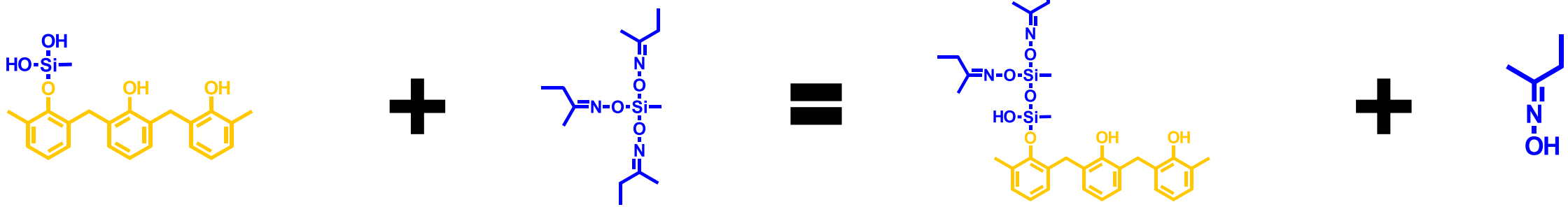

Polysiloxane Curing Process

1B) Crosslinking compounds react with hydroxyl functional units of phenolic resin.

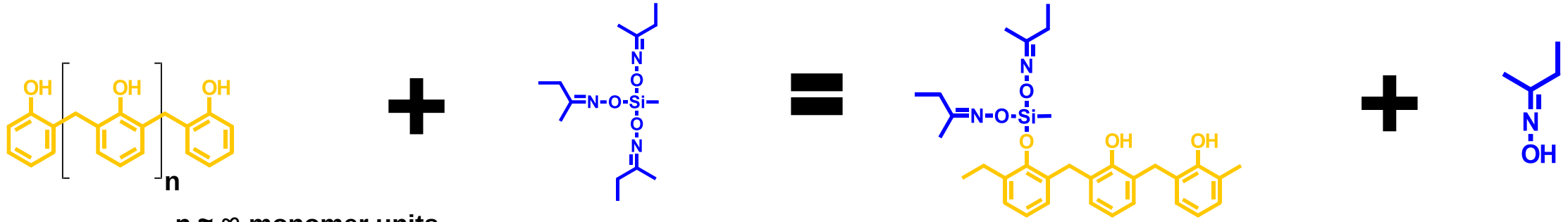

n ≈ ∞ monomer units

- 5 wt. % oxime mixed with naphtha.
- 2 mm. dia. rod of PICA soaked in solution overnight.
- PICA + oxime cured in open air for 1 week.
- Attenuated Total Reflectance (ATR) spectra reveal a decreased intensity of OH stretch (3000 cm^{-1} – 3550 cm^{-1}).

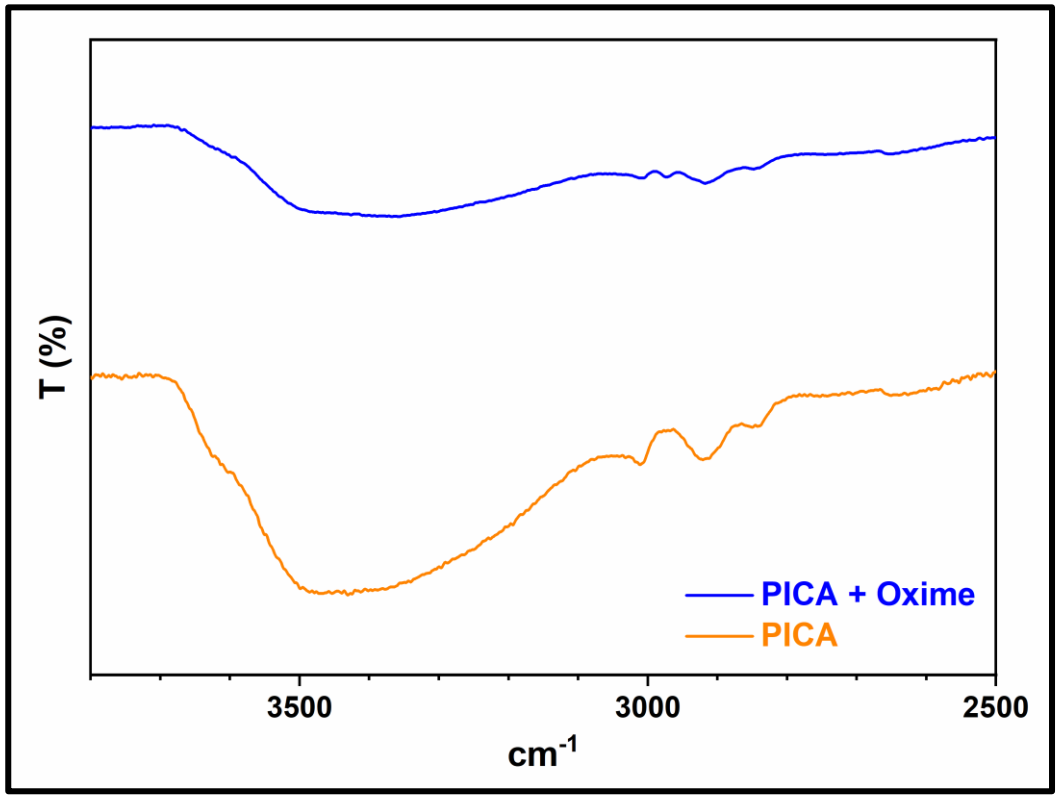

Coating Analysis / FTIR

- **Infrared spectra were collected on PICA and individual components of NuSil.**

A) MEKO - shows a CN stretching mode at 1640 cm^{-1}.

B) NuSil - CN stretching mode from MEKO disappears after NuSil is fully cured.

C) PICA - OH stretch 3700 – 3200 cm^{-1}.

D) PICA + 8 wt. % oxime – bands appear at 1270 cm^{-1} and 1000 cm^{-1} indicating MEKO has reacted with itself to form domains of polysiloxane.

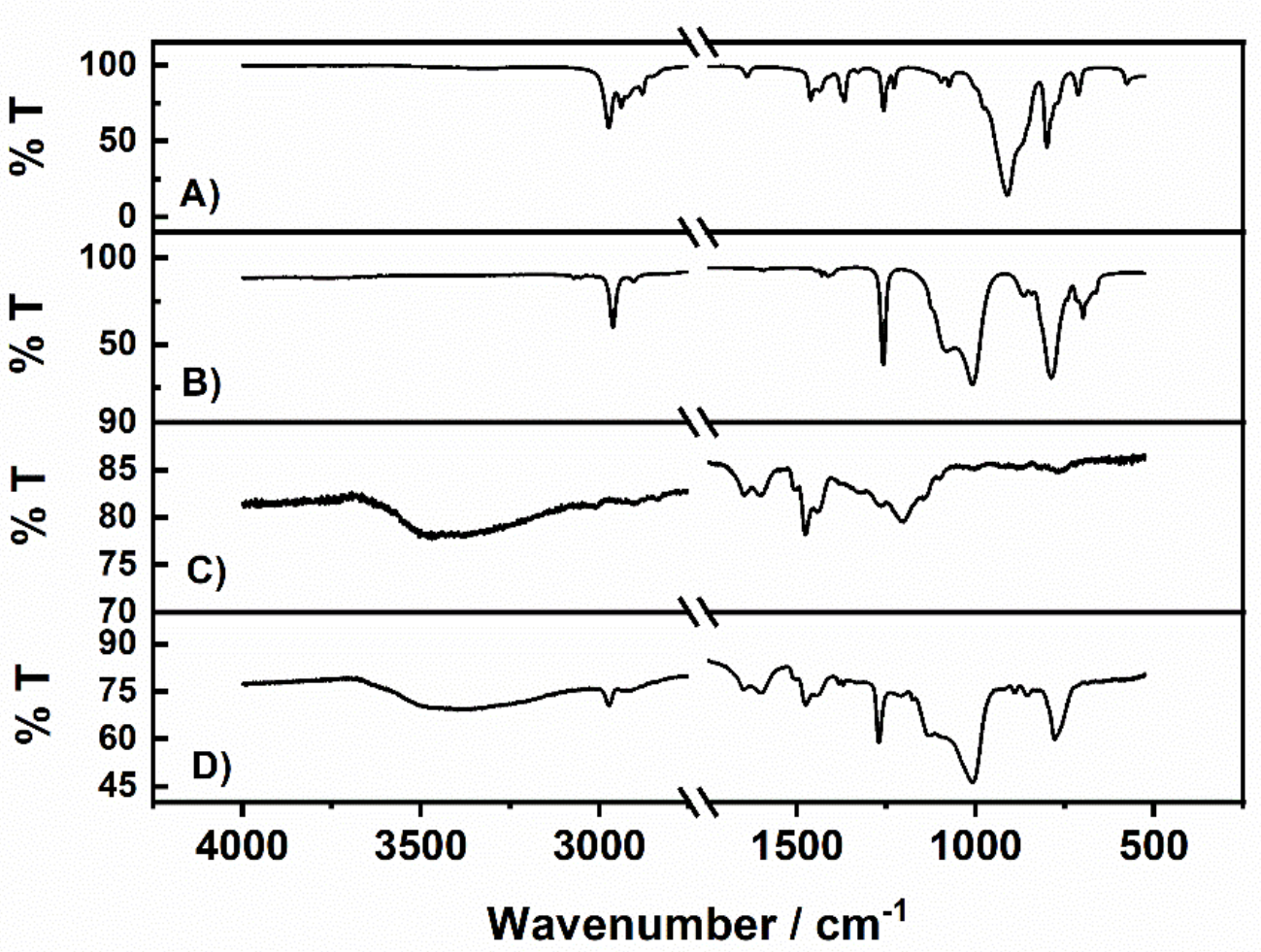

Infrared spectra of: A) methyltris(methylethylketoximino)silane (MEKO), B) cured NuSil® CV-1144-0, C) PICA, and D) PICA cured in a solution of 8 wt. % MEKO and isopropyl alcohol. Infrared spectra of the polymers and molecules in this study do not exhibit absorption data at frequencies between 2700 cm^{-1}–1800 cm^{-1}. Therefore, the spectra have been truncated to illustrate features in the rest of the spectrum in more detail.

PICA – NuSil / Model Architecture

- Sphere-cone geometry was chosen to observe the formation of a viscous melt layer.
- Each model was instrumented with a thermocouple plug to measure the in-depth temperature response.
- Two R-type thermocouples and two K-type thermocouples spaced ~ 5 mm apart.
- 8 sphere-cone models were masked and coated with NuSil.
- Average areal density of NuSil coating ~ 10.0 ± 1.0 mg cm^{-2} (PICA-N).
- One model coated with twice the areal density ~ 19 mg cm^{-2} (PICA-N').

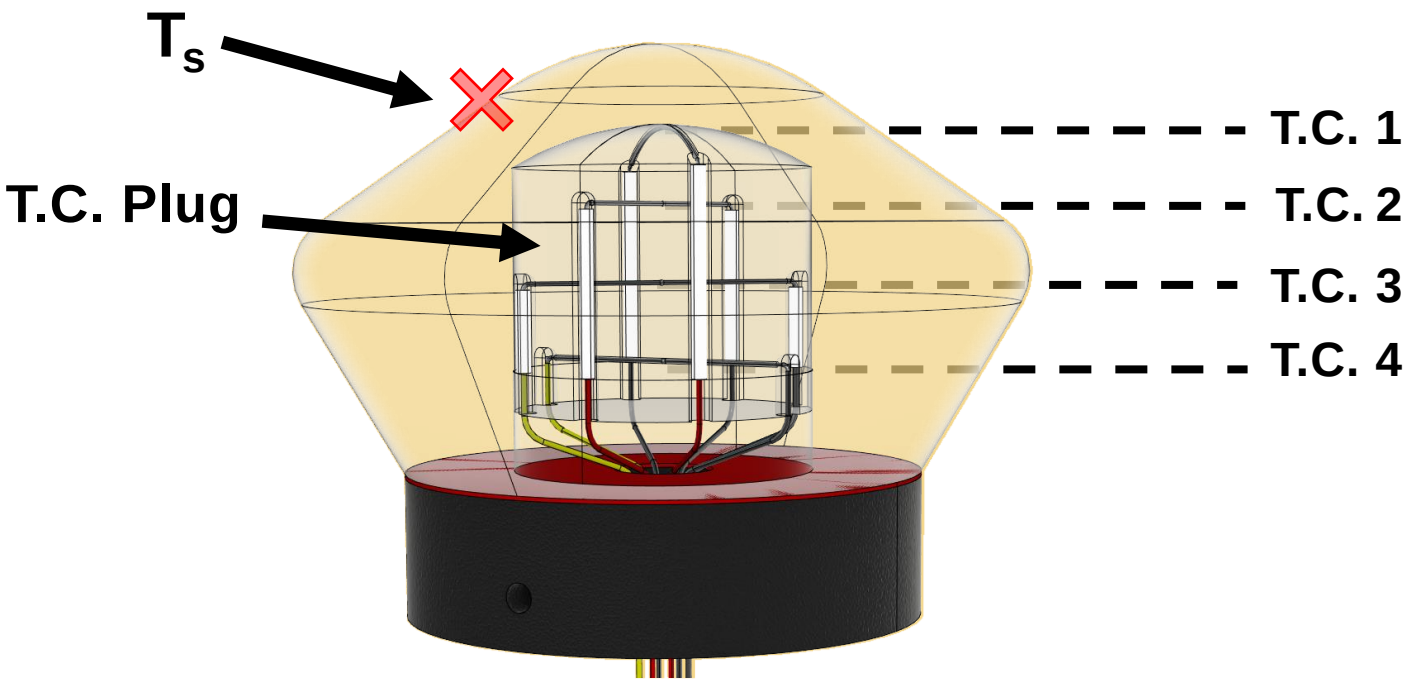

HyMETS / Test Conditions

- A two-color pyrometer was used to measure the surface temperature.
- High-speed cameras were used to observe salient phenomena and measure recession rates.
- A suite of emission spectrometers were used to analyze species in the post-shock region.

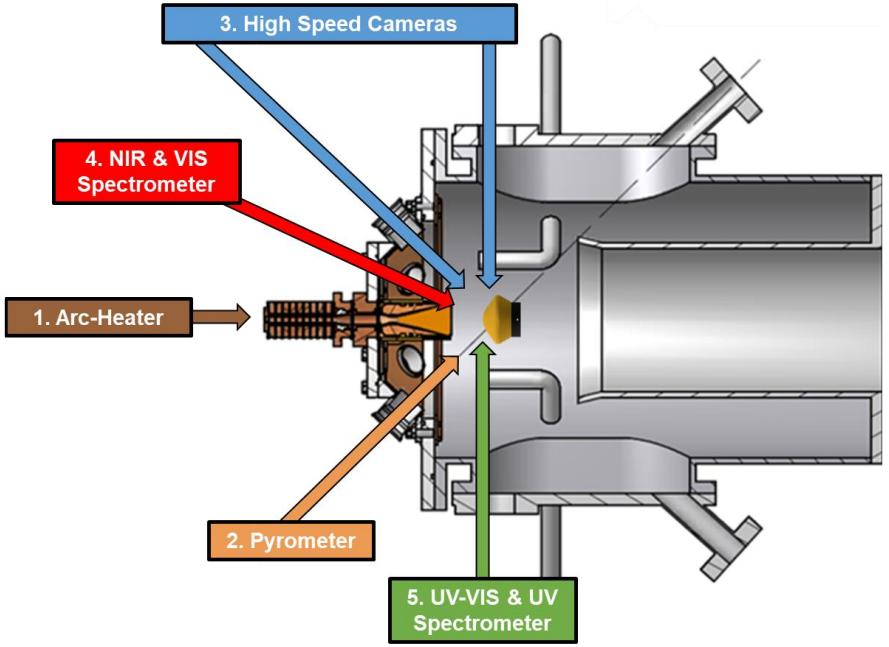

Test Conditions

Test Article	Material	Test Condition	Simulated Atmosphere	Heat Flux (W cm^{-2})	Stagnation Pressure (kPa)	Test Length (s)
PS01	PICA-N′	B	Earth	140	5.6	28
PS02	PICA-N	B	Earth	140	5.6	30
PS03	PICA-N	B	Earth	140	5.6	30
PS04	PICA-N	C	Earth	60	4.1	67
PS05	PICA-N	A	Earth	224	6.6	29
PS06	PICA-N	B	N_2	131	5.3	29
PS07	PICA-N	B	Mars	127	5.2	33
PS08	PICA-N	C	Earth	60	3.9	30
PS09	PICA	B	Earth	140	5.6	30
PS10	PICA	B	N_2	130	5.3	30
PS11	PICA	A	Earth	223	6.6	21
PS12	PICA	B	Mars	126	5.3	31

Flow Composition

Flow Composition		
Earth	Mars	Titan
N_2: 75%	CO_2: 85%	N_2: 95%
O_2: 21%	N_2: 10%	Ar: 5%
Ar: 4%	Ar: 5%	

- Data collected in 3 gas flow compositions (e.g., Air, CO_2, N_2).

PICA-NuSil / Thermal Response

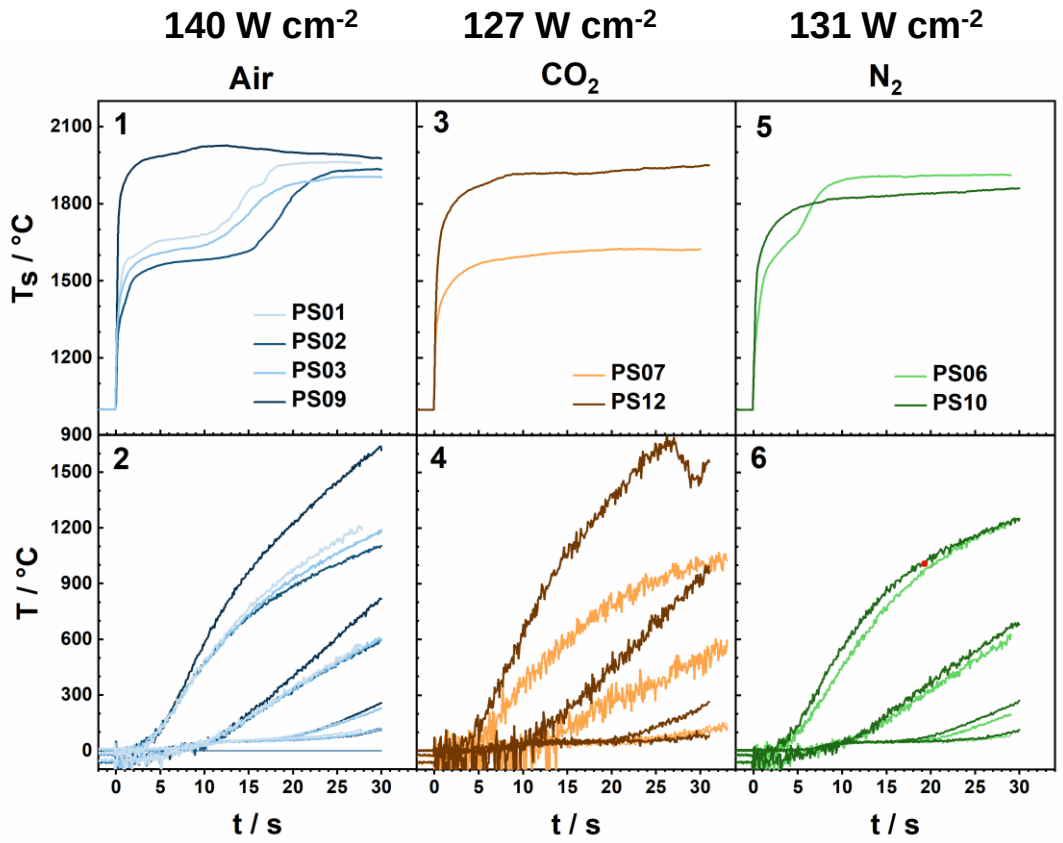

- NuSil lowers the measured surface temperature and in-depth response in oxidizing atmospheres.

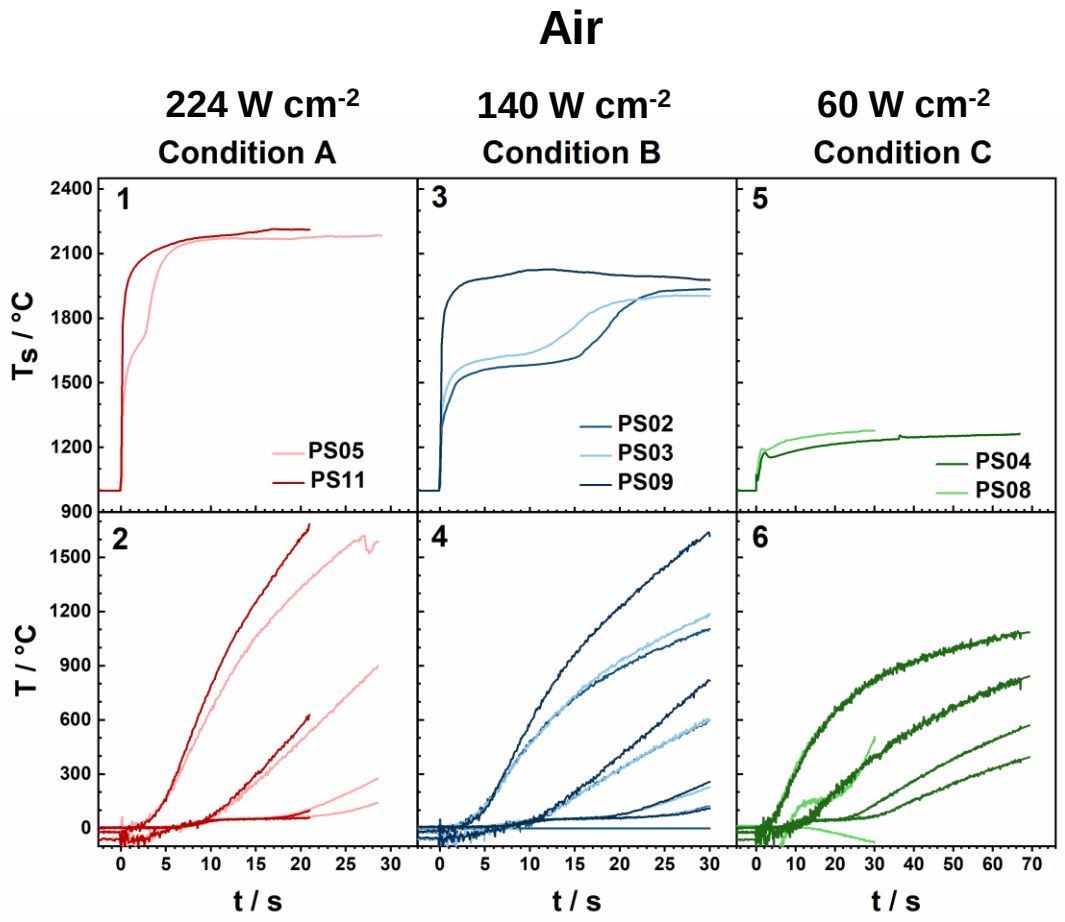

- Survival of the coating increases at lower heating rates.

PICA-NuSil / Post-Test Analysis

Panel figures illustrating changes in morphology, surface temperature, and emission.

Panel A)

- **Emission signal indicates rapid pyrolysis in the stagnation region.**
- **Pyrolysis is followed by a stagnation in emission signal.**
- **Si emission indicates that NuSil decomposes over the course of 2 seconds.**
- **A rise in Ca emission (t = 11s) indicates that FiberForm has been exposed to the reactive flow.**

Panel B)

- **Similar phenomena observed in panel B but on a compressed timescale.**

Panel C)

- **Surface temperature and emission data indicate that the coating is relatively stable in CO_2.**

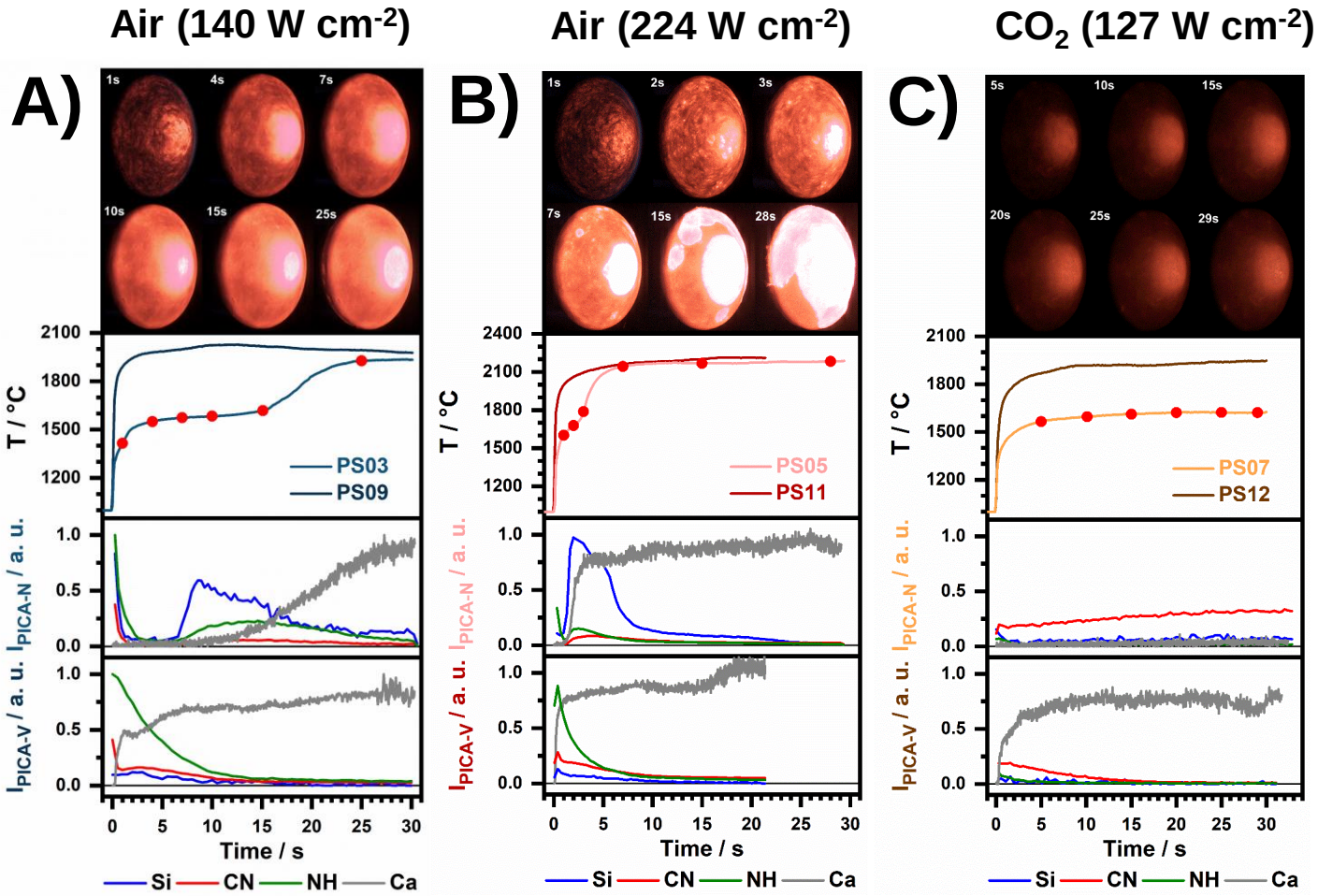

Panel figures showing still images from high-speed video, surface temperature data, and traces of species emitting in the boundary layer (e.g., Si – 251.6 nm, CN – 358.5, & NH – 336.1 nm) and stagnation surface (Ca – 422.7 nm). Panel A) illustrates the ablation process for PS03 and condition B. Panel B) illustrates the ablation process for PS05 and condition A. Panel C) illustrates the ablation process for PS07 and condition B.

Material Response Mechanism

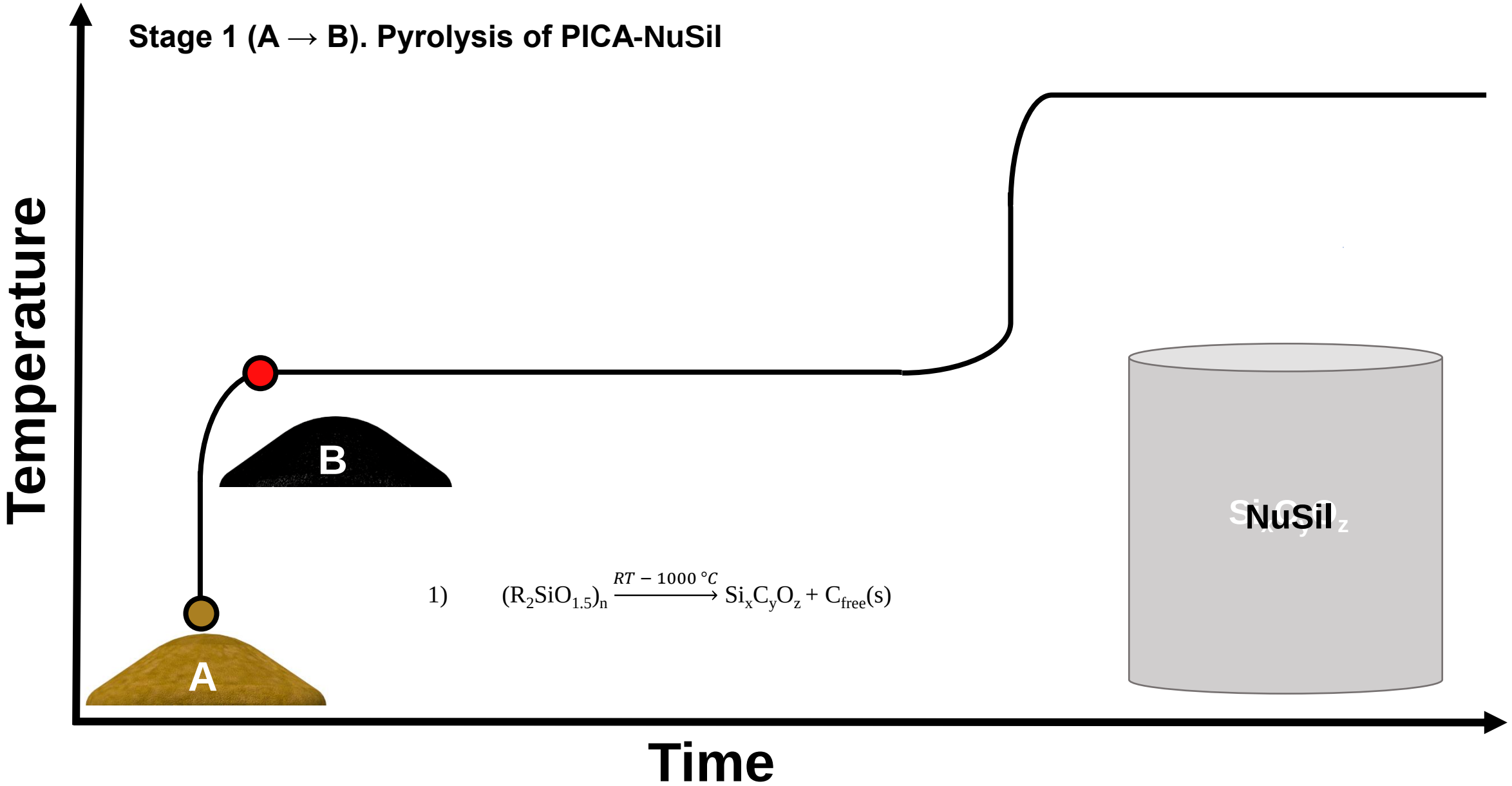

NuSil / Thermogravimetric Analysis (TGA)

- **MEKO – Nitrogen (orange trace, A)**

  a) Multistep decomposition process.

  b) Char yield > NuSil (64 wt. %).

- **NuSil – Nitrogen**

  a) TGA data show significant mass loss at T > 450 ºC (green trace, A).

  b) DSC data indicate that overall process is endothermic (green trace, B).

- **NuSil – Air**

  a) Char yield is comparable to pyrolysis.

  b) DSC data show intense exotherm which is attributed to the oxidation of NuSil.

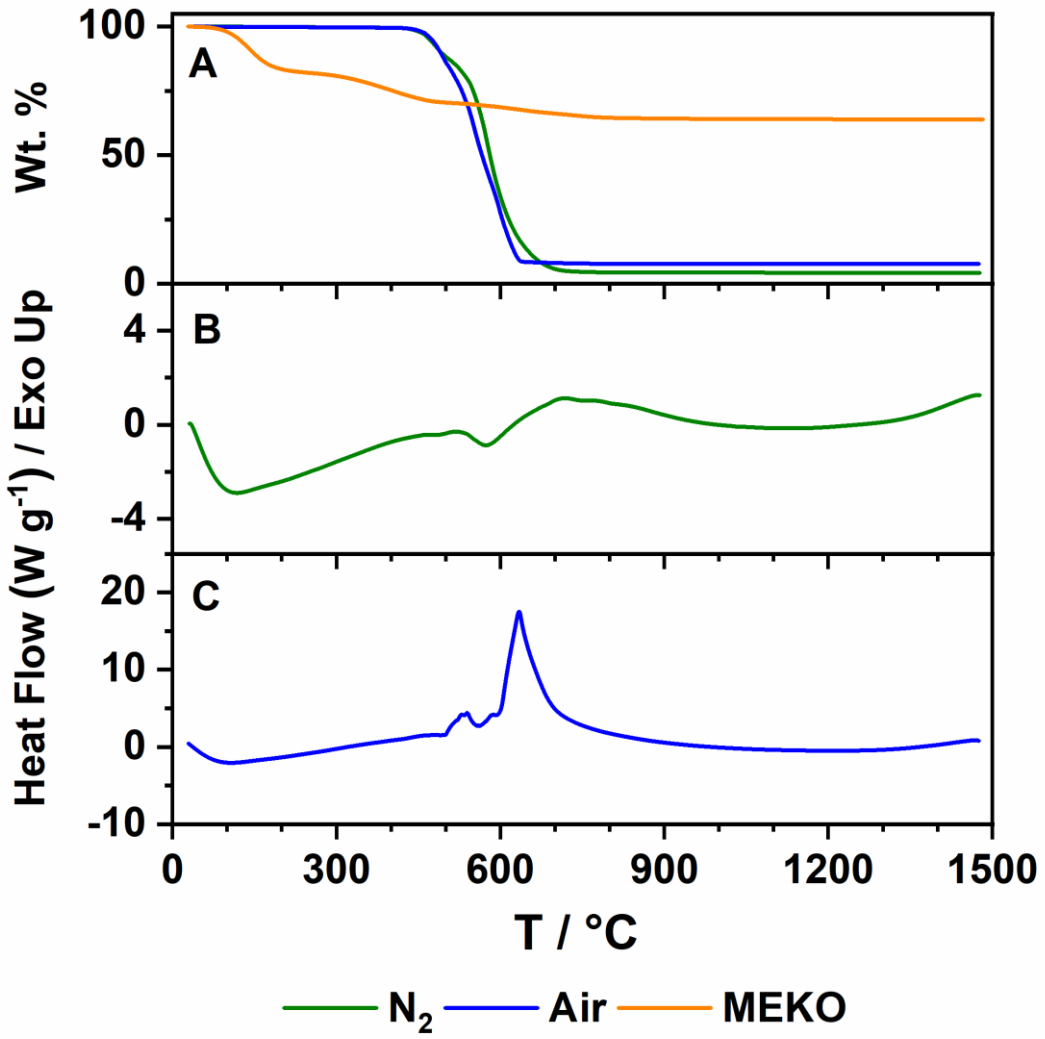

TGA/DSC data were collected on samples of NuSil at a heating rate of 40 ºC min^{-1} between T = ambient - 1475 ºC.

Material Response Mechanism

Stage 1 (A → B). Pyrolysis of PICA-NuSil

Stage 2 (B → C). Passive Oxidation and Phase Separation

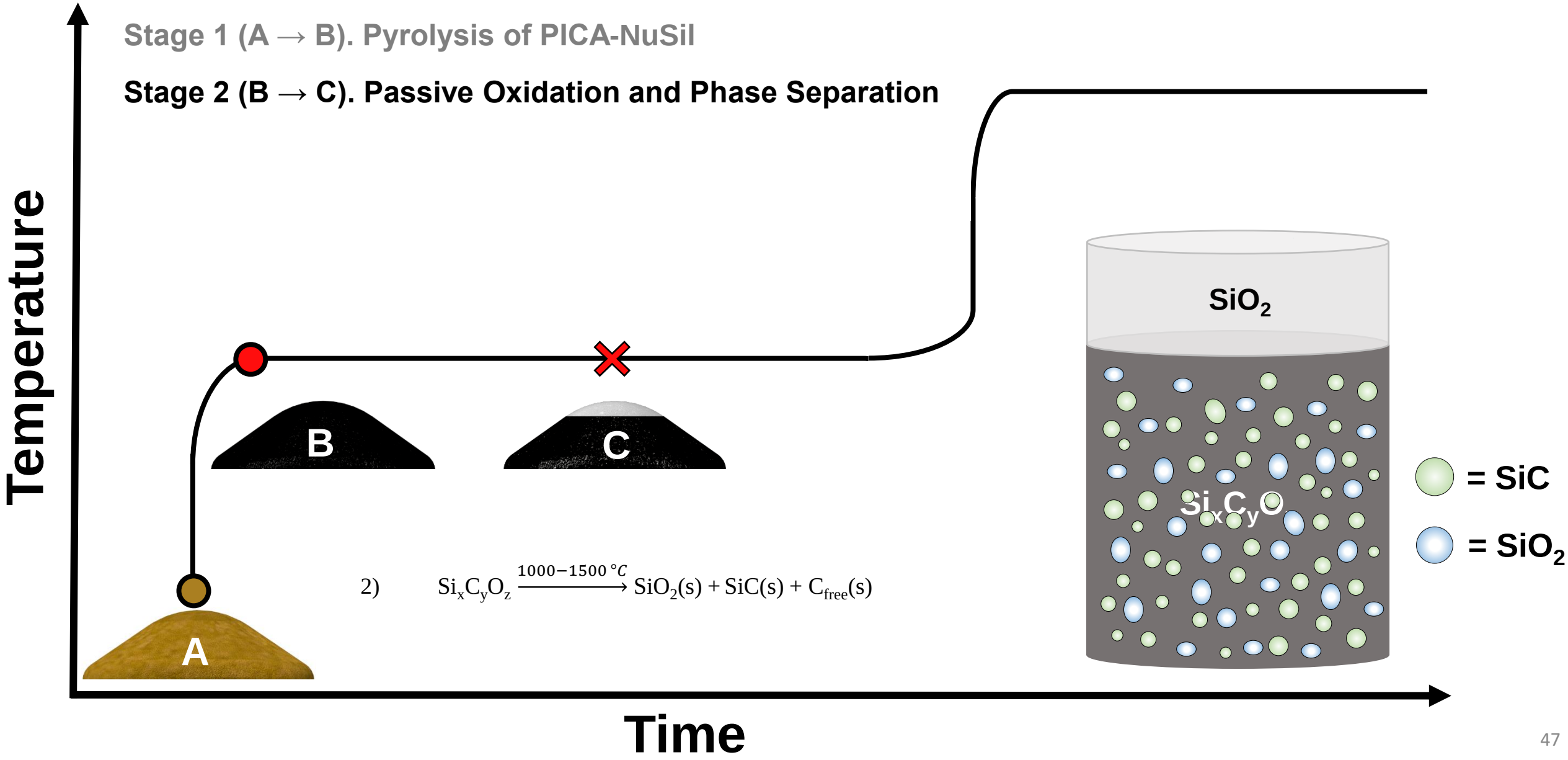

2) $Si_xC_yO_z \xrightarrow{1000-1500\,^{\circ}C} SiO_2(s) + SiC(s) + C_{free}(s)$

Post-Test Analysis / Surface Morphology (Air)

A) Post-test photo of PS03 shows a dark coating on the frustum and a ring of silica near the nose cone.

B) S.E.M. image shows a ring of silica that separates the coated frustum and region of exposed char.

C) Recession measurements indicate that the coated surface recedes slower than the exposed char, as evidenced by the flat region at the model's center.

D) E.D.S. spectrum collected on the frustum (panel B, red x) indicates that the surface is primarily composed of Si and O.

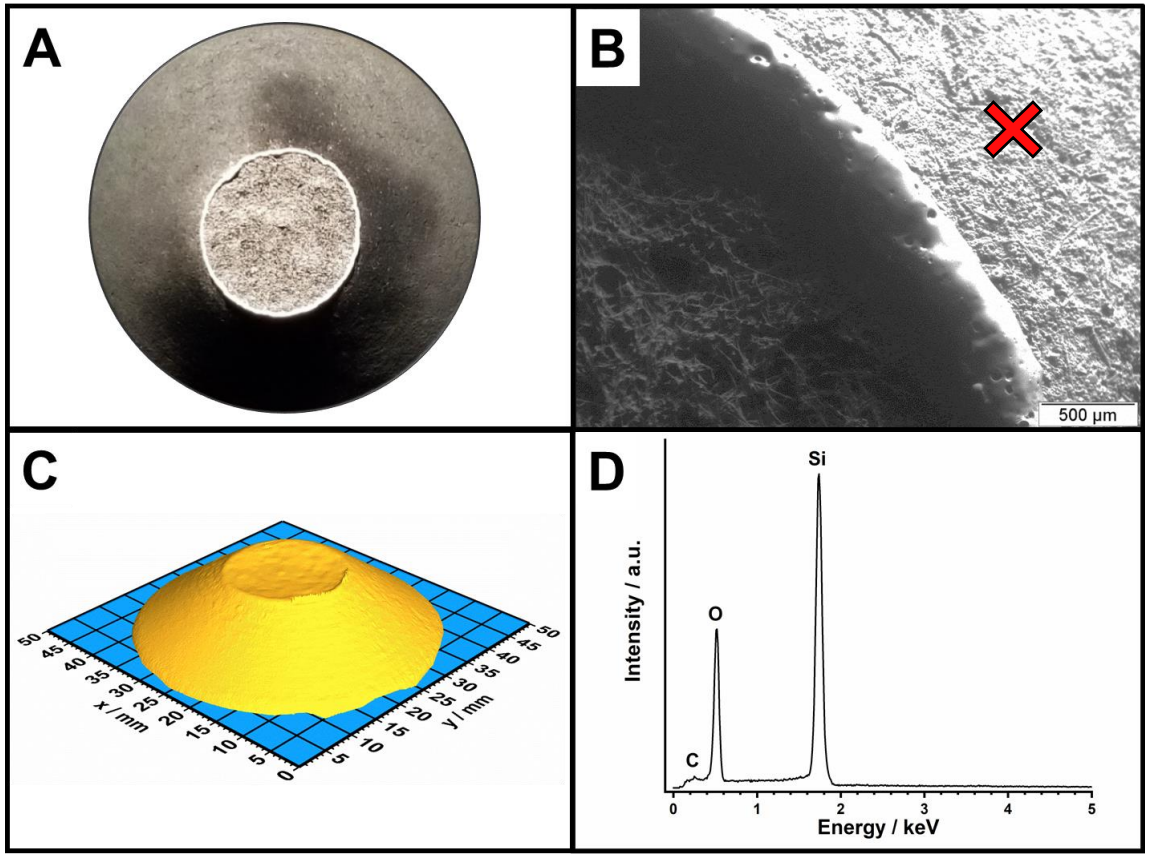

Surface characterization of PS03 showing: A) Post-test photo of the surface of PS03, B) S.E.M. image collected at the char and surface coating interface, C) 3D recession profile, and D) E.D.S. spectrum collected on the frustum of the post-test surface.

Post-Test Analysis / Surface Morphology (CO_2)

A) Post-test photo of PS07 shows a dark coating on the frustum and frustum covered with SiO_2.

B) S.E.M. image shows that the subsurface morphology consists of bundles of carbon fibers bound together with a solid phase. Additionally, the image shows the presence of silica microspheres.

C) Recession measurements indicate a stable surface morphology in the CO_2 environment.

D) E.D.S. spectrum collected on the solid phase in panel B (red dot) indicates the presence of Si and C.

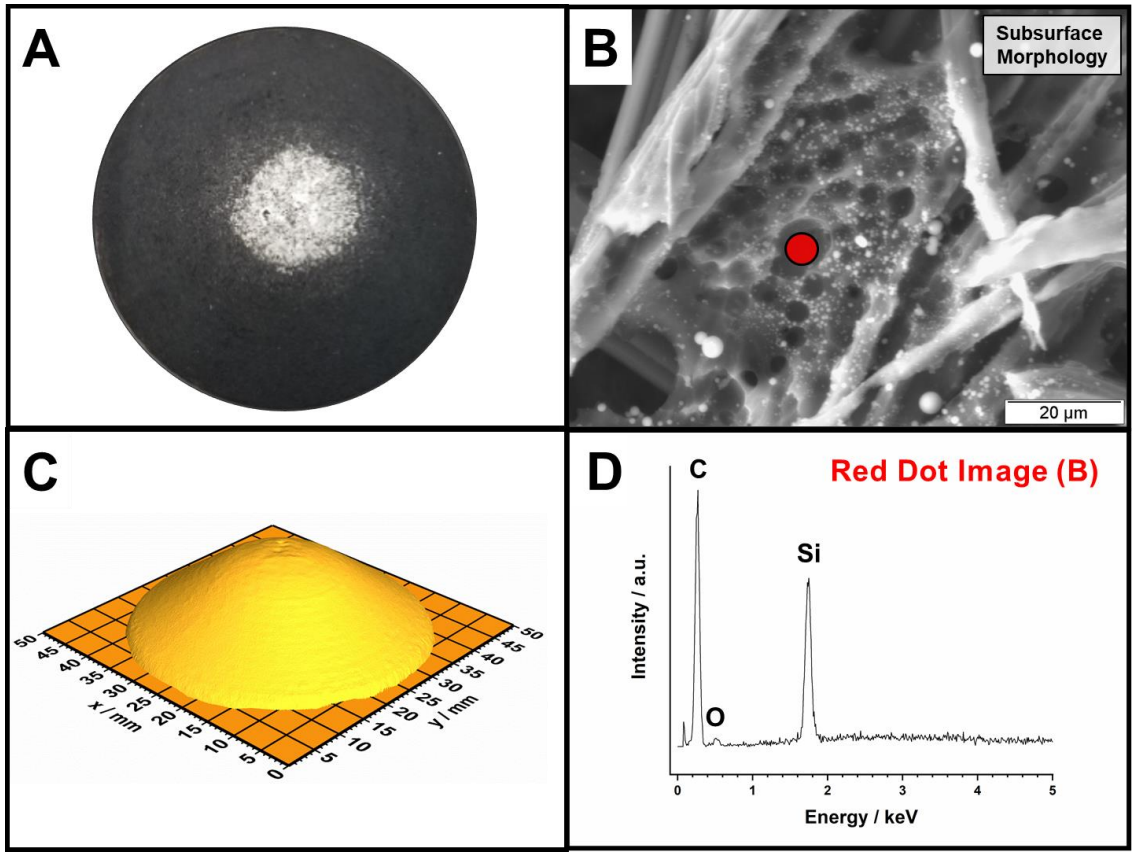

Surface characterization of PS07 showing: A) Post-test photo of the surface of PS07, B) S.E.M. image of the TPS microstructure beneath the SiO_2 surface, C) 3D recession profile, and D) EDS spectra collected in the area covered by the red dot in B).

Post-Test Analysis / XRD

- Post-test coatings were collected from the surface of models subjected to oxidizing atmospheres.
- Signal for SiC appears in post-test coatings collected from models with a surface temperature T_s > 1500 ºC (e.g., A, B, E).
- Signal for SiC did not appear in coatings collected from models that were subjected to condition C (e.g., T_s < 1300 ºC, 60 W cm^{-2}). Note that this observation remains true even after the length of the test is doubled (e.g., PS04 vs. PS08).

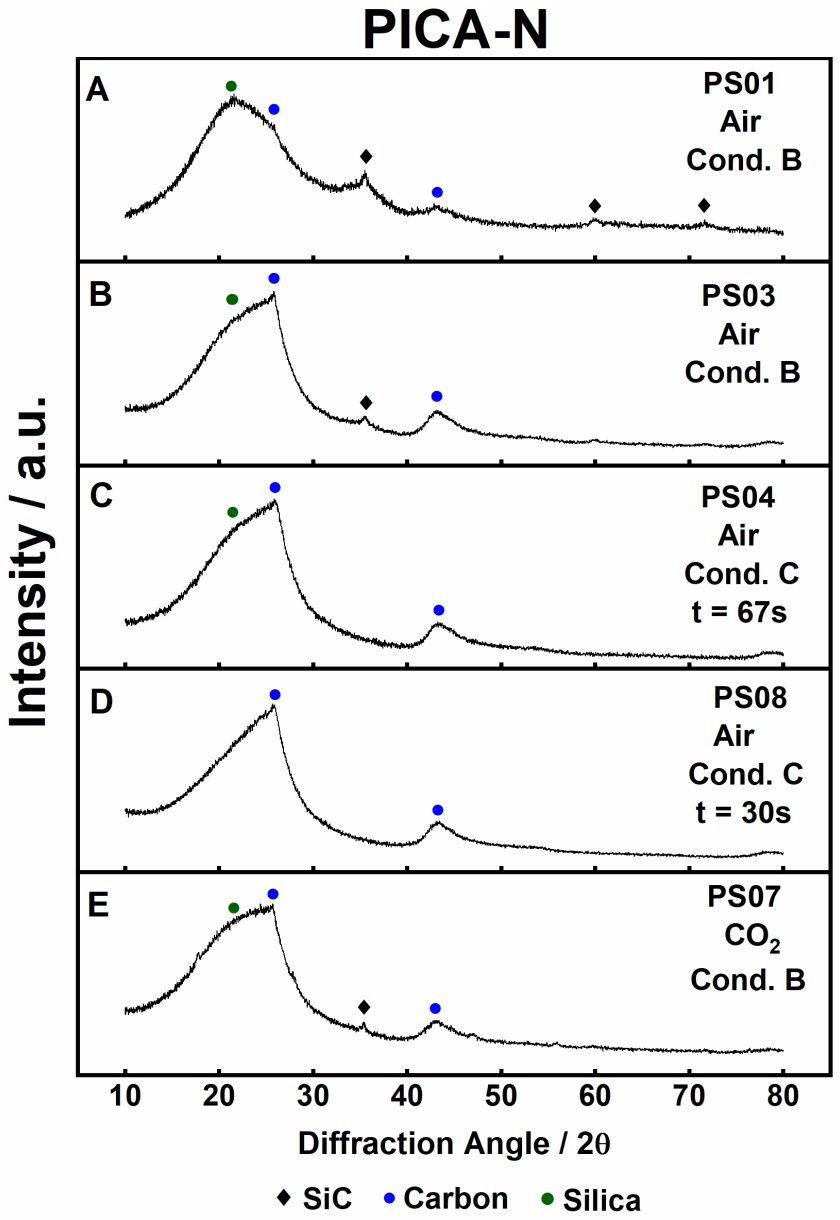

Material Response Mechanism

Stage 1 (A → B). Pyrolysis of PICA-NuSil

Stage 2 (B → C). Passive Oxidation and Phase Separation

Stage 3 (C → D). Coating Decomposition

Temperature

Time

A

B

C

D

3) $SiO_2(s) + 3C_{free}(s) \xrightarrow[\Delta H\ @\ \Delta G=0:\ +14{,}688\ (kj/kg)]{\Delta G=0\ @\ T=1520\ ^\circ C} SiC(s) + 2CO(g)$

4) $2SiO_2(s) + SiC(s) \longrightarrow 3SiO(g) + CO(g)$

5) $SiO(g) + \frac{1}{2}O_2(g) \longrightarrow SiO_2(s)$

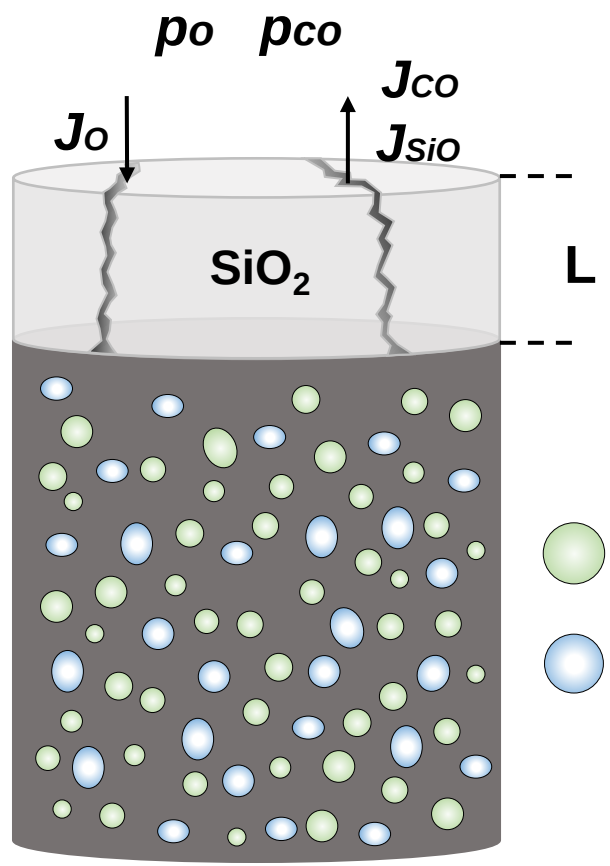

NuSil / Isothermal Analysis (TGA)

- **Isothermal TGA experiments.**

  a) NuSil loses mass at a greater rate in nitrogen than in air.

- **Microscope images of the post-test resin from TGA experiments performed on NuSil® in (A) air and (B) nitrogen.**

  a) Passivating layer of SiO_2 forms at the surface of each material.

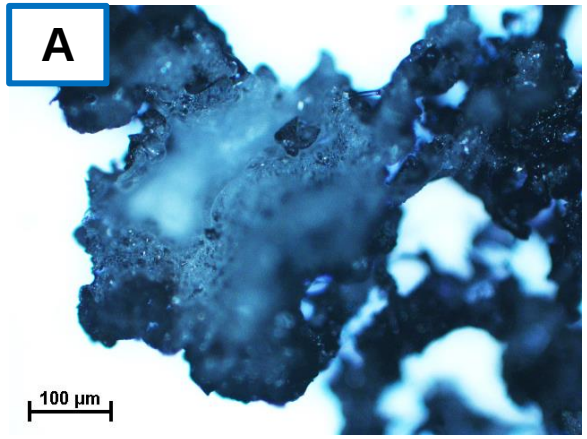

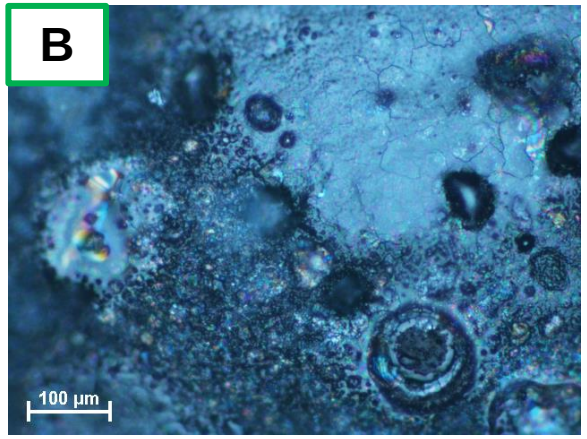

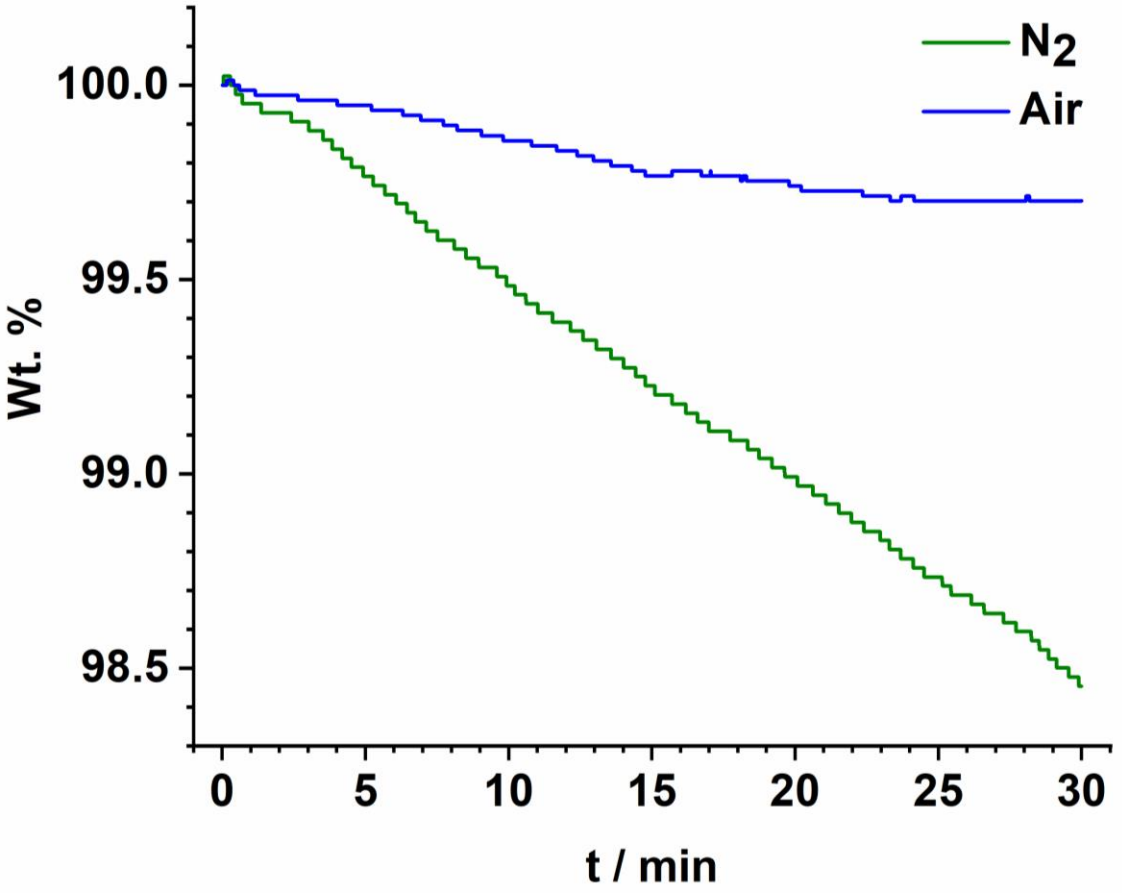

Mass loss rates as a function of time during the isothermal (T = 1475 °C) stage of the TGA experiments.

PICA-NuSil / Ablation Mechanism

Stage 1 (A → B). Pyrolysis of PICA-NuSil

Stage 2 (B → C). Passive Oxidation and Phase Separation

Stage 3 (C → D). Coating Breakdown

Temperature

Time

A

B

C

D

3) $SiO_2(s) + 3C_{free}(s) \xrightarrow[\Delta H\ @\ \Delta G=0:\ +14{,}688\ (kj/kg)]{\Delta G=0\ @\ T=1520\ ^\circ C} SiC(s) + 2CO(g)$

4) $2SiO_2(s) + SiC(s) \longrightarrow 3SiO(g) + CO(g)$

5) $SiO(g) + \frac{1}{2}O_2(g) \longrightarrow SiO_2(s)$

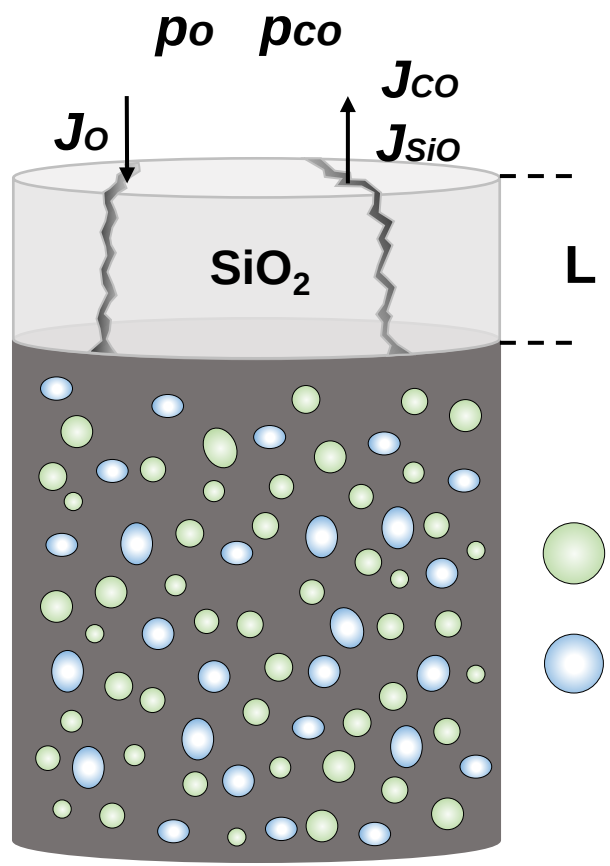

Material Response Mechanism

Stage 1 (A → B). Pyrolysis of PICA-NuSil

Stage 2 (B → C). Passive Oxidation and Phase Separation

Stage 3 (C → D). Coating Breakdown

Temperature

Time

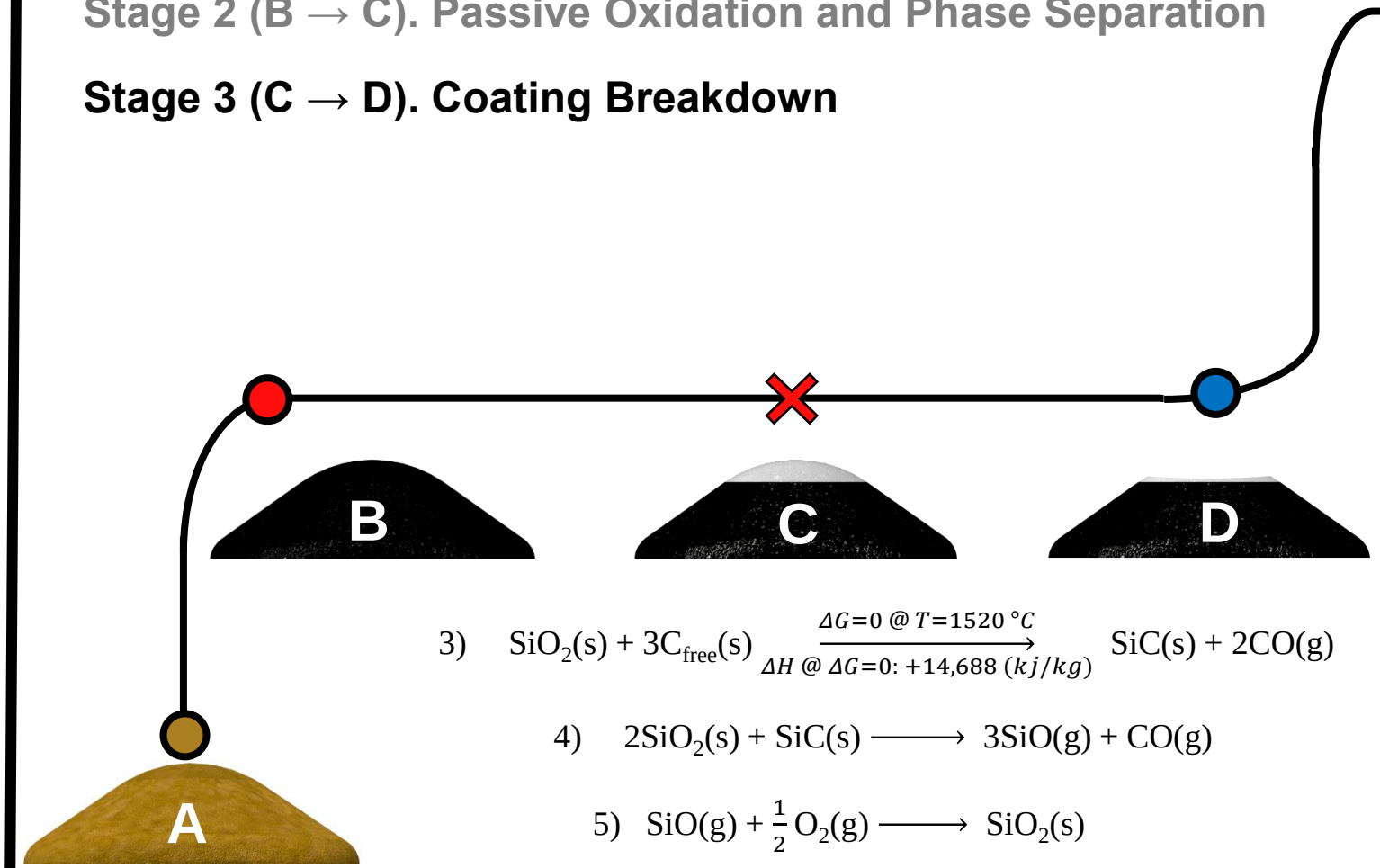

3) $SiO_2(s) + 3C_{free}(s) \xrightarrow[\Delta H\ @\ \Delta G=0:\ +14{,}688\ (kj/kg)]{\Delta G=0\ @\ T=1520\ ^\circ C} SiC(s) + 2CO(g)$

4) $2SiO_2(s) + SiC(s) \longrightarrow 3SiO(g) + CO(g)$

5) $SiO(g) + \frac{1}{2}O_2(g) \longrightarrow SiO_2(s)$

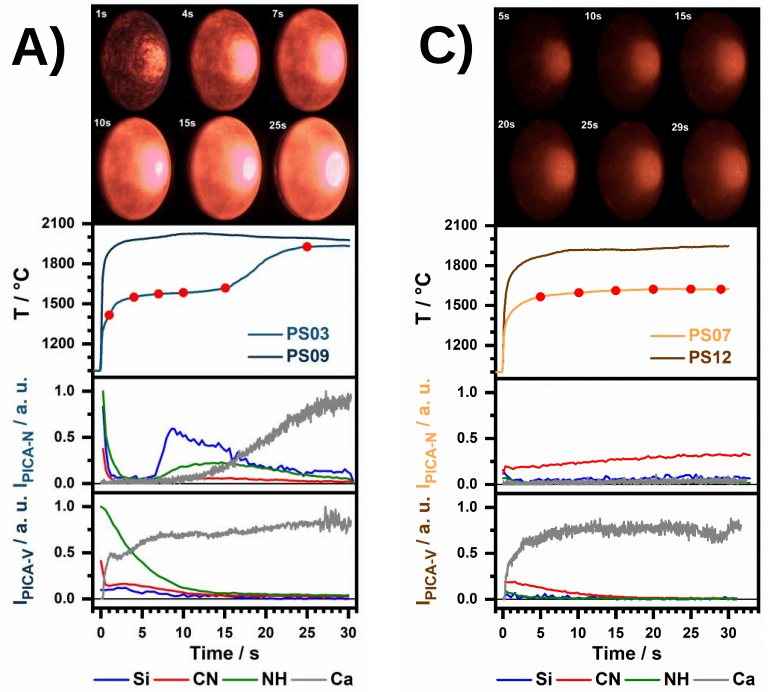

Material Response Mechanism

Stage 1 (A → B). Pyrolysis of PICA-NuSil

Stage 2 (B → C). Passive Oxidation and Phase Separation

Stage 3 (C → D). Coating Breakdown

Stage 3 (C → D′). CO_2 Environment

Temperature

Time

A

B

C

D

3) $SiO_2(s) + 3C_{free}(s) \xrightarrow[\Delta H\ @\ \Delta G=0:\ +14{,}688\ (kj/kg)]{\Delta G=0\ @\ T=1520\ ^\circ C} SiC(s) + 2CO(g)$

4) $2SiO_2(s) + SiC(s) \longrightarrow 3SiO(g) + CO(g)$

5) $SiO(g) + \frac{1}{2}O_2(g) \longrightarrow SiO_2(s)$

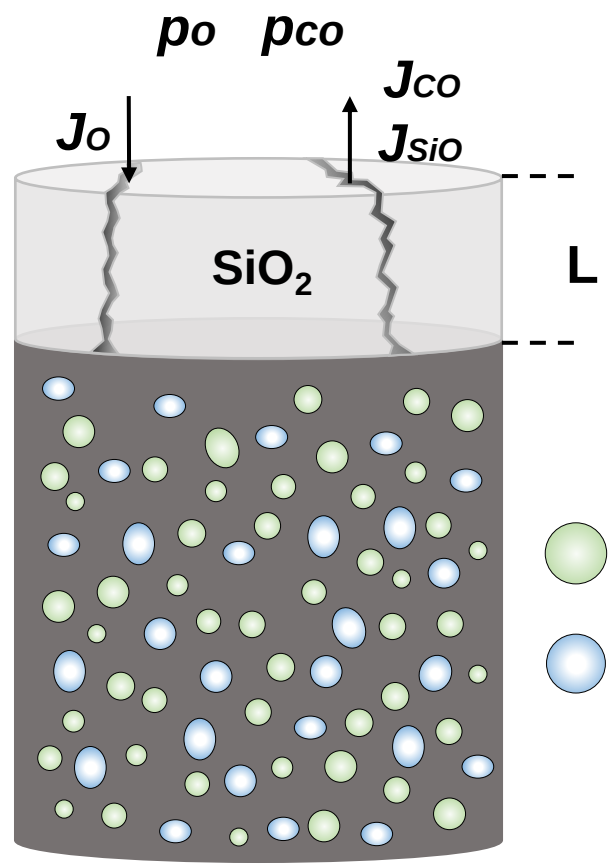

Material Response Mechanism

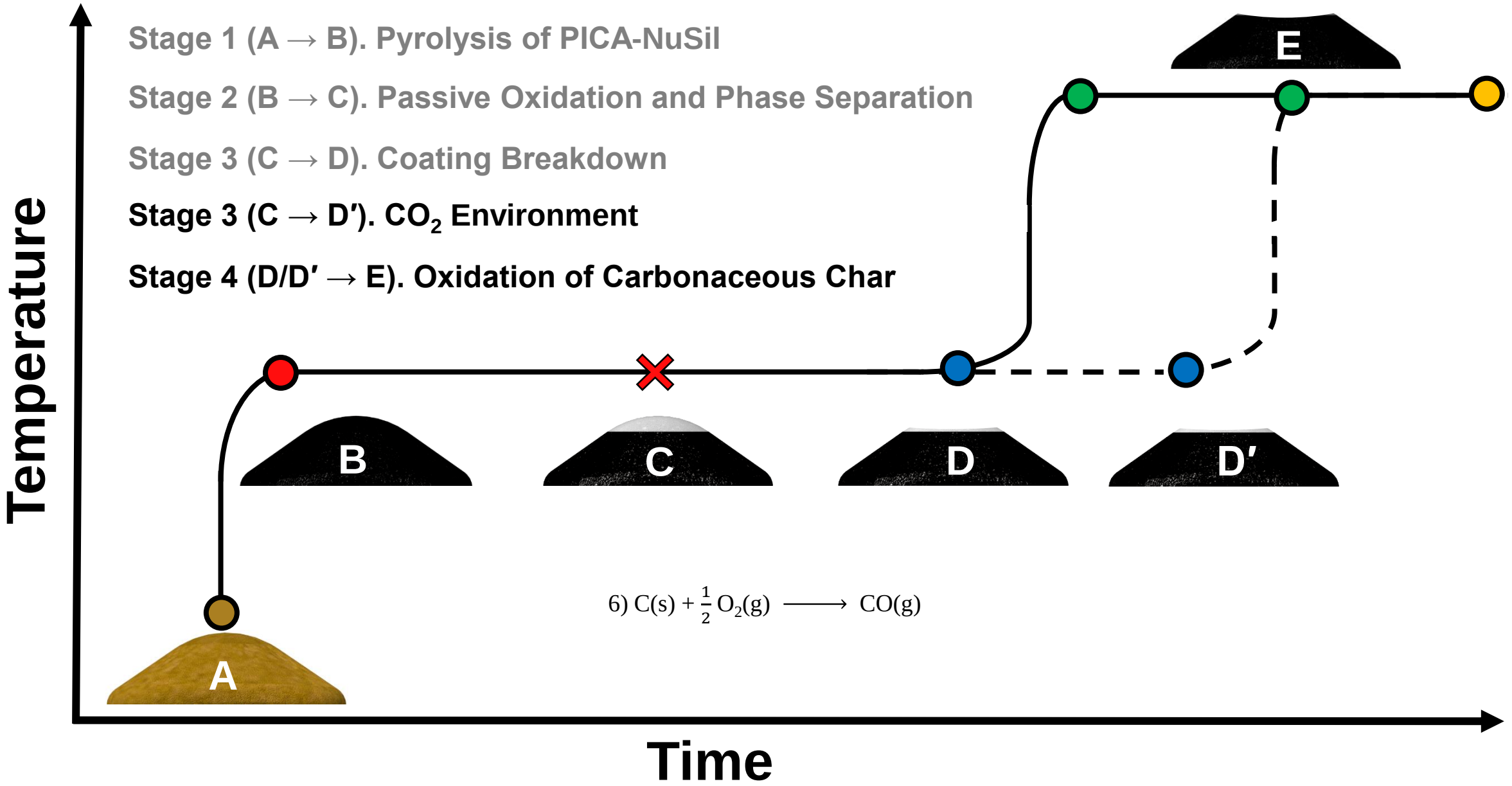

Conclusions

- **NuSil lowers the surface temperature and in-depth response in oxidizing conditions.**
- **NuSil survives for longer periods of time at lower heating rates.**
- **The ablation mechanism of NuSil consists of four steps:**

Stage 1 (A → B). Pyrolysis of PICA-NuSil

- Formation of $Si_xC_yO_z$
- Char yield ∝ crosslinking density of NuSil

Stage 2 (B → C). Passive Oxidation and Phase Separation

- Formation of protective oxide layer
- $Si_xC_yO_z \rightarrow SiC(s) + SiO_2(s) + C(s)_{free}$

Stage 3 (C → D). Coating Breakdown

- NuSil breaks down via carbothermal reduction.

Stage 4 (D → E). Oxidation of Carbonaceous Char

- Surface temperature rises due after carbonaceous char layer is exposed to the reactive flow environment.

SOLAR SYSTEM DESTINATIONS

Venus

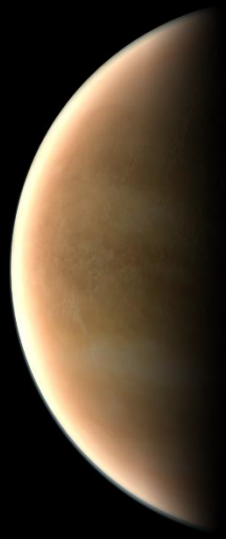

Atmosphere:

CO_2 ~ 96.5 %

N_2 ~ 3.5 %

Mars

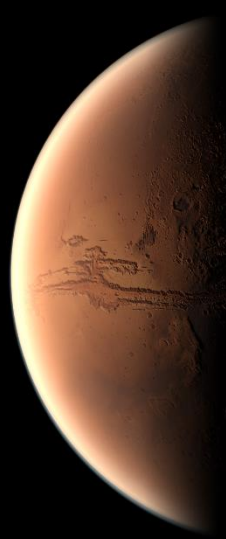

Atmosphere:

CO_2 ~ 95.3 %

N_2 ~ 2.6 %

Ar ~ 1.9 %

Titan

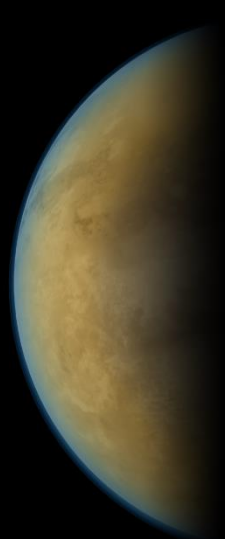

Atmosphere:

N_2 ~ 95 %

CH_4 ~ 5 %

Neptune

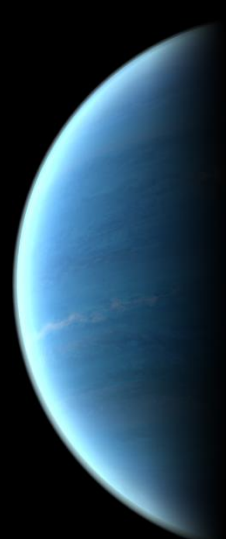

Atmosphere:

H_2 ~ 80 %

He ~ 19 %

CH_4 ~ 1 %

ATMOSPHERIC ENTRY / MATERIAL RESPONSE

- Block, Absorb, and Dissipate Thermal Energy.
- Maximize the Thermal Gradient Between the Recession Front and Spacecraft Substructure.

OXIDATION RESISTANCE

THERMAL CONDCUTIVITY

PAYLOAD CAPACITY

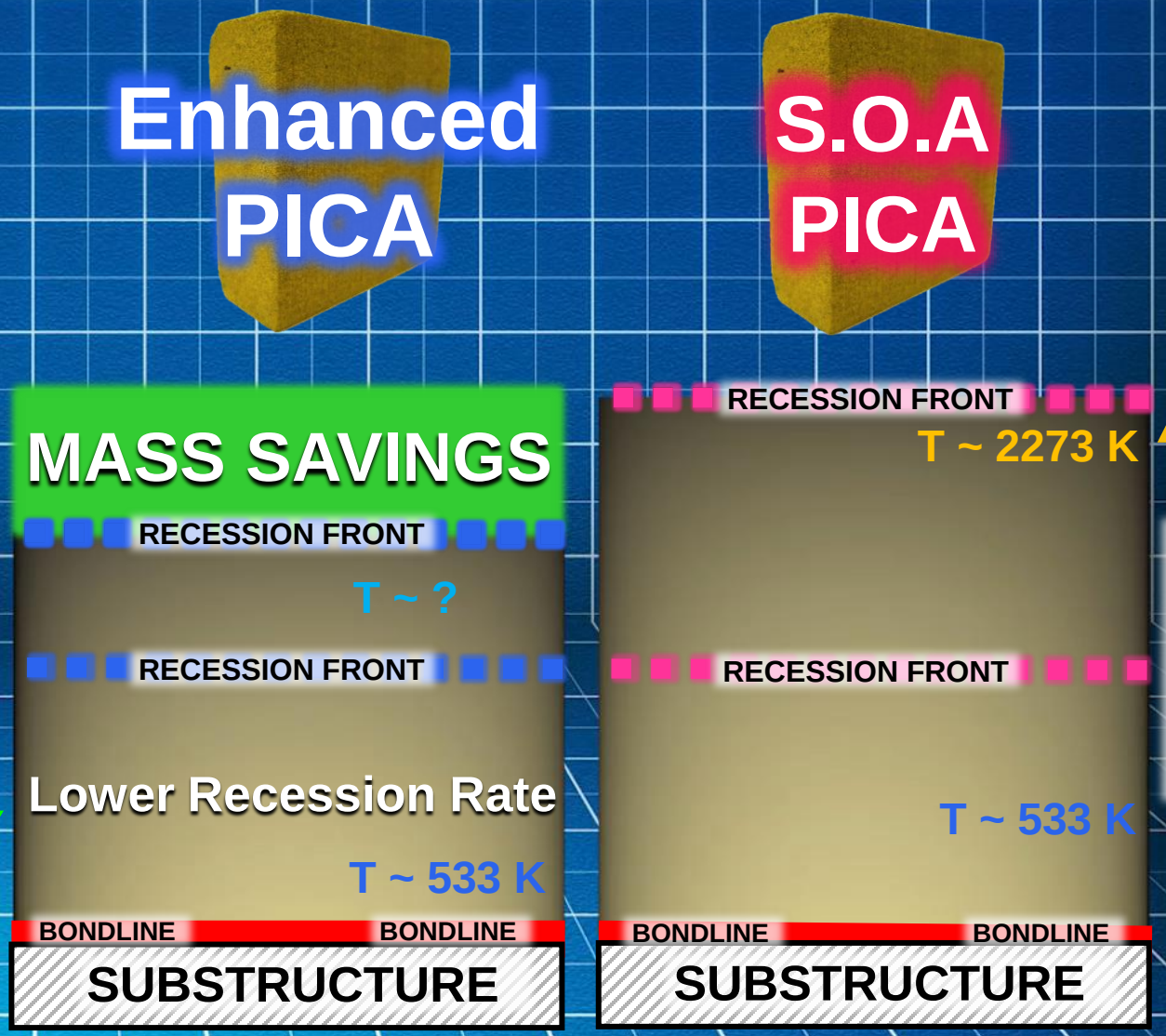

SURFACE COATINGS VS. VOLUME COATINGS

- GROUND BASED COATINGS WILL INFLUENCE PERFORMANCE.
- ALL COATINGS WILL BE APPLIED TO THE ENITRE VOLUME.

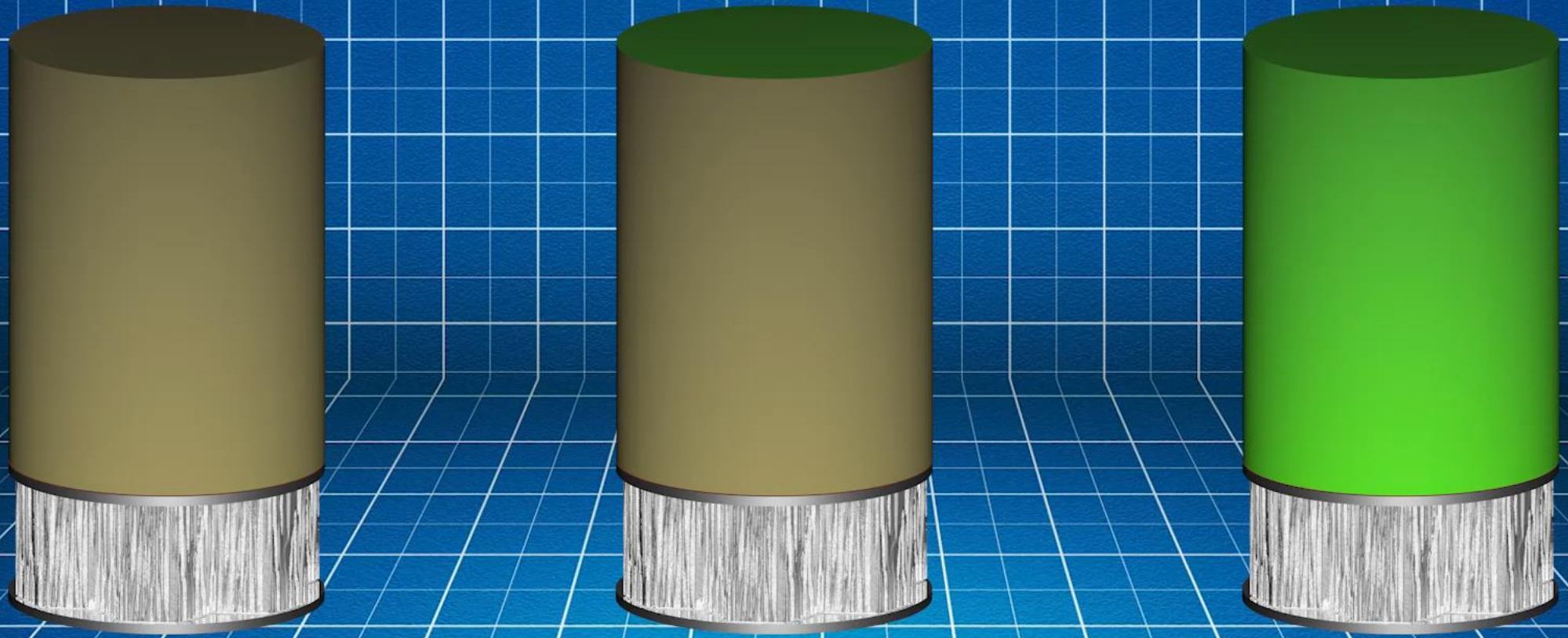

VIRGIN SURFACE VOLUME

WHAT IS ATOMIC LAYER DEPOSITION?

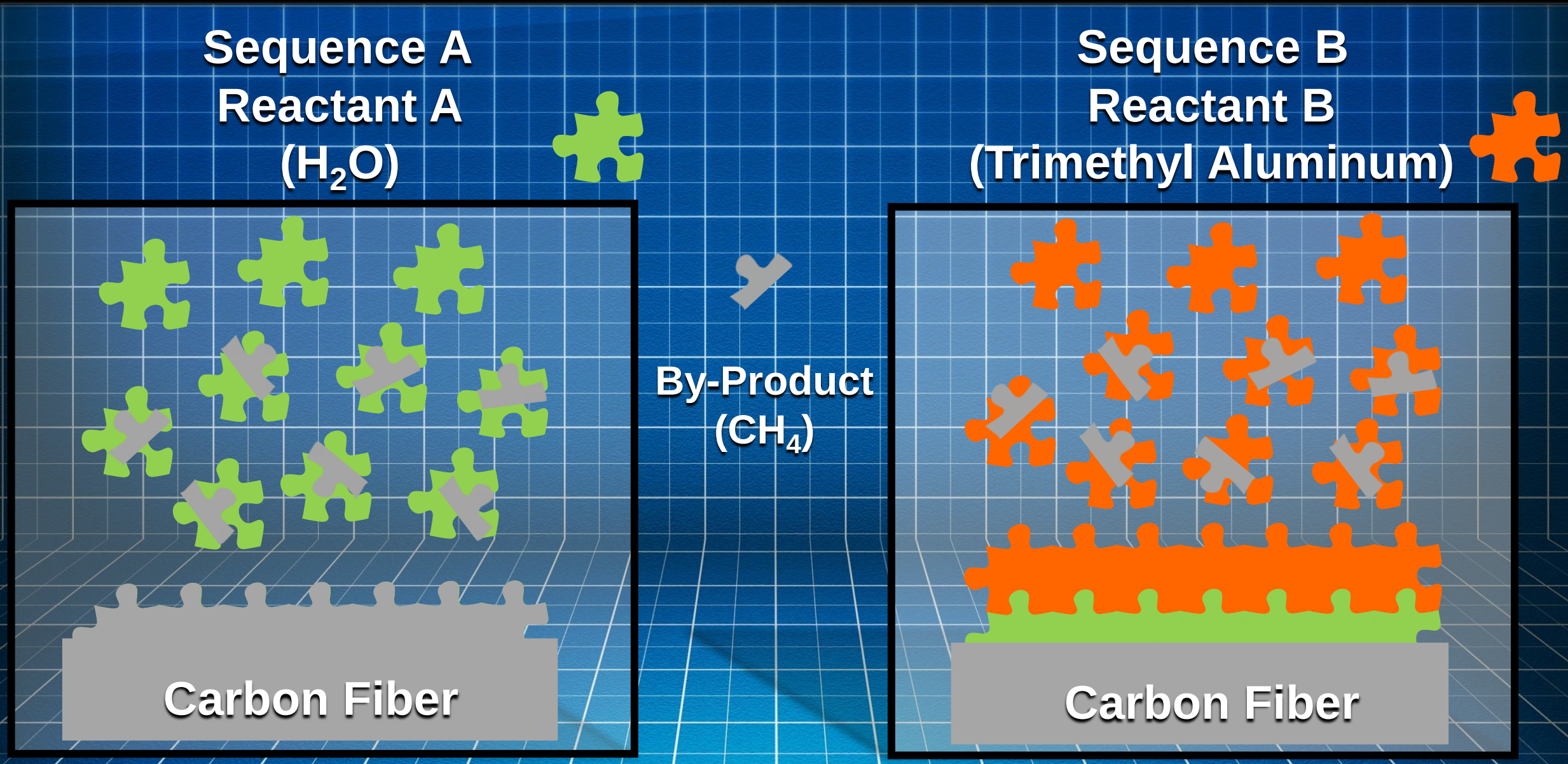

WHAT IS ATOMIC LAYER DEPOSITION?

COATING THICKNESS (L)
~ HUNDREDS of NANOMETERS

FiberForm

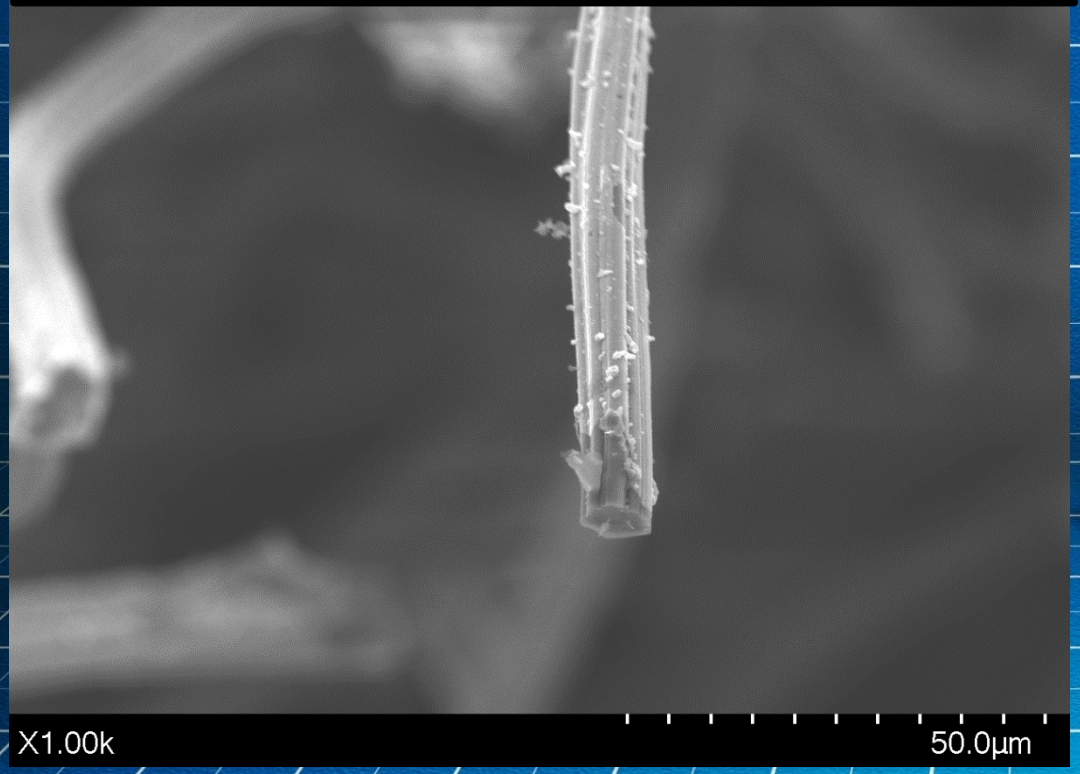

L

A-B Sequence

WHAT IS ATOMIC LAYER DEPOSITION?

COATING THICKNESS (L)
~ HUNDREDS of NANOMETERS

Carbon Felt

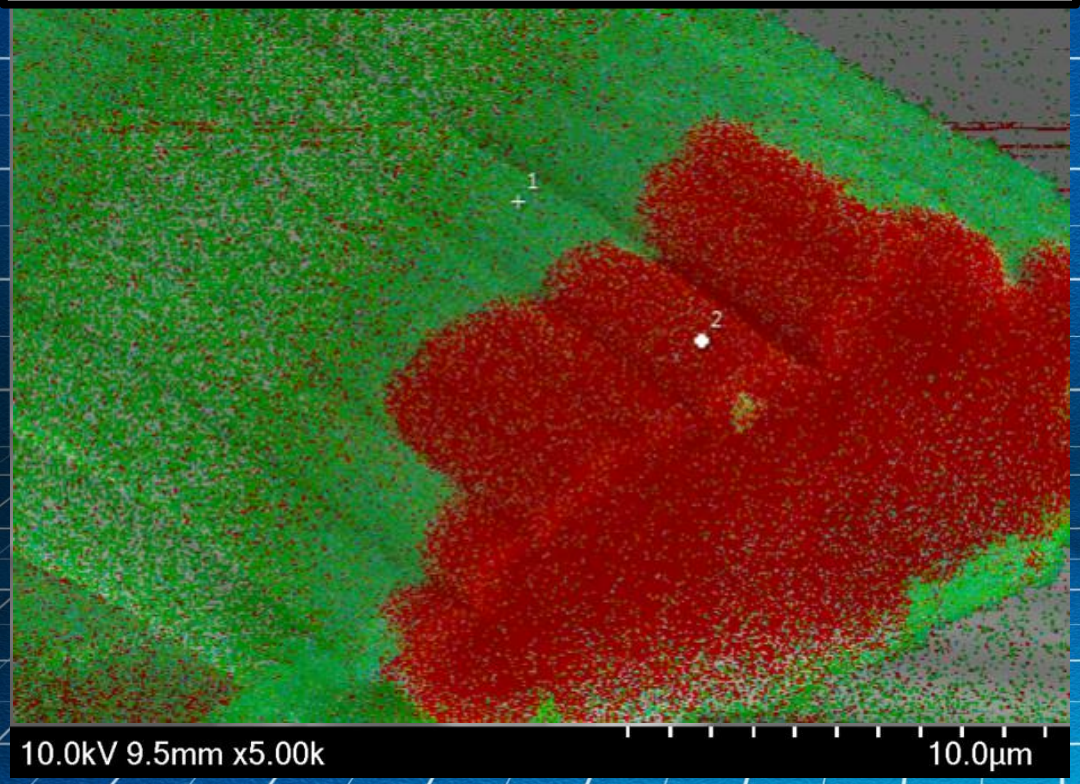

L

A-B Sequence

FY20 & FY21 Center Innovation Fund

Oxidation Resistance

- Heating Rate: 20 °C min^{-1}
- ∆T: Ambient – 1,000 °C
- Virgin FiberForm.
  - Onset of Oxidation: T ~ 550 °C.
- FiberForm + 50 nm Al_2O_3.
  - Onset of Oxidation: T ~ 750 °C.
- FiberForm + 100 nm Al_2O_3.
  - Onset of Oxidation: T ~ 750 °C.

T.G.A. Data - Air

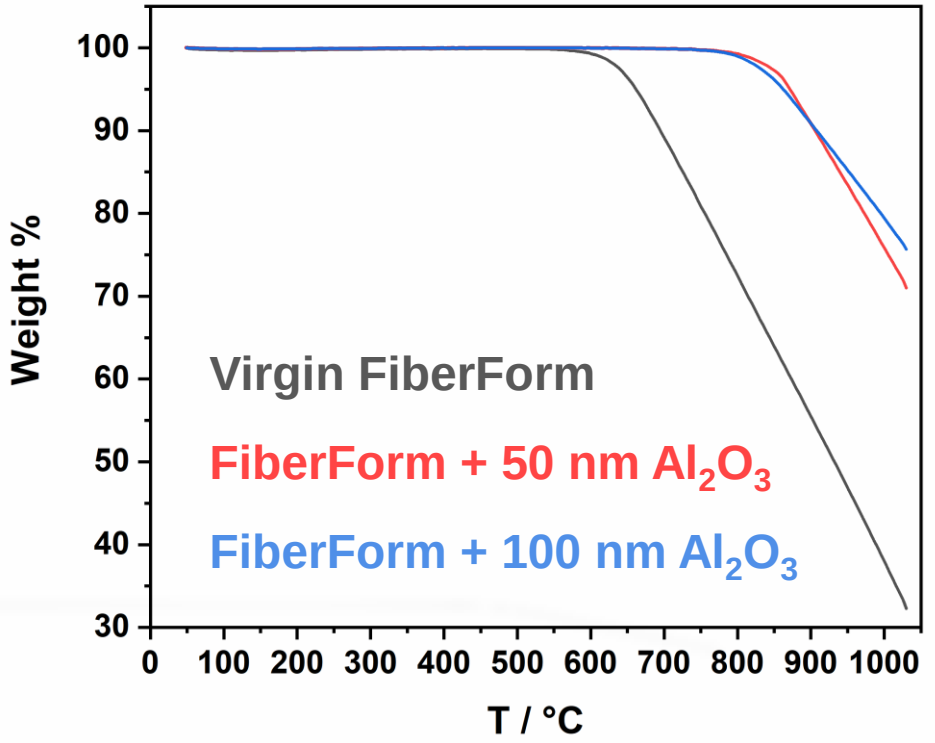

Alumina Coatings Increase the Onset of Oxidation By 36%

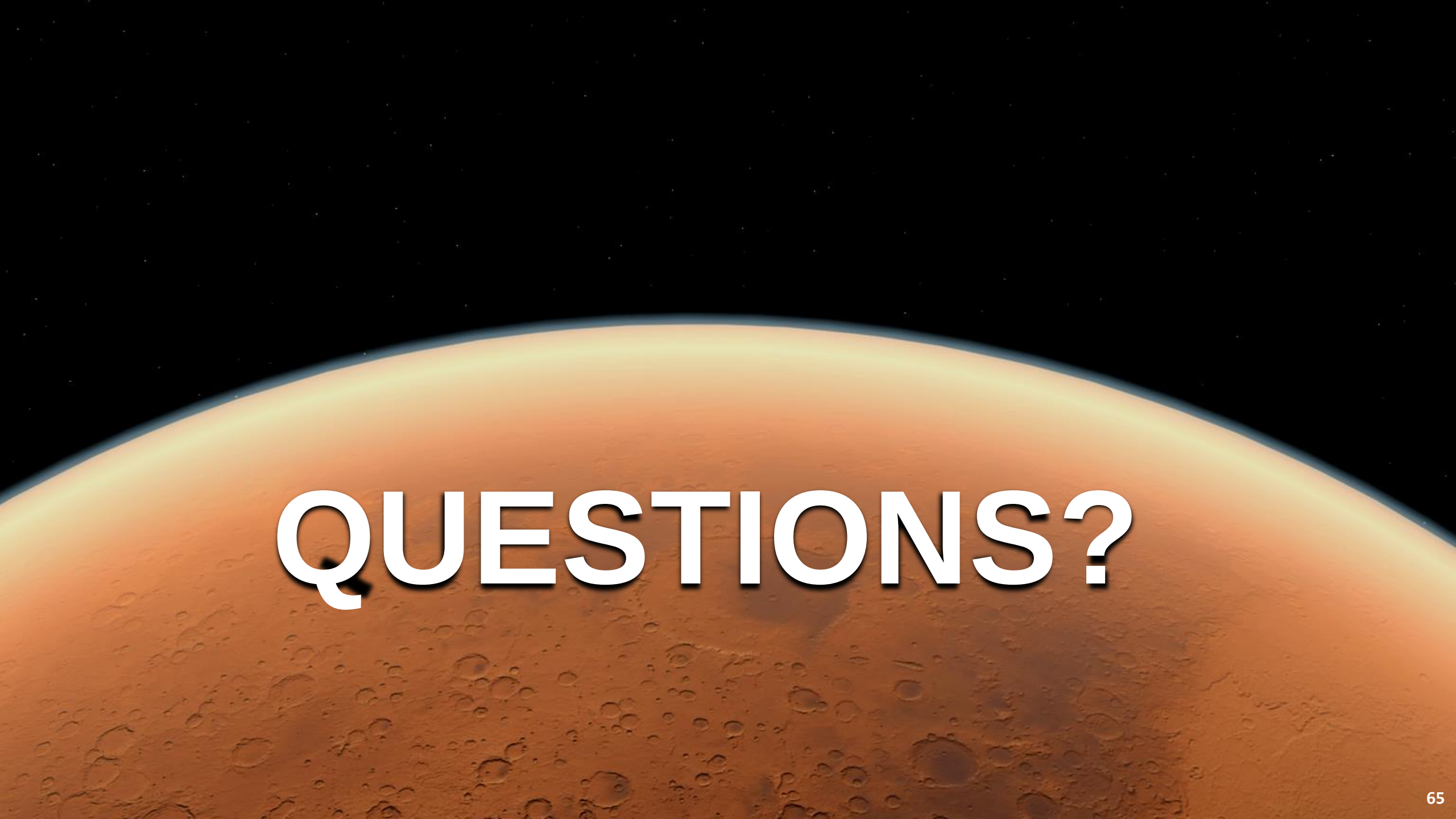
QUESTIONS?